$\mathcal{L}_1$ ADAPTIVE CONTROL WITH QUANTIZATION AND DELAY

BY

HUI SUN

DISSERTATION

Submitted in partial fulfillment of the requirements
for the degree of Doctor of Philosophy in Electrical and Computer Engineering
in the Graduate College of the
University of Illinois at Urbana-Champaign, 2013

Urbana, Illinois

Doctoral Committee:

Professor Tamer Başar, Chair
Professor Naira Hovakimyan, Co-Chair
Professor Daniel Liberzon
Professor Rayadurgam Srikant

ABSTRACT

This dissertation involves $\mathcal{L}_1$ adaptive control development and analysis in the presence of quantization and system delays, addressing quantized uncertain systems and delayed uncertain systems.

We discuss three cases of control of quantized systems: the state feedback control for systems with input quantization, state feedback control for systems with both input and state quantization, and output feedback control for systems with input quantization. Some of the theoretical results are later applied to a buck-converter. The quantization schemes considered are introduced, detailed performance analysis and simulation/application results for different cases are included, and detailed proofs are given in an appendix.

We discuss control design and performance results for adaptive control of uncertain systems with internal delays. The results are subsequently applied to control of the drilling bit in a rotary steerable system, where the spatial delays come from the difference of equipment positions.

Based on $\mathcal{L}_1$ adaptive control theory for classical nonlinear systems in *Hovakimyan and Cao (2010)*, we further develop the control for quantized and delayed systems. For each case we develop control design according to the available state information, analyze the performance of the closed-loop system, and demonstrate the results in simulations and applications.

To my baby Leshan, for being the first annotator of my thesis.

ACKNOWLEDGMENTS

I would like to express my utmost and deepest gratitude and appreciation to my advisors, Professor Naira Hovakimyan and Tamer Başar, for their guidance, patience and detailed advice through these years. Thanks to Professor Hovakimyan for her patience in working with me on detailed problems and nurturing our group so we discuss and share ideas. Thanks to Professor Başar for always finding time for me in his busy work, for his guidance and support in my projects and papers, and for his broad knowledge in the decision and control area. I am most grateful to them for giving me the opportunity to carry out my research and for always being there when I need help.

I would also like to express my appreciation to my committee: Professor Daniel Liberzon and Professor Rayadurgam Srikant. Thanks for the valuable questions and comments, which helped me towards the improvement and completion of my thesis.

My warmest appreciation to all my friends and labmates. Thank you for your invaluable friendship and encouragement, for your help and discussions.

Special thanks to my family for their love and support.

TABLE OF CONTENTS

CHAPTER 1

INTRODUCTION

"Faith is taking the first step even when you don't see the whole staircase." –Martin Luther King, Jr.

This dissertation considers two types of uncertain systems: quantized systems and delayed systems.

Quantized systems have gained increasing notice and coverage for their role in modeling hardware and communication limitations. Real world systems are usually described by continuous-value continuous-time models. The variables used in the models take values in finite-dimensional Euclidean spaces. However, the values can be obtained only with finite precision. Quantization is a mapping from a larger set (such as a finite-dimensional Euclidean space) to a smaller set of finite or countably many symbols. It describes both hardware and software limitations. For instance, for hardware, it can describe the imprecise measurement, where only finite digits can be read from a meter, or the constrained control, where only selected values of control are allowed. A motivating application in this dissertation uses quantization to model the A/D and D/A conversion errors in an electric circuit system. In communication systems, quantization provides an approximation to a continuous-value variable, and thus reduces the transmission bits for a single value from infinite to finite.

A variety of different types of quantized systems have been studied in recent years. Stabilization of LTI systems is covered in [1–4], supervisory control of quantized uncertain systems is considered in [5, 6], with applications in [7], the limitations of performance in adaptive dynamical systems are addressed in [8]. We consider two types of quantization in this dissertation. In [2, 9], the problem of stabilizing an unstable LTI system has been studied. The logarithmic quantizer has been shown to be the coarsest quantizer to stabilize the system. The idea of logarithmic quantizer is to maintain a small relative error. So it gets finer around the origin and coarser away from the origin. In [4], the problem of state estimation has been considered. Using information theoretic criteria, such as mono-

tonic boundedness of entropy of the estimation error, it has been shown that the uniform quantization is the one that achieves the minimum rate. The variety of hysteresis quantization is first introduced in cellular neural networks by [10–12], and is shown to help improve the Lyapunov stability of the cellular neural networks (CNN). Later, [13] shows that the switching frequency between two adjacent quantization intervals is locally finite, which is useful to reduce the chattering phenomenon.

Delayed system study in this dissertation is motivated by the control of a rotary steerable system. The spatial delays in the system come from the modeling of distance displacements of the equipment. On the drill pipes stabilizers or force actuators are placed at a certain distance to the drilling bit to displace the bit and change the angle of the drilling direction while measurement-while-drilling tools are equipped to send directional data back to the surface without disturbing drilling operations. In a rotary steerable system the actual drilling trajectory depends on a variety of factors, such as assembly configuration and dimensions, lithology, dip, bit type, hole curvature, magnitude of inclination, bit weight, and rotary speed, and is difficult to predict [14]. The dynamic vibration response of the drillstring as a mechanical structure has been studied in many works [15–18]. Due to the imprecision in modeling and measurement, the controller design that is robust and handles large parametric uncertainty becomes an important aspect in the directional drilling technology.

To deal with the uncertainty in the aforementioned two types of systems, we use an adaptive controller to estimate the uncertainty and adjust the control according to the estimate. We refer to the $\mathcal{L}_1$ adaptive controller due to its ability of incorporating system structures as well as fast adaptation with guaranteed robustness (bounded away from zero time-delay margin) [19, 20]. The $\mathcal{L}_1$ adaptive controller runs a state predictor in parallel with the plant, decoupled from the control laws, which together with proper filtering makes the incorporation of different system constraints, such as quantization, delays, and saturation, possible when other model-inversion type of control is inapplicable. Meanwhile, the $\mathcal{L}_1$ adaptive controller uses a fast estimation scheme, which leads to uniform guaranteed performance in both transient state and steady state [20, 21]. Moreover, it is proved to have a time-delay margin, bounded away from zero [19]. The fast adaptation and guaranteed robustness make it especially suitable for environments rich in measurement noise and disturbances.

The dissertation is organized as follows. Chapter 2 introduces two different

types of quantization: uniform and logarithmic, as well as their variations with hysteresis, which are used later in Chapters 3, 4, and 5. Chapter 3 analyzes state feedback control of input-quantized systems; Chapter 4 analyzes state feedback control of state-quantized systems; and Chapter 5 analyzes output feedback control of input-quantized systems. Chapter 6 discusses adaptive control of uncertain delayed systems. Finally, the concluding remarks of Chapter 7 and two appendices conclude the thesis.

CHAPTER 2

QUANTIZATION

"I do not pretend to start with precise questions. I do not think you can start with anything precise. You have to achieve such precision as you can, as you go along." –Bertrand Russell

This chapter introduces the quantization schemes used in this dissertation. Two typical quantization schemes are considered in the control problems formulated in later chapters: uniform and logarithmic quantization. Motivated by the possible frequent switching and chattering phenomenon in quantized systems, the variety of hysteresis quantization for both uniform and logarithmic types are also introduced.

Widely used in compressing data and modeling imprecision problems, a quantization function $Q : X \to X_{\mathrm{q}}$ maps a continuous range of values into a set of countably many or finite elements. Though quantization can be done on both finite and infinite dimensional spaces, we consider a quantization function on $\mathbb{R}^n$. For each subset of $X \subset \mathbb{R}^n$, the quantization function outputs a single element in $X_{\mathrm{q}} \subset \mathbb{R}^n$.

When a time varying signal is quantized, we consider the quantization of the signal value $x(t)$ at time t. At each time t, the input $x(t) \in X$ and the output $x_{\mathrm{q}}(t) \in X_{\mathrm{q}}$ of the quantizer satisfy $x_{\mathrm{q}}(t) = Q(x(t))$.

2.1 Uniform quantization

In uniform quantization, the outputs of the quantization function are equispaced. The elements in the space are represented with equal resolution.

We start with the scalar case of classical uniform quantization. Let $Q_{\mathrm{unif}}(\cdot)$ be the quantization function. If the input signal is $x(t) \in \mathbb{R}$, the quantization function

$x_{\mathrm{q}}(t) = Q_{\mathrm{unif}}(x(t))$ is defined by

$$x_{\mathrm{q}}(t) = Q_{\mathrm{unif}}(x(t)) = \begin{cases} x_i, & \alpha_i \leq x(t) < \alpha_{i+1}, \\ 0, & -\alpha_0 < x(t) < \alpha_0, \\ -x_i, & -\alpha_{i+1} < x(t) \leq -\alpha_i, \end{cases} \tag{2.1}$$

where $\alpha_0 = \frac{1}{2}l$, $l > 0$, $-\alpha_0 < x_0 < \alpha_0$, $\alpha_{i+1} = \alpha_i + l$, and $i \in \mathcal{I}$. A uniform quantization function is shown in Figure 2.1. The quantization error in this case

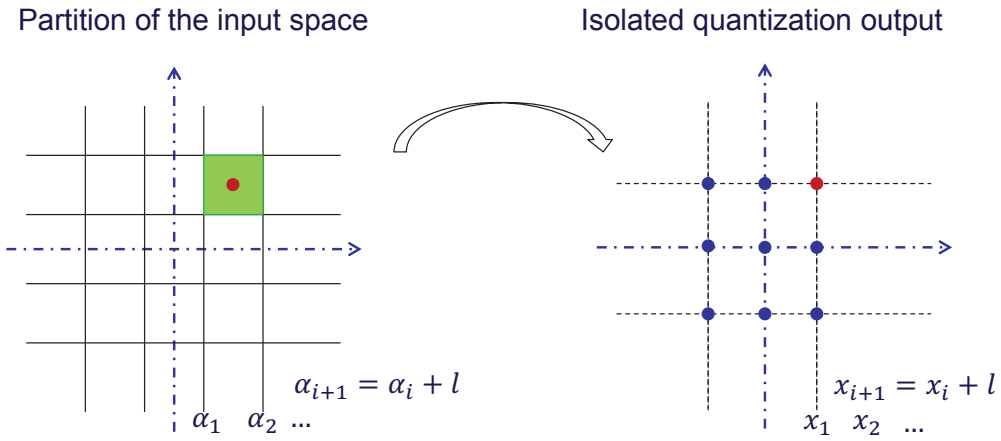

Figure 2.1: Uniform quantization function.

is bounded by

$$|x_q - x| \leq \frac{1}{2}l. \tag{2.2}$$

In the vector case, for a vector $x = [x_1, x_2, \ldots, x_n] \in \mathbb{R}^n$, we apply the quantization function defined above elementwise. This way the quantization error bound carries to the vector case. Let the quantization interval lengths be l_j, $j = 1, \ldots, n$. Then $l = \max_{j=1,\ldots,n} l_j$.

2.2 Logarithmic quantization

The logarithmic quantization is developed with the concept of minimal attention control, where the values around the equilibrium get higher resolution than the values far away from the equilibrium.

Similarly, we first introduce the scalar case logarithmic quantization. Let $Q_{\log}(\cdot)$

be the quantization function. If the input signal is $x(t)$, the quantization density is ρ, and the parameters for the quantization intervals are α_0 and x_0, the quantization function is defined by [22]

$$x_{\mathrm{q}}(t) = Q_{\log}(x(t)) = \begin{cases} x_i, & \alpha_i \le x(t) < \alpha_{i+1}, \\ 0, & x(t) = 0, \\ -x_i, & -\alpha_{i+1} \le x(t) < -\alpha_i, \end{cases} \tag{2.3}$$

where $\alpha_0 > 0$, $0 < \rho < 1$, $x_0 = \frac{2}{1+\rho}\alpha_0$, $\alpha_{i+1} = \frac{1}{\rho}\alpha_i$, $x_{i+1} = \frac{1}{\rho}x_i$, $i \in \mathcal{I}$. The concept of minimal attention control refers to the case in which the values around the equilibrium get higher resolution than the values far away from the equilibrium. The logarithmic quantization function $Q_{\log}$ is shown in Figure 2.2.

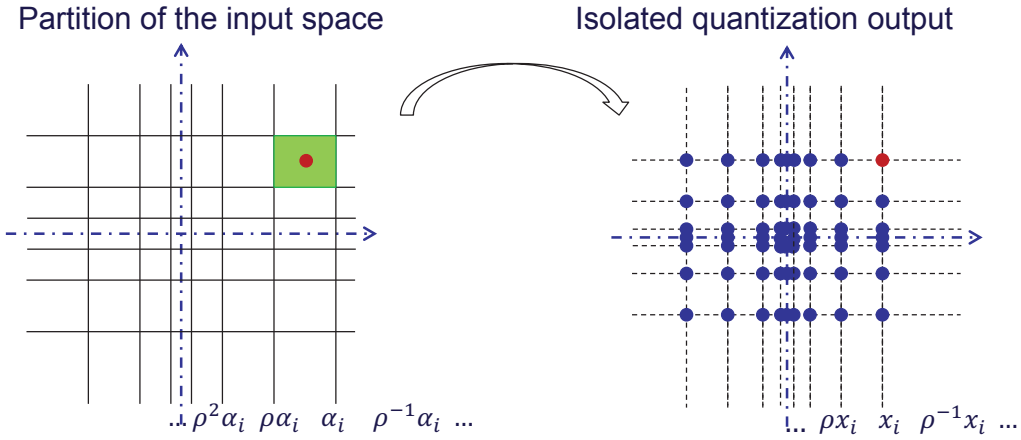

Figure 2.2: Logarithmic quantization function.

Let $M_1 \triangleq \frac{x_i}{\alpha_i} = \frac{x_0}{\alpha_0} = \frac{2}{1+\rho}$ and $M_2 \triangleq \frac{x_i}{\alpha_{i+1}} = \rho\frac{x_0}{\alpha_0} = \rho M_1$. We know from the definition in (2.3) that the quantization output follows the sector bound [9]

$$M_2|x| \le |x_{\mathrm{q}}| \le M_1|x|. \tag{2.4}$$

Let the quantization error be defined by $x_{\mathrm{qe}}(t) = x(t) - x_{\mathrm{q}}(t)$. It is bounded by

$$\begin{aligned} &(1 - M_2)|x| \le |x_{\mathrm{q}} - x| \le (M_1 - 1)|x|, \\ &|x_{\mathrm{q}} - x| \le \delta_x|x|, \quad \delta \triangleq \frac{1-\rho}{1+\rho}. \end{aligned} \tag{2.5}$$

Remark 1 *Note that δ is also a constant representing the coarseness of the quan-*

tization in addition to ρ. The variables δ and ρ have one-to-one correspondence. Thus, the logarithmic quantization can also be defined by specifying δ instead of ρ. When the quantization is finer, ρ increases, δ decreases, and when the quantizer is coarser, ρ decreases, δ increases, $0 < \rho < 1$, $0 < \delta < 1$.

The quantization error bound carries to the vector case $x(t) \in \mathbb{R}^n$. For each entry, assign a logarithmic quantizer as described above. Let the constants be δ_j, $j = 1, \ldots, n$. Then $\delta = \max_{j=1,\ldots,n} \delta_j$.

2.3 Hysteresis uniform quantization

In quantized systems, quantization introduces nonlinearity and discontinuity into the system, which can lead to undesirable switching and chattering phenomena. Hysteresis quantization is one scheme that has a memory of the past input signal and uses the signal history to avoid this phenomenon. Two typical quantization schemes are considered in the control problems formulated in later chapters: uniform and logarithmic hysteresis quantization. This section starts with the first one and the next section considers the second one.

The multi-level hysteresis quantization function is first introduced in cellular neuron networks by [10–12], and is shown to help improve the Lyapunov stability of the cellular neural networks. The discontinuity of quantized systems and the reduction of chattering phenomena with hysteresis quantization are later analyzed in [13].

The hysteresis uniform quantization is defined by a multi-valued map $Q_{h\text{unif}}(x)$ as follows:

$$Q_{h\text{unif}}(x) = \begin{cases} x_i, & \alpha_i - h \le x < \alpha_{i+1} + h, \\ 0, & -\alpha_0 - h \le x < \alpha_0 + h, \\ -x_i, & -\alpha_{i+1} - h \le x < -\alpha_i + h, \end{cases} \tag{2.6}$$

where $0 < p_h < 50\%$ is the hysteresis percentage, $h = p_h l$ is the hysteresis width constant, and $d \triangleq l + 2h$ is the quantization interval length.

The evolution of $x_{\text{q}}(t) \triangleq Q_{h\text{unif}}(x(t))$ is described as follows. At $t = 0$, $x_{\text{q}}(0) = Q_{\text{unif}}(x(0))$, where $Q_{\text{unif}}(\cdot)$ is the uniform quantization function defined

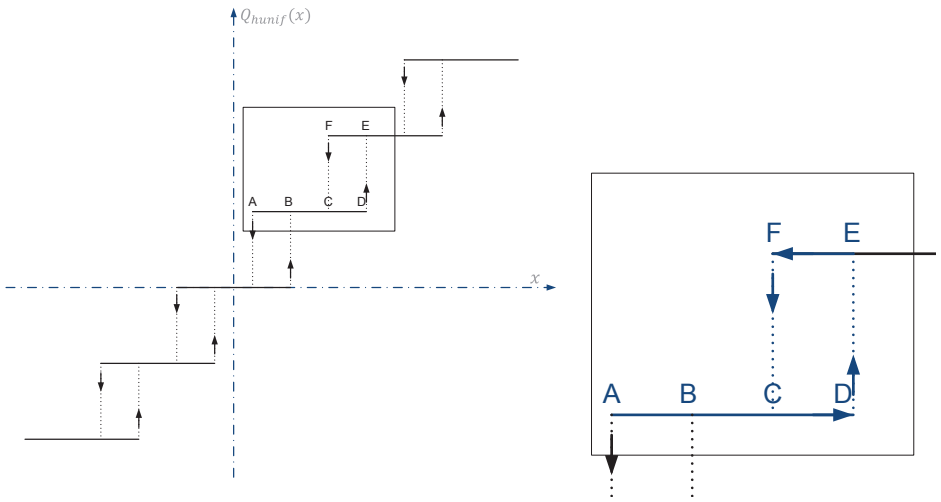

Figure 2.3: Hysteresis uniform quantization function.

in (2.1). Let $x_{\mathrm{q}}(t) \triangleq Q_{h\mathrm{unif}}(x(t))$ and $x_{\mathrm{q}}^{+} \triangleq \lim_{s\to t^{+}} Q_{h\mathrm{unif}}(x(s))$.

$$x_{\mathrm{q}}^{+} = \begin{cases} x_{\mathrm{q}}(t) + l, & x \geq x_{\mathrm{q}}(t) + \dfrac{1}{2}l + h, \\ x_{\mathrm{q}}(t) - l, & x \leq x_{\mathrm{q}}(t) - \dfrac{1}{2}l - h, \\ x_{\mathrm{q}}(t), & x_{\mathrm{q}}(t) - \dfrac{1}{2}l - h < x < x_{\mathrm{q}}(t) + \dfrac{1}{2}l + h. \end{cases}$$

The quantization error in this case is bounded by

$$|x_q - x| \leq \frac{1}{2}d. \tag{2.7}$$

In vector case, the quantized vector is obtained by applying the scalar quantization function defined above elementwise. The quantization error bound carries to the vector case. Let the quantization interval lengths be d_{xj}, $j = 1, \ldots, n$. Then $d_x = \max_{j=1,\ldots,n} d_{xj}$.

Remark 2 *The hysteresis quantization scheme is shown to reduce the chattering phenomenon. The hysteresis characteristics ensure that for the given time intervals the solution of the quantized system has finite switching times. [13].*

Remark 3 *Hysteresis characteristics prevent the quantized signal from infinitely switching at the discontinuity points, at the price of requiring more quantization levels to maintain the same error bound.*

The quantization error in the hysteresis case has an additive term h. Compare it with the classical uniform quantization, and let the quantization interval length for the classical case be l_c, and the length for the hysteresis case be $d_h = l_h + 2h$. To achieve the same upper bound of the quantization error, we need $l_c = d_h, l_h = l_c - 2h$. The hysteresis quantization needs a higher resolution. If the quantized signal is then coded and sent, the size of the source alphabet in the hysteresis case is increased to $\frac{l_c}{l_c - 2h}$ times of the classical one. For example, in [13], $h = \frac{1}{4}l_c$, the size of source alphabet is doubled.

2.4 Hysteresis logarithmic quantization

The hysteresis logarithmic quantization is defined by a multi-valued map $Q_{h\log}(x)$, as follows:

$$Q_{h\log}(x) = \begin{cases} x_i, & \alpha_i - h_i \le x < \alpha_{i+1} + h_{i+1}, \\ 0, & -\alpha_0 - h_0 \le x < \alpha_0 + h_0, \\ -x_i, & -\alpha_{i+1} - h_{i+1} \le x < -\alpha_i + h_i, \end{cases} \tag{2.8}$$

where $0 < p_h < 1$ is the hysteresis percentage, $h_0 = p_h \delta \alpha_0$, and $h_{i+1} = \frac{1}{\rho} h_i$.

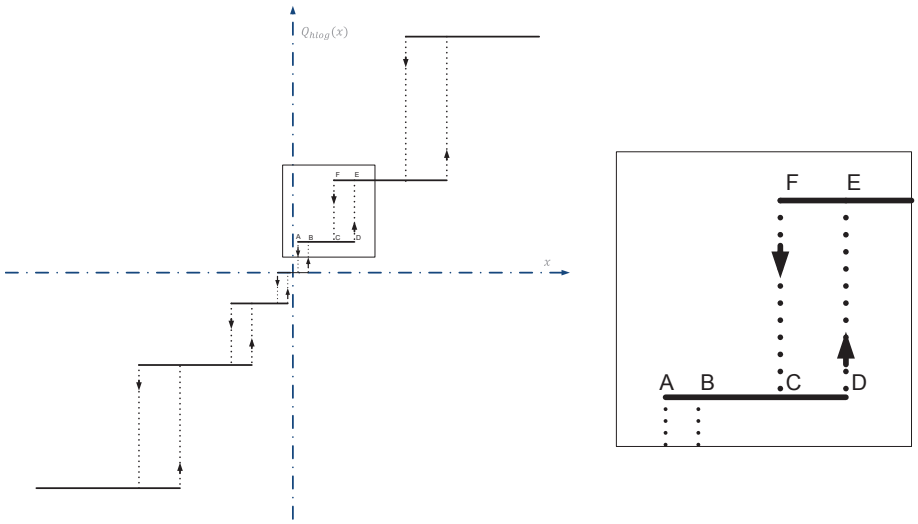

Figure 2.4: Hysteresis logarithmic quantization function.

The evolution of $x_{\mathrm{q}}(t) \triangleq Q_{h\log}(x(t))$ is described as follows. At $t = 0$, $x_{\mathrm{q}}(0) = Q_{\log}(x(0))$, where $Q_{\log}(\cdot)$ is the standard logarithmic quantization func-

tion defined in (2.3). Let $x_{\mathrm{q}}(t) \triangleq Q_{h\log}(x(t))$ and $x_{\mathrm{q}}^{+} \triangleq \lim_{s\to t^{+}} Q_{h\log}(x(s))$.

$$x_{\mathrm{q}}^{+} = \begin{cases} \dfrac{1}{\rho}x_{\mathrm{q}}(t), & x \geq \dfrac{1+\rho}{2\rho}\left(1 + p_h\dfrac{1-\rho}{\rho}\right)x_{\mathrm{q}}(t), \\ \rho x_{\mathrm{q}}(t), & x \leq \dfrac{1+\rho}{2}\left(1 - p_h\dfrac{1-\rho}{\rho}\right)x_{\mathrm{q}}(t), \\ x_{\mathrm{q}}(t), & \text{otherwise.} \end{cases}$$

The quantization error in this case is bounded by

$$|x_q - x| \leq \delta_e|x|, \quad \delta_e = \frac{\rho + p_h(1+\rho)}{\rho - p_h(1-\rho)}. \tag{2.9}$$

In the vector case, the quantized vector is obtained by applying the scalar quantization function defined above elementwise. This way the quantization error bound carries to the vector case. Let the quantization constants be δ_{ej}, $j = 1, \ldots, n$. Then $\delta_e = \max_{j=1,\ldots,n} \delta_{ej}$.

CHAPTER 3

STATE FEEDBACK CONTROL FOR INPUT-QUANTIZED SYSTEMS

"Imperfect action is better than perfect inaction." –Harry Truman

In this chapter, we consider input-quantized uncertain systems, their control design and performance evaluation problems. Due to the discontinuity introduced by quantization, the ODE that describe the system dynamics have discontinuous right-hand sides. The notions of solutions for this type of ODEs and the existence of classical solutions are worth discussing. The first part of this chapter discusses the solution of the input-quantized systems. Then the control problems are dealt with in two cases for systems with matched and unmatched uncertainties.

An input-quantized system is shown in Figure 3.1. The development proceeds as follows. The existence of a solution is motivated by a scalar linear example, and generalizes to a certain type of linear/nonlinear interconnected system. Then SISO linear uncertain systems with matched uncertainties are considered. Next, general nonlinear systems with unmatched uncertainties are considered. The controller uses the state feedback of the plant and generates the control signal $u(t)$ for the quantization block, and the quantization block generates $u_{\mathrm{q}}(t)$ and provides it to the plant.

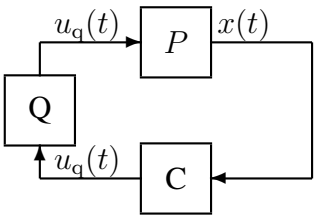

Figure 3.1: System with quantized input

3.1 Existence of solutions

We start with an example showing that when quantization is added to the loop, the existence of solution cannot be addressed by classical results.

Example 1 *Consider the linear system*

$$\dot{x}(t) = x(t) + u(t),$$

which can be stabilized by the linear feedback control $u(t) = -2x(t)$.

Consider the same linear system with the same control, and let the control loop be closed by quantization

$$\begin{aligned} \dot{x}(t) =& x(t) + Q_{\text{unif}}(u(t)) \\ =& x(t) - Q_{\text{unif}}(2x(t)). \end{aligned} \tag{3.1}$$

Let the right hand side be $f(x) \triangleq x(t) - Q_{\text{unif}}(2x(t))$*, and the constants used in quantization function be* $\alpha_0 = \frac{1}{2}l$*. If the system starts from the discontinuity point* $x_o = \frac{1}{4}l$*, there does not exist a Carathéodory solution.*

Suppose there is a Carathéodory solution. Assume the solution leaves x_o *in the direction of increasing* x*. Then* $f(t, x_o^+) \triangleq \lim_{x \searrow x_o} f(t, x) = -\frac{3}{4}l < 0$*. In another case, assume the solution leaves* x_o *in the direction of decreasing* x*. Then* $f(t, x_o^-) \triangleq \lim_{x \nearrow x_o} f(t, x) = \frac{1}{4}l > 0$*. In the third case, assume the solution stays at* x_o*. Then* $f(t, x_o) = -\frac{3}{4}l \neq 0$*. Thus in all possible cases the solution violates* (3.1)*, and there does not exist a Carathéodory solution.*

After the example showing possible existence problem of the classical solutions to input-quantized systems, we introduce several solution notions for the differential equation

$$\dot{x} = f(t, x), \quad x(0) = x_o, \tag{3.2}$$

where $x(t) \in \mathbb{R}^n$ and the function $f : \mathbb{R} \times \mathbb{R}^n \to \mathbb{R}^n$ is assumed to be piecewise continuous in t.

Before the definitions, we introduce the following notations. Let $J_T \triangleq [0, T)$ be a time interval of length T; $B_\delta(x_o) \triangleq \{x : \|x - x_o\| < \delta\}$ be the open ball of radius δ at x_o; $\bar{S}$ be the closure of a set S; and $\text{cvx}S$ be the convex hull of the set S.

Definition 1 ([23]) *A function* $\phi(t) : J_T \to \mathbb{R}^n$ *is a Carathéodory solution of*

(3.2)*, if* $x(0) = x_o$*,* $x(t)$ *is absolutely continuous on each compact subinterval of* J_T*, and*

$$\dot{\phi}(t) = f(t, \phi(t))$$

is satisfied almost everywhere on J_T*.*

The existence and uniqueness of classical solutions follows from the Lipschitz continuity of the right hand side and is provided by the Picard-Lindelöf Theorem [24, 25]. However, when the right-hand side of (3.2) is not continuous in x, this standard result is no longer applicable and the classical definition of the solution is insufficient. A more general definition is introduced by A. F. Filippov [26, 27].

Next, we first introduce a more general definition of solutions to ODEs, with which a more general class of ODEs with discontinuous right-hand sides have solutions, and then show that a certain type of input-quantized systems have Filippov solutions that coincide with Carathéodory solutions.

Definition 2 ([23]) *A function* $\phi(t) : J_T \to \mathbb{R}^n$ *is a Filippov solution of* (3.2)*, if* $x(0) = x_o$*,* $x(t)$ *is absolutely continuous on each compact subinterval of* J_T*, and*

$$\dot{\phi}(t) \in \mathscr{F}[f(t, \phi(t))]$$

is satisfied a.e. on $[0, T)$*, where*

$$\mathscr{F}[f(t,x)] = \cap_{\delta>0} \cap_{N:\mu(N)=0} \overline{\text{cvx}} f(t, B_\delta(x) - N),$$

where μ *is the Lebesgue measure.*

Consider a partially quantized interconnected system with the structure given by

$$\dot{\boldsymbol{x}} = \boldsymbol{f}(x, s), \tag{3.3}$$

where the state consists of two parts $x \in \mathbb{R}^n$, $s \in \mathbb{R}^m$, and the dynamics take the following form

$$\boldsymbol{x} = \begin{bmatrix} x \\ s \end{bmatrix}, \ \boldsymbol{f} = \begin{bmatrix} f_x(x, Q(s)) \\ f_s(x, s) \end{bmatrix},$$

where $f_x : \mathbb{R}^{n+m} \to \mathbb{R}^n$, $f_s : \mathbb{R}^{n+m} \to \mathbb{R}^m$ are Lipschitz continuous functions and $Q : \mathbb{R}^m \to \mathbb{R}^m$ is a quantization function. The x-dynamics depend on the quantized state s, while the s-dynamics depend on the states directly.

The discontinuities happen on the switching surface $\Gamma_{ki} \triangleq \{x : \xi_{ki}(\boldsymbol{x}) \triangleq s_k - \alpha_{ki} = 0\}$. When $\boldsymbol{x}$ approaches some point $\boldsymbol{x}^* = [x^* \ \alpha_i]^\top$ on the hyperplane $s_k = \alpha_{ki}$, let the function $\boldsymbol{f}(x, s)$ have limiting values

$$\boldsymbol{f}(x^*, s_1, \ldots, s_{k-1}, \alpha_{ki}^+, s_{k+1}, \ldots, s_m) \triangleq \boldsymbol{f}(x^*, s_{-i}, \alpha_{ki}^+) \triangleq \lim_{\substack{x \to x^* \\ s \searrow \alpha_{ki}}} \boldsymbol{f}(x, s),$$

$$\boldsymbol{f}(x^*, s_1, \ldots, s_{k-1}, \alpha_{ki}^-, s_{k+1}, \ldots, s_m) \triangleq \boldsymbol{f}(x^*, s_{-i}, \alpha_{ki}^-) \triangleq \lim_{\substack{x \to x^* \\ s \nearrow \alpha_{ki}}} \boldsymbol{f}(x, s).$$

The switching surface Γ_i has a normal vector $\nabla \xi_{ki}$. Note that

$$\langle \nabla \xi_{ki}, \boldsymbol{f}(x^*, s_{-i}, \alpha_{ki}^+) \rangle = f(x^*, \alpha_i) = \langle \nabla \xi_{ki}, \boldsymbol{f}(x^*, s_{-i}, \alpha_{ki}^-) \rangle$$

The vectors $\boldsymbol{f}(x^*, \alpha_i^+)$ and $\boldsymbol{f}(x^*, \alpha_i^-)$ lie on one side of the switching surface. The dynamic behavior on the surface is referred to as regular switching motion and the solution passes from one side of the plane to the other [27, 28].

Similar arguments hold for other switching surfaces. Then there exists a Carathéodory solution, which is equivalent to the Fillipov solution [23, 27, 28].

Remark 4 *Let s be the state of the controller; $f_s(x, s) = A_c s + B_c \eta(x)$ be a linear function on a state-dependent signal $\eta(x)$; and the quadruple $(A_c, B_c, \mathbb{I}, 0)$ be a state-space model of a low-pass filter. The dynamics in* (3.3) *become:*

$$\begin{aligned} \dot{x} =& f(x, Q(s)) \\ \dot{s} =& A_c s + B_c \eta(x). \end{aligned}$$

It is a closed-loop system with filtered and quantized input. According to the previous discussion, there exists a Carathéodory solution.

3.2 Input-quantized systems with matched uncertainties

In the following four sections, we consider the system with linear matched uncertainties as follows:

$$\begin{aligned}\dot{x}(t) =& A_m x(t) + b\left(-\theta^\top x(t) + u_{\mathrm{q}}(t)\right),\\ y(t) =& c^\top x(t), \quad x(0) = x_0,\\ u_{\mathrm{q}}(t) =& Q(u_{\mathrm{q}}(t)),\end{aligned} \tag{3.4}$$

where A_m is a known $n \times n$ Hurwitz matrix, $b, c \in \mathbb{R}^n$ are known constant vectors, $\theta \in \mathbb{R}^n$ is an unknown constant vector, $x(t) \in \mathbb{R}^n$ is the system state vector (measured), $y(t) \in \mathbb{R}$ is the regulated output, $u(t)$ is the designed control signal, and $Q(\cdot)$ is the quantization function.

Assumption 1 *The unknown parameter θ belongs to a given compact convex set Θ_B, $\theta \in \Theta_B$. Let $\theta_{1\max} \triangleq \max_{\theta\in\Theta_B} \|\theta\|_1$.*

The objective is to design an adaptive controller that would compensate for the uncertainties in the system and ensure analytically quantifiable uniform transient and steady-state performance bounds in the presence of input quantization.

3.3 Control design

In this section we present the $\mathcal{L}_1$ adaptive controller for the system in (3.4). The $\mathcal{L}_1$ adaptive controller consists of a state predictor, an adaptive law and a control law. For the linearly parameterized system in (3.4), we consider the following state predictor:

$$\begin{aligned}\dot{\hat{x}}(t) =& A_m \hat{x}(t) + b\left(-\hat{\theta}^\top(t) x(t) + u_{\mathrm{q}}(t)\right)\\ \hat{y}(t) =& c^\top \hat{x}(t), \quad \hat{x}(0) = x_0,\end{aligned} \tag{3.5}$$

where $\hat{x}(t) \in \mathbb{R}^n$, $\hat{y}(t) \in \mathbb{R}$ are the state and the output of the state predictor and $\hat{\theta}(t) \in \mathbb{R}^n$ is an estimate of the parameter θ. The projection-type adaptive law for

$\hat{\theta}(t)$ is given by

$$\dot{\hat{\theta}}(t) = \Gamma \mathrm{Proj}(\hat{\theta}(t), x(t)\tilde{x}^\top(t)Pb),\ \hat{\theta}(0) = \hat{\theta}_0, \tag{3.6}$$

where $\tilde{x}(t) \triangleq \hat{x}(t) - x(t)$ is the prediction error, $\Gamma > 0$ is the adaptation rate, $\mathrm{Proj}(\cdot,\cdot)$ denotes the projection operator (Definition 3 [29]), which ensures that $\hat{\theta}(t) \in \Theta_B$ for all $t \geq 0$, and $P = P^\top > 0$ solves the algebraic Lyapunov equation $A_m^\top P + PA_m = -Q$ for some symmetric $Q > 0$.

The control signal is defined by

$$u(s) = C(s)\left(\hat{\eta}(s) + k_g r(s)\right), \tag{3.7}$$

where $k_g \triangleq 1/(c^\top H(0))$, $H(s) \triangleq (s\mathbb{I} - A_m)^{-1}b$, $\hat{\eta}(t) \triangleq \hat{\theta}^\top(t)x(t)$, while $C(s)$ is a BIBO stable and strictly proper transfer function with DC gain $C(0) = 1$, and its state-space realization assumes zero initialization. Let

$$G(s) \triangleq H(s)(C(s) - 1). \tag{3.8}$$

The $\mathcal{L}_1$ adaptive controller consists of (3.5), (3.6) and (3.7), with $C(s)$ verifying the following upper bound for the $\mathcal{L}_1$ norm of $G(s)$

$$\lambda \triangleq \|G(s)\|_{\mathcal{L}_1}\theta_{1\max} < 1. \tag{3.9}$$

3.4 Performance analysis

We first introduce the reference system and analyze its stability, and then show that the input and the output signals of the closed-loop system track those of the reference system with uniform transient and steady-state performance bounds.

3.4.1 Stability of reference system

Consider the reference system

$$\begin{aligned} \dot{x}_{\mathrm{ref}}(t) =& A_m x_{\mathrm{ref}}(t) + b\left(-\theta^\top x_{\mathrm{ref}}(t) + u_{\mathrm{ref}}(t)\right) \\ y_{\mathrm{ref}}(t) =& c^\top x_{\mathrm{ref}}(t), \quad x_{\mathrm{ref}}(0) = x_0, \end{aligned} \tag{3.10}$$

with the following reference controller:

$$u_{\rm ref}(s) = C(s)\left(\theta^\top x_{\rm ref}(s) + k_g r(s)\right) . \tag{3.11}$$

We notice that in the absence of $C(s)$ this reference controller reduces to the nominal controller of model reference adaptive control architecture (MRAC), by perfectly canceling the uncertainties. Since in the presence of $C(s)$ it only partially cancels the uncertainties, we need first to prove that this reference system is stable.

Substituting (3.11) into (3.10), we have

$$\begin{aligned} x_{\rm ref}(s) &= H(s)k_g C(s)r(s) + G(s)\theta^\top x_{\rm ref}(s) + (s\mathbb{I} - A_m)^{-1}x_0 \,, \\ x_{\rm ref}(s) &= (\mathbb{I} - G(s)\theta^\top)^{-1}[H(s)C(s)k_g r(s) + (s\mathbb{I} - A_m)^{-1}x_0]. \end{aligned} \tag{3.12}$$

Lemma 1 ([21]) *If the condition in (3.9) holds, then* $(\mathbb{I} - G(s)\theta^\top)^{-1}$ *and* $(\mathbb{I} - G(s)\theta^\top)^{-1}G(s)$ *are BIBO stable.*

Then (3.12) leads to the following bound on $x_{\rm ref}(t)$:

$$\begin{aligned} \|x_{\rm ref}\|_{\mathcal{L}_\infty} \leq & k_g \|(\mathbb{I} - G(s)\theta^\top)^{-1}H(s)C(s)\|_{\mathcal{L}_1}\|r\|_{\mathcal{L}_\infty} \\ & + \|(\mathbb{I} - G(s)\theta^\top)^{-1}\|_{\mathcal{L}_1}\|(s\mathbb{I} - A_m)^{-1}x_0\|_{\mathcal{L}_\infty}. \end{aligned} \tag{3.13}$$

Since $u_{\rm ref}(s) = C(s)\left(\theta^\top x_{\rm ref}(s) + k_g r(s)\right)$, we have

$$\|u_{\rm ref}\|_{\mathcal{L}_\infty} \leq \|C(s)\theta^\top\|_{\mathcal{L}_1}\|x_{\rm ref}\|_{\mathcal{L}_\infty} + k_g\|r\|_{\mathcal{L}_\infty}. \tag{3.14}$$

3.4.2 Prediction error

Let $\tilde{x}(t) \triangleq \hat{x}(t) - x(t)$, and $\tilde{\theta}(t) \triangleq \hat{\theta}(t) - \theta$. From (3.4) and (3.5), we have the prediction error dynamics

$$\dot{\tilde{x}}(t) = A_m\tilde{x}(t) - b\tilde{\theta}^\top(t)x(t)\,, \quad \tilde{x}(0) = 0\,. \tag{3.15}$$

Lemma 2 ([21]) *For the system in (3.4) and the controller defined by (3.7), we have the following uniform bound*

$$\|\tilde{x}\|_{\mathcal{L}_\infty} \leq \sqrt{\frac{\theta_{2\max}}{\lambda_{\min}(P)\Gamma}}, \quad \theta_{2\max} \triangleq 4\max_{\theta\in\Theta_B}\|\theta\|_2^2,\ \forall t \geq 0,$$

and asymptotic convergence

$$\lim_{t\to\infty} \tilde{x}(t) = 0.$$

3.4.3 Tracking error

First we introduce several notations. Let $e_x(t) = x(t) - x_{\rm ref}(t)$, $e_u(t) = u_{\rm q}(t) - u_{\rm ref}(t)$, $u_{qe}(t) = u_{\rm q}(t) - u(t)$.

Since (A_m, b) is controllable, and $H(s)$ is strictly proper and stable, there exists $c_o \in \mathbb{R}^n$ such that $c_o^\top H(s)$ is minimum phase with relative degree one (by Lemma 4 in [21]).

Lemma 3 *Consider the system in (3.4) and the controller in (3.7). We have*

$$\begin{aligned}\|e_{x_\tau}\|_{\mathcal{L}_\infty} \leq & \|(\mathbb{I} - G(s)\theta^\top)^{-1}[G(s)\theta^\top + (C(s)-1)\mathbb{I}]\|_{\mathcal{L}_1} \|\tilde{x}_\tau\|_{\mathcal{L}_\infty} \\ & + \left\| \left(\left(\mathbb{I} - G(s)\theta^\top\right)^{-1} H(s) u_{qe} \right)_\tau \right\|_{\mathcal{L}_\infty}, \qquad (3.16) \\ \|e_{u_\tau}\|_{\mathcal{L}_\infty} \leq & \left\| C(s) \frac{1}{c_o^\top H(s)} c_o^\top \right\|_{\mathcal{L}_1} \|\tilde{x}_\tau\|_{\mathcal{L}_\infty} + \|C(s)\theta^\top\|_{\mathcal{L}_1} \|e_{x_\tau}\|_{\mathcal{L}_\infty} + \|u_{qe_\tau}\|_{\mathcal{L}_\infty}. \qquad (3.17)\end{aligned}$$

Proof. See Appendix B.1.

3.4.4 Uniform quantization

As introduced in Section 2.1, the error introduced by a uniform quantization function is bounded by a constant. Together with the analysis in Lemma 3, we have the following theorem.

Theorem 1 *For the system in (3.4) with uniform quantization as defined in Section 2.1 and the controller in (3.7), we have*

$$\|e_x\|_{\mathcal{L}_\infty} \leq \gamma_{xu}, \quad \|e_u\|_{\mathcal{L}_\infty} \leq \gamma_{uu}, \qquad (3.18)$$

where

$$\gamma_{xu} = \frac{1}{2} l \left\| \left(\mathbb{I} - G(s)\theta^\top\right)^{-1} H(s) \right\|_{\mathcal{L}_1} + \|(\mathbb{I} - G(s)\theta^\top)^{-1}[G(s)\theta^\top + (C(s)-1)\mathbb{I}]\|_{\mathcal{L}_1} \sqrt{\frac{\theta_{2\max}}{\lambda_{\min}(P)\Gamma}},$$

$$\gamma_{uu} = \left\| C(s) \frac{1}{c_o^\top H(s)} c_o^\top \right\|_{\mathcal{L}_1} \sqrt{\frac{\theta_{2\max}}{\lambda_{\min}(P)\Gamma}} + \|C(s)\theta^\top\|_{\mathcal{L}_1} \gamma_{xu} + \frac{1}{2} l \,.$$

Proof. By substituting (2.2) into (3.16) in Lemma 3, we have $\|e_{x_\tau}\|_{\mathcal{L}_\infty} \leq \gamma_{xu}$. Since γ_{xu} is uniform over all $\tau \in (0, \infty)$, we have $\|e_x\|_{\mathcal{L}_\infty} \leq \gamma_{xu}$.

Similarly, we substitute (3.18) and (2.2) into (3.17) in Lemma 3 to get $\|e_{u_\tau}\|_{\mathcal{L}_\infty} \leq \gamma_{uu}$. Since the right hand side is uniform over all $\tau \in (0, \infty)$, we have the first bound in (3.18). □

Remark 5 *From Theorem 1, we note that the error bound B_{unif} has two terms. The first term can be made arbitrarily small by increasing the adaptation rate Γ. The second one decreases as the interval length l decreases, i.e., as the quantizer gets finer. As l goes to zero, the second term goes to zero, and the error bound reduces to the case without quantization [20, 21].*

Remark 6 *In* (3.18), $\left\| C(s) \frac{1}{c_o^\top H(s)} c_o^\top \right\|_{\mathcal{L}_1}$ *needs to be bounded for $e_u(t)$ to be bounded. This is ensured by the strictly proper low pass filter $C(s)$. In the case when $C(s) = 1$, which corresponds to the MRAC, $\left\| C(s) \frac{1}{c_o^\top H(s)} c_o^\top \right\|_{\mathcal{L}_1}$ is unbounded, since $c_o^\top H(s)$ in the denominator is strictly proper. In this case, we have $\gamma_{uu} \to \infty$, implying that one cannot obtain a similar uniform bound for the control signal of MRAC.*

For the logarithmic quantization, $C(s)$ is also crucial for the same arguments.

Remark 7 *We notice that the matrix A_m in* (3.4) *is Hurwitz. The presented solution in this paper can be generalized to any matrix A, as long as (A, b) is controllable. There are two methods to analyze this new system. On one hand, since (A, b) is controllable, there exists $k \in \mathbb{R}^n$, such that $A_m = A + bk^\top$. Then, one can introduce $\theta_{new} = k + \theta$, and the system will assume the same form as in* (3.4). *On the other hand, one can design $u_{new}(t) = u(t) + k^\top x(t)$ and proceed with similar derivations. The linear part $k^\top x(t)$ will not affect the performance bounds for uniform quantization, but will add additional conditions and change the bounds for logarithmic quantization.*

Remark 8 *From* (3.14) *and* (3.18)*, we know both* $\|u_{\text{ref}}\|_{\mathcal{L}_\infty}$ *and* $\|e_u\|_{\mathcal{L}_\infty}$ *are bounded. Further,*

$$\begin{aligned}\|u\|_{\mathcal{L}_\infty} \leq & \|u_{\text{ref}}\|_{\mathcal{L}_\infty} + \|e_u\|_{\mathcal{L}_\infty} \leq \rho_{u_r} + \gamma_{uu}\,,\\ \rho_{u_r} = & \|C(s)\theta^\top\|_{\mathcal{L}_1}\rho_{x_r} + k_g\|r\|_{\mathcal{L}_\infty}\,,\\ \rho_{x_r} = & k_g\|(\mathbb{I} - G(s)\theta^\top)^{-1}H(s)C(s)\|_{\mathcal{L}_1}\|r\|_{\mathcal{L}_\infty}\\ & + \|(\mathbb{I} - G(s)\theta^\top)^{-1}\|_{\mathcal{L}_1}\|(s\mathbb{I} - A_m)^{-1}x_0\|_{\mathcal{L}_\infty}\,.\end{aligned}$$

We know the range of the control $u(t)$*, and the number of quantization intervals we may use. Hence, using this uniform quantization, the required number of bits for a control signal is*

$$n_{uni} = \log\left(\frac{1}{l}(\rho_{u_r} + \gamma_{uu})\right).$$

3.4.5 Logarithmic quantization

For the system with logarithmic quantization, we have the following performance bounds.

Theorem 2 *For the system in (3.4) with logarithmic quantizer and the controller in (3.7), when*

$$\Delta < \frac{1}{\left\|(\mathbb{I} - G(s)\theta^\top)^{-1}H(s)\right\|_{\mathcal{L}_1}\|C(s)\|_{\mathcal{L}_1}\theta_{1\max}},$$

we have

$$\begin{aligned}\|e_x\|_{\mathcal{L}_\infty} \leq & \gamma_{xl}\,, \qquad (3.19)\\ \gamma_{xl} = & \frac{1}{1 - \left\|(\mathbb{I} - G(s)\theta^\top)^{-1}H(s)\right\|_{\mathcal{L}_1}\Delta\|C(s)\|_{\mathcal{L}_1}\theta_{1\max}}\\ & \Big(\|\left(\mathbb{I} - G(s)\theta^\top\right)^{-1}[G(s)\theta^\top + (C(s)-1)\mathbb{I}]\|_{\mathcal{L}_1}\sqrt{\tfrac{\theta_{2\max}}{\lambda_{\min}(P)\Gamma}}\\ & + \Delta(\mathbb{I} - G(s)\theta^\top)^{-1}H(s)\|_{\mathcal{L}_1}\|C(s)\|_{\mathcal{L}_1}(\theta_{1\max}\rho_{x_r} + k_g\|r\|_{\mathcal{L}_\infty})\Big),\\ \rho_{x_r} = & k_g\|(\mathbb{I} - G(s)\theta^\top)^{-1}H(s)C(s)\|_{\mathcal{L}_1}\|r\|_{\mathcal{L}_\infty}\\ & + \|(\mathbb{I} - G(s)\theta^\top)^{-1}\|_{\mathcal{L}_1}\|(s\mathbb{I} - A_m)^{-1}x_0\|_{\mathcal{L}_\infty}\,,\end{aligned}$$

and

$$\|e_u\|_{\mathcal{L}_\infty} \leq \left\| C(s)\frac{1}{c_o^\top H(s)}c_o^\top \right\|_{\mathcal{L}_1} \sqrt{\frac{\theta_{2\max}}{\lambda_{\min}(P)\Gamma}} + \Delta\theta_{1\max}\|C(s)\|_{\mathcal{L}_1}\rho_{x_r} + \Delta\|C(s)\|_{\mathcal{L}_1}k_g\|r\|_{\mathcal{L}_\infty} + \left(\|C(s)\theta^\top\|_{\mathcal{L}_1} + \Delta\theta_{1\max}\|C(s)\|_{\mathcal{L}_1}\right)\gamma_{xl}\,. \tag{3.20}$$

Proof. See Appendix B.2.

Remark 9 *In Theorem 2, for any fixed Δ, the first term of γ_{xl} decreases as the adaptation rate Γ increases. Also, γ_{xl} decreases as Δ decreases, i.e., as the quantizer gets finer. Since the terms multiplying Δ are constants, then as Δ goes to zero, the error bound γ_{xl} reduces to the one in [21]. The same arguments hold for the control bound $\|e_u\|_{\mathcal{L}_\infty}$.*

Remark 10 *In the absence of quantization, one can prove that the $\mathcal{L}_1$ adaptive controller ensures also asymptotic tracking of constant $r(t)$ ([21], Theorem 2 and Lemma 6). Since the obtained performance bounds are decoupled into two terms, one of which is identical to the bounds in [21] and the other is linear in the quantization parameter, then as the quantizer gets finer, one recovers the asymptotic properties of the $\mathcal{L}_1$ adaptive controller.*

3.5 Simulation

Consider the system in (3.4) with

$$A_m = \begin{bmatrix} 0 & 1 \\ -1 & -1.4 \end{bmatrix}, b = \begin{bmatrix} 0 \\ 1 \end{bmatrix}, c = \begin{bmatrix} 1 \\ 0 \end{bmatrix}, x_0 = \begin{bmatrix} 1 \\ 1 \end{bmatrix}, \theta = \begin{bmatrix} 4 \\ -4.5 \end{bmatrix}, \tag{3.21}$$

and let $\Theta_B = \{\theta_1 \in [-10, 10], \theta_2 \in [-10, 10]\}$, which gives $\theta_{1\max} = 20$. Letting the low pass filter be $C(s) = \frac{\omega}{s+\omega}$, we plot $\lambda = \|G(s)\|_{\mathcal{L}_1}\theta_{1\max}$ with respect to ω in Figure 3.2. Notice that for $\omega > 30$, we have $\lambda < 1$. The $\mathcal{L}_1$ adaptive controller is designed with $C(s) = \frac{160}{s+160}$, which leads to $\lambda = 0.1725 < 1$, and let the adaptation rate be $\Gamma = 10^5$. We now show the performance of $\mathcal{L}_1$ adaptive controller for both kinds of quantizers under different reference signals without any retuning of the controller.

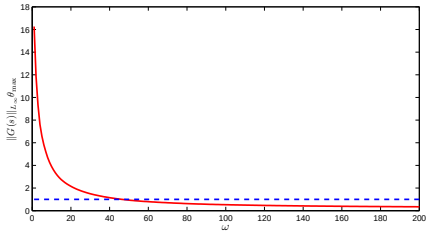

Figure 3.2: λ with respect to ω and constant 1.

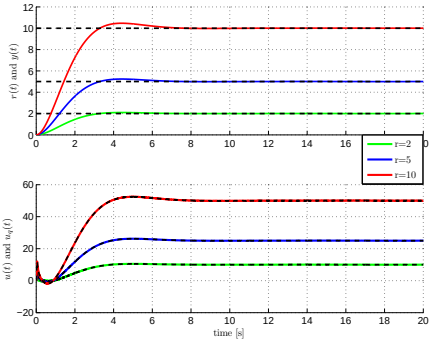

Figure 3.3: $y(t)$ and $u(t)$ for uniform quantizer with $l = 0.1$ and step references $r(t) = 2\,, 5\,, 10$.

Figure 3.3 shows the performance of system output $y(t)$ and input $u_{\mathrm{q}}(t)$ for uniform quantizer with quantization interval $l = 0.1$ and step references $r = 2\,, 5\,, 10$. We note that it leads to scaled control inputs and system outputs for scaled reference inputs. Increasing the quantization interval to $l = 1$, with the same scaled step references, the performance degradation is shown in Figure 3.4.

We can see that the coarse quantizer results in high frequency oscillation in the control input $u_{\mathrm{q}}(t)$ and in the tracking error $y(t)$, but the system still has the scaled characteristics typical for $\mathcal{L}_1$ adaptive controller. This type of performance degradation is expected from the performance bounds. Figure 3.5 shows that with the same coarse uniform quantizer ($l = 1$), but with sinusoidal reference signal $r(t) = 20\sin(0.2t)$, the tracking performance is reasonably good, and there is no high frequency oscillation in the control input.

Figures 3.6-3.8 show similar phenomena for the logarithmic quantizer without any retuning of the $\mathcal{L}_1$ controller. The quantization constants for the 3 cases are $\Delta = 0.005$, $\Delta = 0.01$ and $\Delta = 0.01$, respectively.

We finally notice that we do not redesign or retune the $\mathcal{L}_1$ controller in these

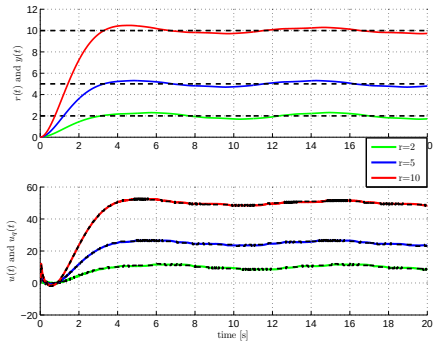

Figure 3.4: $y(t)$ and $u(t)$ for uniform quantizer with $l = 1$ and step references $r(t) = 2\,, 5\,, 10$.

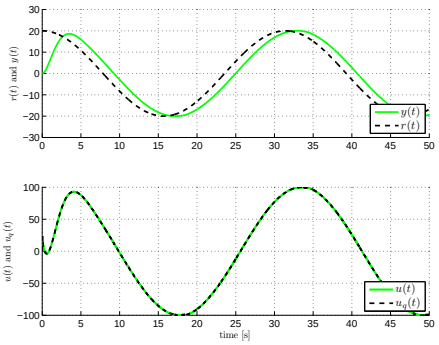

Figure 3.5: $y(t)$ and $u(t)$ for uniform quantizer with $l = 1$ and sinusoidal references $r(t) = 20\sin(0.2t)$.

simulations, from one reference input to another, or from one quantizer to the other.

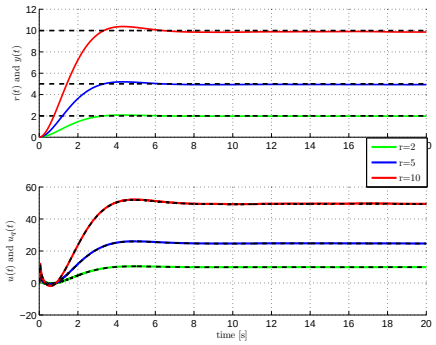

Figure 3.6: $y(t)$ and $u(t)$ for logarithmic quantizer with $\Delta = 0.005$ and step references $r(t) = 2\,, 5\,, 10$.

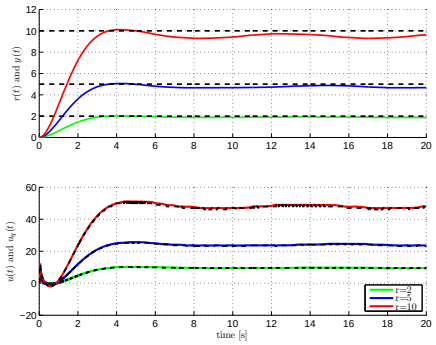

Figure 3.7: $y(t)$ and $u(t)$ for logarithmic quantizer with $\Delta = 0.01$ and step references $r(t) = 2\,, 5\,, 10$.

3.6 Input-quantized systems with unmatched uncertainties

In Sections 3.6-3.9, we consider a general input-quantized nonlinear uncertain system, without any matched assumptions on the uncertainty. We recall the system diagram shown in Figure 3.1 in the beginning of this chapter, the $\mathcal{L}_1$ adaptive controller uses state feedback to generate $u(t)$. The quantized output is $u_{\rm q}(t)$, which controls the plant.

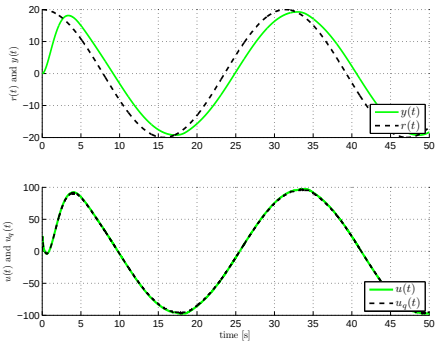

Figure 3.8: $y(t)$ and $u(t)$ for logarithmic quantizer with $\Delta = 0.01$ and sinusoidal references $r(t) = 20\sin(0.2t)$.

Let the system dynamics be described by

$$\begin{aligned}
\dot{x}(t) &= A_m x(t) + B_m \omega u_{\mathrm{q}}(t) + f(x(t), z(t), t)\,, \quad x(0) = x_0\,,\\
\dot{x}_z(t) &= g\left(x_z(t), x(t), t\right)\,, \quad x_z(0) = x_{z0}\,,\\
y(t) &= Cx(t)\,, \quad z(t) = g_o\left(x_z(t), t\right)\,, \quad u_{\mathrm{q}}(t) = Q(u(t))\,,
\end{aligned} \tag{3.22}$$

where $x(t) \in \mathbb{R}^n$ is the system state vector (measured); $u_{\mathrm{q}}(t) \in \mathbb{R}^m$ ($n \geq m$) is the quantized control signal; $y(t) \in \mathbb{R}^m$ is the regulated output; A_m is a known Hurwitz $n \times n$ matrix; $B_m \in \mathbb{R}^{n\times m}$ and $C \in \mathbb{R}^{m\times n}$ are known constant matrices; $\omega \in \mathbb{R}^{m\times m}$ is the unknown high-frequency gain matrix; $z(t)$ and $x_z(t)$ are the output and the state vector of internal unmodeled dynamics; $f(\cdot)$ $g_o(\cdot)$, and $g(\cdot)$ are unknown nonlinear functions, Lipschitz continuous in x, z, x_z, continuous in t; $u(t)$ is the designed control signal, and $Q(\cdot)$ is the quantization function. The initial condition x_0 is assumed to be inside a known set, i.e., $\|x_0\|_\infty \leq \rho_0$ with known $\rho_0 > 0$.

We can rewrite the system in (3.22) as

$$\begin{aligned}
\dot{x}(t) =& A_m x(t) + B_m\left(\omega u_{\mathrm{q}}(t) + f_1(x(t), z(t), t)\right) + B_{um} f_2(x(t), z(t), t)\,,\\
\dot{x}_z(t) =& g\left(x_z(t), x(t), t\right)\,, \quad x(0) = x_0\,, \quad x_z(0) = x_{z0}\,,\\
y(t) =& Cx(t)\,, \quad z(t) = g_o\left(x_z(t), t\right)\,, \quad u_{\mathrm{q}}(t) = Q(u(t))\,,
\end{aligned} \tag{3.23}$$

where $B_{um} \in \mathbb{R}^{n\times(n-m)}$ is a constant matrix such that

$$B_m^\top B_{um} = 0, \quad \mathrm{rank}([B_m\ B_{um}]) = n;$$

and $f_1(\cdot)$, $f_2(\cdot)$, are unknown nonlinear functions, such that

$$\begin{bmatrix} f_1(x(t), z(t), t) \\ f_2(x(t), z(t), t) \end{bmatrix} = \begin{bmatrix} B_m & B_{um} \end{bmatrix}^{-1} f(x(t), z(t), t)\,.$$

Here $f_1(\cdot)$ represents the matched part of the uncertainties, whereas $B_{um} f_2(\cdot)$ represents the unmatched part (cross-coupling dynamics).

As in the case without quantization [20, 30], we introduce the following assumptions. Let $X(t) = [x^\top(t)\ z^\top(t)]$.

Assumption 2 (Uniform boundedness of $f_i(0,t)$) *There exists $B_{10} > 0$ and $B_{20} > 0$, such that the following bound holds uniformly in t: $\|f_i(0,t)\| \leq B_{i0}, i = 1, 2$.*

Assumption 3 (Semiglobal uniform boundedness of partial derivatives) *For $i = 1, 2$, and any $\nu > 0$, there exist $d_{f_{xi}}(\nu)$ and $d_{f_{ti}}(\nu) > 0$ such that, for any $\|X(t)\|_\infty < \nu$, the partial derivatives of $f_i(X,t)$ are piecewise continuous and bounded:*

$$\left\| \frac{\partial f_i(X,t)}{\partial X} \right\|_\infty \leq d_{f_{xi}}(\nu), \quad \left\| \frac{\partial f_i(X,t)}{\partial t} \right\|_\infty \leq d_{f_{ti}}(\nu),$$

where the first norm is the induced infinity norm of a matrix, while the second is the infinity norm of a vector.

Remark 11 *Assumptions 2 and 3 are fairly mild assumptions on the system dynamics and can be verified for sufficiently broad classes of systems. These assumptions are related to the nature of proofs of $\mathcal{L}_1$ adaptive control architecture and are not due to the quantization schemes. In [30], where an alternative piecewise constant adaptive law is considered for the same $\mathcal{L}_1$ architecture, Assumption 3 is relaxed. Consequently, the proofs of quantization with those adaptive laws will also use less restrictive assumptions.*

Assumption 4 (Conservative knowledge of the high-frequency gain matrix) *The high-frequency gain matrix ω is assumed to be an unknown (nonsingular) strictly row-diagonally dominant matrix with $\mathrm{sgn}(\omega_{ii})$ known. Also, we assume that there exists a known compact set Ω, such that $\omega \in \Omega \subset \mathbb{R}^{m \times m}$.*

Assumption 5 (Stability of internal dynamics) [1] *The x_z-dynamics are BIBO stable both with respect to initial condition x_{z0} and input $x(\cdot)$, i.e. there exist L_z, $B_z > 0$ such that for all $t \geq 0$, $\|z_t\|_{\mathcal{L}_\infty} \leq L_z \|x_t\|_{\mathcal{L}_\infty} + B_z$.*

[1] Note that this assumption applies to time-varying x_z-dynamics as well.

Assumption 6 (Stability of matched transmission zeros) *The transmission zeros of the transfer matrix $H_m(s) = C(s\mathbb{I}-A_m)^{-1}B_m$ from the quantized control input $u_{\rm q}(t)$ to the output of the system $y(t)$ lie in the open left-half plane.*

Given a piecewise continuous, bounded reference signal $r(t)$, the control objective is to design an adaptive state feedback controller for the quantized system to ensure that $y(t)$ tracks the output response $y_m(t)$ of the following system $M(s) \triangleq C\left(s\mathbb{I} - A_m\right)^{-1} B_m K_g(s)$, both in transient and steady-state, where $K_g(s)$ is a feedforward prefilter.

Conventional design methods from multivariable control theory can be used to design the prefilter $K_g(s)$ to achieve desired decoupling properties. As an example, if one chooses $K_g(s)$ as the constant matrix $K_g = -(CA_m^{-1}B_m)^{-1}$, then the diagonal elements of the desired transfer matrix $M(s) = C(s\mathbb{I}_n - A_m)^{-1}B_m K_g$ have DC gain equal to one, while the off-diagonal elements have zero DC gain.

3.7 Control design

In this section we present the $\mathcal{L}_1$ adaptive controller. We first introduce some notation the that will be used in the definition of the controller and the ensuing analysis.

3.7.1 Notation

For any $\nu > 0$, let

$$L_{i\nu} \triangleq \frac{\bar{\nu}}{\nu} d_{f_{xi}}(\bar{\nu}), \quad \bar{\nu} \triangleq \max\{\nu + \bar{\gamma}_x, \; L_z(\nu + \bar{\gamma}_x) + B_z\}, \tag{3.24}$$

where $\bar{\gamma}_x > 0$ is an arbitrary, small constant.

Let $H_{xm}(s) \triangleq (s\mathbb{I}_n - A_m)^{-1}B_m$, $H_{xum}(s) \triangleq (s\mathbb{I}_n - A_m)^{-1}B_{um}$, $H_m(s) \triangleq CH_{xm}(s) = C(s\mathbb{I}_n - A_m)^{-1}B_m$, $H_{um}(s) \triangleq CH_{xum}(s) = C(s\mathbb{I}_n - A_m)^{-1}B_{um}$.

The design of $\mathcal{L}_1$ adaptive controller involves a strictly proper $m \times m$ transfer matrix $D(s)$ and a matrix gain $K \in \mathbb{R}^{m\times m}$, which lead to a strictly proper stable transfer matrix

$$C(s) \triangleq \omega K \left(\mathbb{I}_m + D(s)\omega K\right)^{-1} D(s) \tag{3.25}$$

with DC gain $C(0) = \mathbb{I}_m$. The choice of $D(s)$ needs to ensure also that $C(s)H_m^{-1}(s)$ is a proper stable transfer matrix. For a particular class of systems, a possible choice for $D(s)$ might be $D(s) = \frac{1}{s}\mathbb{I}_m$, which yields a strictly proper $C(s)$ of the form $C(s) = \omega K \left(s\mathbb{I}_m + \omega K\right)^{-1}$, with the condition that the choice of K must ensure that $-\omega K$ is Hurwitz.

For proofs of stability and performance bounds, the choices of $D(s)$ and K also need to ensure that there exists $\rho_{x_r} > \rho_0$, such that

$$\begin{aligned} &\|G_m(s)\|_{\mathcal{L}_1} + \|G_{um}(s)\|_{\mathcal{L}_1}\ell_0 \\ &\leq \frac{\rho_{x_r} - \|H_{xm}(s)C(s)K_g(s)\|_{\mathcal{L}_1}\|r\|_{\mathcal{L}_\infty} - \|s(s\mathbb{I} - A_m)^{-1}\|_{\mathcal{L}_1}\rho_0}{L_{1\rho_{x_r}}\rho_{x_r} + B_0}, \end{aligned} \tag{3.26}$$

where $G_m(s) \triangleq H_{xm}(s)(\mathbb{I}_m - C(s))$, $G_{um}(s) \triangleq (\mathbb{I}_n - H_{xm}(s)C(s)H_m^{-1}(s)C)H_{xum}(s)$, $\ell_0 \triangleq L_{2\rho_{x_r}}/L_{1\rho_{x_r}}$, $B_0 \triangleq \max\{B_{10}, \frac{B_{20}}{\ell_0}\}$, $L_{1\rho_{x_r}}$ and $L_{2\rho_{x_r}}$ were defined in (4.27), and $K_g(s)$ is the proper stable feedforward prefilter.

For the analysis results in the following sections to hold, the inequality in (3.26) is only a sufficient condition and is required only for the real ω. However, since ω is unknown, (3.26) cannot be used to guide the filter design. More conservatively, we can make the choices of $D(s)$ and K to ensure that for all $\omega \in \Omega$ there exists a constant $\rho_{x_r} > \rho_0$, such that (3.26) holds.

The selection of $D(s)$ and K determines the bandwidth and the structure of the low-pass filter $C(s)$. To satisfy the condition, the bandwidth of $C(s)$ should be large enough to make the left-hand-side small. When the bandwidth is large, $C(s) \to \mathbb{I}_m$, $\|G_m(s)\|_{\mathcal{L}_1}$ and $\|G_{um}(s)\|_{\mathcal{L}_1}$ get small. (The existence of ρ_{x_r} and the impact of the unmatched uncertainty are further discussed in Remark 16.) The filter design should also ensure that the high-frequency oscillation is rejected and the control signals stay within the actuator bandwidth limit. Further, $C(s)$ affects the system performance, such as the transient performance bounds and the time-delay margin. Thus the design can be done by solving a multi-objective optimization problem [31–33]. See references [34–36] for related optimization problems, such as $\mathcal{L}_1$ norm minimization.

Define the constants

$$\begin{aligned}\rho_{u_r} &\triangleq \left\|\omega^{-1}C(s)H_m^{-1}(s)H_{um}(s)\right\|_{\mathcal{L}_1}\left(L_{2\rho_{x_r}}\rho_{x_r}+B_{20}\right) \\ &\quad+\left\|\omega^{-1}C(s)\right\|_{\mathcal{L}_1}(L_{1\rho_{x_r}}\rho_{x_r}+B_{10})+\left\|\omega^{-1}C(s)K_g(s)\right\|_{\mathcal{L}_1}\|r\|_{\mathcal{L}_\infty}, \qquad (3.27)\\ c_{ue} &= \|H_{xm}(s)\omega\|_{\mathcal{L}_1}+\|H_{xm}(s)C(s)\|_{\mathcal{L}_1}2\omega_{1\max}, \\ c_{xe} &= \left\|H_{xm}(s)C(s)H_m^{-1}(s)C\right\|_{\mathcal{L}_1}, \qquad (3.28)\end{aligned}$$

where $\omega_{1\max}=\max_{\omega\in\Omega}\|\omega\|_\infty$. Define the functions

$$\begin{aligned}c_{de}(a,b) &= \|G_m(s)\|_{\mathcal{L}_1}a+\|G_{um}(s)\|_{\mathcal{L}_1}b, \qquad (3.29)\\ c_{eu}(a,b) &= \left\|\omega^{-1}C(s)\right\|_{\mathcal{L}_1}a+\left\|\omega^{-1}C(s)H_m^{-1}(s)H_{um}(s)\right\|_{\mathcal{L}_1}b.\end{aligned}$$

3.7.2 $\mathcal{L}_1$ adaptive controller

Next, we introduce the three elements: the state predictor, the adaptive law and the control law for this system.

State predictor: We consider the following state predictor

$$\begin{aligned}\dot{\hat{x}}(t) =& A_m\hat{x}(t)+B_m(\hat{\omega}(t)u_{\rm q}(t)+\hat{\theta}_1(t)\|x_t\|_{\mathcal{L}_\infty}+\hat{\sigma}_1(t)) \\ &+B_{um}(\hat{\theta}_2(t)\|x_t\|_{\mathcal{L}_\infty}+\hat{\sigma}_2(t)),\ \hat{x}(0)=x_0, \qquad (3.30)\end{aligned}$$

where $\hat{\omega}(t)\in\mathbb{R}^{m\times m}$, $\hat{\theta}_1(t)\in\mathbb{R}^m$, $\hat{\sigma}_1(t)\in\mathbb{R}^m$, $\hat{\theta}_2(t)\in\mathbb{R}^{n-m}$, and $\hat{\sigma}_2(t)\in\mathbb{R}^{n-m}$ are the adaptive estimates.

Adaptive laws: The adaptation laws for $\hat{\omega}(t)$, $\hat{\theta}_1(t)$, $\hat{\sigma}_1(t)$, $\hat{\theta}_2(t)$, and $\hat{\sigma}_2(t)$ are defined as

$$\begin{aligned}\dot{\hat{\omega}}(t) &= \Gamma\mathrm{Proj}(\hat{\omega}(t),-(\tilde{x}^\top(t)PB_m)^\top u_{\rm q}^\top(t)), \\ \dot{\hat{\theta}}_1(t) &= \Gamma\mathrm{Proj}(\hat{\theta}_1(t),-(\tilde{x}^\top(t)PB_m)^\top\|x_t\|_{\mathcal{L}_\infty}), \\ \dot{\hat{\theta}}_2(t) &= \Gamma\mathrm{Proj}(\hat{\theta}_2(t),-(\tilde{x}^\top(t)PB_{um})^\top\|x_t\|_{\mathcal{L}_\infty}), \\ \dot{\hat{\sigma}}_1(t) &= \Gamma\mathrm{Proj}(\hat{\sigma}_1(t),-(\tilde{x}^\top(t)PB_m)^\top), \qquad (3.31)\\ \dot{\hat{\sigma}}_2(t) &= \Gamma\mathrm{Proj}(\hat{\sigma}_2(t),-(\tilde{x}^\top(t)PB_{um})^\top),\end{aligned}$$

where $\hat{\omega}(0)=\hat{\omega}_0$, $\hat{\theta}_i(0)=\hat{\theta}_{i_0}$, $\hat{\sigma}_i(0)=\hat{\sigma}_{i_0}$, $i=1,2$; $\tilde{x}(t)=\hat{x}(t)-x(t)$; $\Gamma\in\mathbb{R}^+$ is the adaptation gain; $P=P^\top>0$ is the solution to the algebraic Lyapunov equation $A_m^\top P+PA_m=-Q$, $Q=Q^\top>0$; and the projection operator $\mathrm{Proj}(\cdot,\cdot)$

is given in Definition 3 in the Appendix. The projection operator ensures that $\hat{\omega}(t) \in \Omega$, $\|\hat{\theta}_i(t)\|_\infty \leq \theta_{b_i}$, $\|\hat{\sigma}_i(t)\|_\infty \leq \sigma_{b_i}$, $i = 1, 2$, for all $t > 0$, where θ_{b_i} and σ_{b_i} depend on the bounds of x in different cases, to be defined in (3.36).

Control law: We first design the control signal $u(t)$, given by

$$u(t) = -K\chi(t)\,, \quad \chi(s) = D(s)\hat{\eta}(s)\,, \tag{3.32}$$

where $\hat{\eta}(s)$ is the Laplace transform of the signal

$$\hat{\eta}(t) = \hat{\omega}(t)u(t) + \hat{\eta}_1(t) + \hat{\eta}_{2m}(t) - r_g(t)\,, \tag{3.33}$$

with $r_g(s) = K_g(s)r(s)$, $\hat{\eta}_{2m}(s) = H_m^{-1}(s)H_{um}(s)\hat{\eta}_2(s)$, and $\hat{\eta}_1(t)$ and $\hat{\eta}_2(t)$ are defined by $\hat{\eta}_i(t) = \hat{\theta}_i(t)\,\|x_t\|_{\mathcal{L}_\infty} + \hat{\sigma}_i(t),\ i = 1, 2$.

3.8 Performance analysis

3.8.1 Closed-loop reference system

Let the closed-loop reference system be given as:

$$\begin{aligned}
\dot{x}_{\rm ref}(t) =& A_m x_{\rm ref}(t) + B_m(\omega u_{\rm ref}(t) + f_1(x_{\rm ref}(t), z(t), t)) \\
&+ B_{um} f_2(x_{\rm ref}(t), z(t), t),\ x_{\rm ref}(0) = x_0 \\
u_{\rm ref}(s) =& -\omega^{-1}C(s)\big(\eta_{1\rm ref}(s) + H_m^{-1}(s)H_{um}(s)\eta_{2\rm ref}(s) - K_g(s)r(s)\big) \\
y_{\rm ref}(t) =& Cx_{\rm ref}(t)\,,
\end{aligned} \tag{3.34}$$

where $\eta_{1\rm ref}(s)$ and $\eta_{2\rm ref}(s)$ are the Laplace transforms of the signals $\eta_{i\rm ref}(t) = f_i(x_{\rm ref}(t), z(t), t)$, $i = 1, 2$.

Lemma 4 ([30]) *For the closed-loop reference system in* (3.34)*, subject to the* $\mathcal{L}_1$*-norm condition* (3.26)*, if* $\|x_0\|_\infty < \rho_0$ *and* $\|z_t\|_{\mathcal{L}_\infty} \leq L_z(\|x_{{\rm ref}t}\|_{\mathcal{L}_\infty} + \gamma_x) + B_z$*, then*

$$\|x_{{\rm ref}t}\|_{\mathcal{L}_\infty} < \rho_{x_r}\,,\ \|u_{{\rm ref}t}\|_{\mathcal{L}_\infty} < \rho_{u_r}\,,$$

where ρ_{x_r} *and* ρ_{u_r} *were defined in* (3.26) *and* (3.27)*, respectively.*

Remark 12 *The closed-loop reference system in* (3.34) *can be written as*

$$\begin{aligned} y_{\text{ref}}(s) =& H_m(s)\big(\mathbb{I}_m - C(s)\big)\eta_{1\text{ref}}(s) \\ &+ \big(\mathbb{I}_m - H_m(s)C(s)H_m^{-1}(s)\big)H_{um}(s)\eta_{2\text{ref}}(s) \\ &+ C(s\mathbb{I} - A_m)^{-1}B_mC(s)K_g(s)r(s). \end{aligned}$$

In the limiting case when $C(s) \to \mathbb{I}_m$, the first two terms go to zero, and $y_{\text{ref}}(s) \to M(s)r(s)$, which is the ideal response $y_m(s) = M(s)r(s)$ specified in the control objective in Section 3.6.

3.8.2 Equivalent linear time-varying system

In this subsection we show that the nonlinear system with unmodeled dynamics in (3.23) can be transformed into a linear system with unknown time-varying parameters and time-varying disturbances.

Lemma 5 ([20]) *For the system in* (3.23)*, if*

$$\|x_t\|_{\mathcal{L}_\infty} \leq \rho_x\,, \quad \|u_t\|_{\mathcal{L}_\infty} \leq \rho_u\,, \tag{3.35}$$

then for all $\tau \in [0, t]$, there exist differentiable functions

$$\theta_1(\tau) \in \mathbb{R}^m,\ \sigma_1(\tau) \in \mathbb{R}^m,\ \theta_2(\tau) \in \mathbb{R}^{n-m},\ \sigma_2(\tau) \in \mathbb{R}^{n-m}$$

such that

$$\begin{aligned} &\|\theta_i(\tau)\|_\infty < \theta_{b_i}(\rho_{x_r}),\ \|\dot{\theta}_i(\tau)\|_\infty < d_{\theta_i}(\rho_{x_r}), \\ &\|\sigma_i(\tau)\|_\infty < \sigma_{b_i}(\rho_{x_r}),\ \|\dot{\sigma}_i(\tau)\|_\infty < d_{\sigma_i}(\rho_{x_r}), \\ &f_i(x(\tau), z(\tau), \tau) = \theta_i(\tau)\|x_\tau\|_{\mathcal{L}_\infty} + \sigma_i(\tau), \quad i = 1, 2, \end{aligned}$$

where θ_{b_i} and σ_{b_i} are given by

$$\theta_{b_i}(\rho_{x_r}) \triangleq L_{i\rho_x}, \sigma_{b_i}(\rho_{x_r}) \triangleq L_{i\rho_x}B_z + B_{i0} + \epsilon_i, i = 1, 2, \tag{3.36}$$

and $\epsilon_i > 0$, $i = 1, 2$, are arbitrary small numbers.

If the bounds in (3.35) hold, then Lemma 5 implies that the system in (3.23) can be rewritten over $\tau \in [0, t]$ as

$$\begin{aligned}\dot{x}(\tau) =& A_m x(\tau) + B_m \left(\omega u_{\mathrm{q}}(\tau) + \theta_1(\tau) \left\|x_\tau\right\|_{\mathcal{L}_\infty} + \sigma_1(\tau)\right) \\ &+ B_{um} \left(\theta_2(\tau) \left\|x_\tau\right\|_{\mathcal{L}_\infty} + \sigma_2(\tau)\right) , \\ y(\tau) =& Cx(\tau) , \quad x(0) = x_0 , \end{aligned} \tag{3.37}$$

where $\theta_1(\tau)$, $\sigma_1(\tau)$, $\theta_2(\tau)$, and $\sigma_2(\tau)$ are unknown bounded time-varying signals with bounded derivatives.

3.8.3 Prediction error

Let $\theta_m(\rho_{x_r})$ and $\tilde{\eta}_i(t)$ be defined as

$$\begin{aligned}\theta_m(\rho_{x_r}) \triangleq& 4\Big(\max_{\omega \in \Omega} \mathrm{tr}(\omega^\top \omega) + (\theta_{b_1}^2 + \sigma_{b_1}^2)m + (\theta_{b_2}^2 + \sigma_{b_2}^2)(n-m)) \\ &+ 4\frac{\lambda_{\max}(P)}{\lambda_{\min}(Q)}((\theta_{b_1} d_{\theta_1} + \sigma_{b_1} d_{\sigma_1})m + (\theta_{b_2} d_{\theta_2} + \sigma_{b_2} d_{\sigma_2})(n-m)\Big) , \end{aligned} \tag{3.38}$$

$$\tilde{\eta}_i(t) = \hat{\eta}_i(t) - \eta_i(t), \quad \eta_i(t) = f_i(x(t), z(t), t), i = 1, 2. \tag{3.39}$$

Also, let $\tilde{\omega}(t) = \hat{\omega}(t) - \omega$, $\tilde{\theta}_i(t) = \hat{\theta}_i(t) - \theta_i(t)$, $\tilde{\sigma}_i(t) = \hat{\sigma}_i(t) - \sigma_i(t)$, $i = 1, 2$. Using the notations above, the following error dynamics can be derived from (3.37) and (3.30)

$$\dot{\tilde{x}}(t) = A_m \tilde{x}(t) + B_m \left(\tilde{\omega}(t) u_{\mathrm{q}}(t) + \tilde{\eta}_1(t)\right) + B_{um} \tilde{\eta}_2(t), \tag{3.40}$$

where $\tilde{x}(0) = 0$. Next we show that given $\gamma_0 > 0$, if the adaptation gain Γ is lower bounded by

$$\Gamma > \frac{\theta_m(\rho_{x_r})}{\lambda_{\min}(P)\gamma_0^2} , \tag{3.41}$$

and the projection is confined to the following bounds

$$\hat{\omega}(t) \in \Omega, \ \|\hat{\theta}_i(t)\|_\infty \leq \theta_{b_i}, \ \|\hat{\sigma}_i(t)\|_\infty \leq \sigma_{b_i}, \ i = 1, 2, \tag{3.42}$$

then the prediction error $\tilde{x}(t)$ between the state of the system and the predictor can be systematically reduced both in transient and steady-state by increasing the

adaptation gain. The following lemma summarizes this result.

Lemma 6 ([20,30]) *Let the adaptation gain be lower bounded as in* (3.41)*, and the projection be confined to the bounds in* (3.42)*. Given the system in* (3.23) *and the $\mathcal{L}_1$ adaptive controller defined by* (3.30)-(3.32) *subject to* (3.26)*, if*

$$\|x_t\|_{\mathcal{L}_\infty} \leq \rho_x \,,\ \|u_t\|_{\mathcal{L}_\infty} \leq \rho_u \,,$$

then we have

$$\|\tilde{x}_t\|_{\mathcal{L}_\infty} < \gamma_0,$$

where γ_0 was introduced in (3.41)*.*

The proof is similar to that of Lemma 3 in [30] and is omitted.

3.8.4 Logarithmic quantization

Given the constant Δ, we introduce a few more notations. Let $\rho_{x_{\log}}$ be defined as

$$\rho_{x_{\log}} \triangleq \rho_{x_r} + \bar{\gamma}_x \,. \tag{3.43}$$

Also define the following constants

$$\begin{aligned}
\gamma_{x_{\log}} \triangleq & \gamma_{x\mathrm{o}_{\log}} + \gamma_{x\mathrm{q}_{\log}} + \epsilon, \qquad (3.44)\\
\gamma_{x\mathrm{o}_{\log}} \triangleq & \frac{c_{xe} + \frac{c_{ue}\Delta \left\| \omega^{-1}C(s)H_m^{-1}(s)C \right\|_{\mathcal{L}_1}}{1-2\omega_{1\max}\Delta\|\omega^{-1}C(s)\|_{\mathcal{L}_1}}}{1 - c_{de}(L_{1\rho_{x_r}}, L_{2\rho_{x_r}}) - \frac{c_{ue}\Delta c_{eu}(L_{1\rho_{x_r}}, L_{2\rho_{x_r}})}{1-2\omega_{1\max}\Delta\|\omega^{-1}C(s)\|_{\mathcal{L}_1}}}\gamma_0,\\
\gamma_{x\mathrm{q}_{\log}} \triangleq & \frac{\frac{c_{ue}}{1-2\omega_{1\max}\Delta\|\omega^{-1}C(s)\|_{\mathcal{L}_1}}}{1 - c_{de}(L_{1\rho_{x_r}}, L_{2\rho_{x_r}}) - \frac{c_{ue}\Delta c_{eu}(L_{1\rho_{x_r}}, L_{2\rho_{x_r}})}{1-2\omega_{1\max}\Delta\|\omega^{-1}C(s)\|_{\mathcal{L}_1}}}\Delta\rho_{u_r},
\end{aligned}$$

where $\epsilon < \bar{\gamma}_x$ is a small positive constant, c_{xe} and c_{ue} were defined in (3.28), $c_{de}(a,b)$ and $c_{eu}(a,b)$ were defined in (3.29), and γ_0 and Δ are sufficiently small

so that $\gamma_{x_{\log}} = \gamma_{xo_{\log}} + \gamma_{xq_{\log}} + \epsilon \leq \bar{\gamma}_x$. Similarly, let

$$\rho_{u_{\log}} \triangleq \rho_{u_r} + \gamma_{u_{\log}}\,, \tag{3.45}$$

$$\begin{aligned}\gamma_{u_{\log}} \triangleq & \frac{(1+\Delta)c_{eu}(L_{1\rho_{x_r}}, L_{2\rho_{u_r}})}{1 - 2\omega_{1\max}\Delta \left\|\omega^{-1}C(s)\right\|_{\mathcal{L}_1}}\gamma_{x_{\log}} + \frac{(1+\Delta)\left\|\omega^{-1}C(s)H_m^{-1}(s)C\right\|_{\mathcal{L}_1}}{1 - 2\omega_{1\max}\Delta \left\|\omega^{-1}C(s)\right\|_{\mathcal{L}_1}}\gamma_0 \\ & + \frac{1 + 2\omega_{1\max}\left\|\omega^{-1}C(s)\right\|_{\mathcal{L}_1}}{1 - 2\omega_{1\max}\Delta \left\|\omega^{-1}C(s)\right\|_{\mathcal{L}_1}}\Delta\rho_{u_r}.\end{aligned} \tag{3.46}$$

Theorem 3 *Let the adaptive gain be lower bounded as in* (3.41) *and the projection be confined to the bounds in* (3.42)*. Given the closed-loop system with logarithmic quantization* (2.3) *and the $\mathcal{L}_1$ adaptive controller defined via* (3.30)-(3.32)*, subject to the $\mathcal{L}_1$-norm condition in* (3.26)*, and the closed-loop reference system in* (3.34)*, if $\|x_0\|_\infty \leq \rho_{x_r}$, then we have the performance bounds*

$$\begin{aligned}&\|x\|_{\mathcal{L}_\infty} \leq \rho_{x_{\log}},\ \|u_{\rm q}\|_{\mathcal{L}_\infty} \leq \rho_{u_{\log}},\ \|x_{\rm ref}\|_{\mathcal{L}_\infty} \leq \rho_{x_r}, \\ &\|u_{\rm ref}\|_{\mathcal{L}_\infty} \leq \rho_{u_r},\ \|\tilde{x}\|_{\mathcal{L}_\infty} < \gamma_0,\ \|x - x_{\rm ref}\|_{\mathcal{L}_\infty} < \gamma_{x_{\log}}, \\ &\|u_{\rm q} - u_{\rm ref}\|_{\mathcal{L}_\infty} < \gamma_{u_{\log}},\ \|y - y_{\rm ref}\|_{\mathcal{L}_\infty} < \|C\|_\infty \gamma_{x_{\log}},\end{aligned} \tag{3.47}$$

where $\gamma_{x_{\log}}$ and $\gamma_{u_{\log}}$ were defined in (3.44) *and* (3.46)*, respectively.*

Proof. See Appendix B.3.

Remark 13 *The performance bounds for the state signal in* (3.47) *have two parts (as seen in* (3.44)*). One of them has a factor γ_0, which can be systematically reduced by increasing the adaptation rate. The other one has a factor Δ, which is the quantization parameter for the logarithmic quantizer. When Δ goes to zero and there is no quantization, this term vanishes and the bounds reduce to the ones in Theorem 1 of [30], as to be expected.*

Remark 14 *The unmatched uncertainty $f_2(x(t), z(t), t)$ adds several terms to both the numerator and the denominator of the performance bound. The bounds $\gamma_{x_{\log}}$ and $\gamma_{u_{\log}}$ of the tracking error in Theorem 3 are given in* (3.44) *and* (3.46)*. From* (3.44)*,* (3.46)*, and the notations in* (3.28) *and* (3.29) *we can see that the unmatched uncertainties contribute to the terms with $H_{um}(s)$ and $G_{um}(s)$. If there is no unmatched uncertainty in the system, i.e. $f_2(x(t), z(t), t) = 0$, $B_{um} = 0$, we will have degenerated results. First, the condition in* (3.26) *will be reduced to Equation (3) in [37]. Second, the performance bounds will be reduced to $\gamma_{x_{\log}} = \gamma_{xo_{\log}} + \gamma_{xq_{\log}} + \epsilon$, where*

$$
\begin{aligned}
\gamma_{x\mathrm{o}_{\log}} =& \frac{c_{xe} + \frac{c_{ue}\Delta\left\|\omega^{-1}C(s)H_m^{-1}(s)C\right\|_{\mathcal{L}_1}}{1-2\omega_{1\max}\Delta\|\omega^{-1}C(s)\|_{\mathcal{L}_1}}}{1 - \|G_m(s)\|_{\mathcal{L}_1} L_{1\rho_{x_r}} - \frac{c_{ue}\Delta\|\omega^{-1}C(s)\|_{\mathcal{L}_1} L_{1\rho_{x_r}}}{1-2\omega_{1\max}\Delta\|\omega^{-1}C(s)\|_{\mathcal{L}_1}}}\gamma_0, \\
\gamma_{x\mathrm{q}_{\log}} =& \frac{\frac{c_{ue}}{1-2\omega_{1\max}\Delta\|\omega^{-1}C(s)\|_{\mathcal{L}_1}}}{1-\|G_m(s)\|_{\mathcal{L}_1} L_{1\rho_{x_r}} - \frac{c_{ue}\Delta\|\omega^{-1}C(s)\|_{\mathcal{L}_1} L_{1\rho_{x_r}}}{1-2\omega_{1\max}\Delta\|\omega^{-1}C(s)\|_{\mathcal{L}_1}}}\Delta\rho_{u_r}, \\
\gamma_{u_{\log}} =& \frac{(1+\Delta)\left\|\omega^{-1}C(s)\right\|_{\mathcal{L}_1} L_{1\rho_{x_r}}}{1 - 2\omega_{1\max}\Delta\left\|\omega^{-1}C(s)\right\|_{\mathcal{L}_1}}\gamma_{x_{\log}} + \frac{(1+\Delta)\left\|\omega^{-1}C(s)H_m^{-1}(s)C\right\|_{\mathcal{L}_1}}{1 - 2\omega_{1\max}\Delta\left\|\omega^{-1}C(s)\right\|_{\mathcal{L}_1}}\gamma_0 \\
& + \frac{1 + 2\omega_{1\max}\left\|\omega^{-1}C(s)\right\|_{\mathcal{L}_1}}{1 - 2\omega_{1\max}\Delta\left\|\omega^{-1}C(s)\right\|_{\mathcal{L}_1}}\Delta\rho_{u_r}.
\end{aligned}
$$

Further, if the input signal is not quantized, $\Delta \to 0$, the limiting $\gamma_{x_{\log}}$ and $\gamma_{u_{\log}}$ agree with the previous result in Theorem 1 in [37].

Remark 15 *The nonlinearities, unmodeled dynamics and unmatched uncertainties add complexity to the condition for selecting the low-pass filter as well as to the performance bounds. A simple version of the $\mathcal{L}_1$ adaptive controller for SISO quantized linear uncertain systems is analyzed in [38]. As stated in the previous remark, the condition in* (3.26) *will be reduced to Equation (3) in [37]. If we further reduce the nonlinear function $f(x(t),z(t),t)$ to a linear term $\theta^\top x(t)$, following a limiting argument (Remark 1 in [37]) we will recover the condition (6) in [38]. For the performance bounds, in the absence of nonlinearities, unmodeled dynamics and unmatched uncertainties, the terms with $\tilde{\omega}(t)$, $z(t)$, $H_{um}(s)$ disappear, and we can obtain the results of Theorems 1 and 2 in [38].*

Remark 16 *To obtain the result in Theorem 3, the selection of $C(s)$ should satisfy the condition in* (3.26)*. Without the unmatched uncertainty, $G_{um}(s) = 0$, this condition can always be satisfied by increasing the bandwidth of $C(s)$. When $C(s) \to \mathbb{I}$, $\|G_m(s)\|_{\mathcal{L}_1} \to 0$. However, in the presence of unmatched uncertainty, the existence of ρ_{x_r} is not obvious. We can see that when the unmatched uncertainty is small, i.e., either $\|G_{um}(s)\|_{\mathcal{L}_1}$ or the Lipschitz constant $L_{2\rho_{x_r}}$ are small, the left-hand-side is small, and a ρ_{x_r} can be determined. When the unmatched uncertainty is large, for the same ρ_{x_r}, the possible ρ_0 need to be smaller. This shows the impact of the unmatched uncertainty on the stability of the reference system and the performance bounds. The constant ρ_{x_r} characterizes a positive invariant*

set of the closed-loop reference system. If the unmatched uncertainty increases, the positive invariant set shrinks, which agrees with intuition.

3.8.5 Uniform quantization

As shown in Section 2.1, the error introduced by uniform quantization is bounded by half of the quantization interval length. Given the quantization interval length l, we introduce a few more notations. Let $\rho_{x_{\rm unif}}$ be defined as

$$\rho_{x_{\rm unif}} \triangleq \rho_{x_r} + \bar{\gamma}_x \,. \tag{3.48}$$

$$\gamma_{x_{\rm unif}} \triangleq \gamma_{x{\rm o}_{\rm unif}} + \gamma_{x{\rm q}_{\rm unif}} + \epsilon, \tag{3.49}$$

$$\gamma_{x{\rm o}_{\rm unif}} \triangleq \frac{c_{xe}}{1 - c_{de}(L_{1\rho_{x_r}}, L_{2\rho_{x_r}})}\gamma_0, \gamma_{x{\rm q}_{\rm unif}} \triangleq \frac{\frac{1}{2}c_{ue}}{1 - c_{de}(L_{1\rho_{x_r}}, L_{2\rho_{x_r}})l},$$

where $\epsilon < \bar{\gamma}_x$ is a small positive constant, c_{xe} and c_{ue} are defined in (3.28), $c_{de}(a, b)$ is defined in (3.29), γ_0 and Δ are sufficiently small, so that $\gamma_{x_{\rm unif}} = \gamma_{x{\rm o}_{\rm unif}} + \gamma_{x{\rm q}_{\rm unif}} + \epsilon \leq \bar{\gamma}_x$.

Similarly, let

$$\rho_{u_{\rm unif}} \triangleq \rho_{u_r} + \gamma_{u_{\rm unif}} \,, \tag{3.50}$$

$$\begin{aligned}\gamma_{u_{\rm unif}} \triangleq & c_{eu}(L_{1\rho_{x_r}}, L_{2\rho_{u_r}})\gamma_{x_{\rm unif}} + \left\|\omega^{-1}C(s)H_m^{-1}(s)C\right\|_{\mathcal{L}_1}\gamma_0 \\ & + (1 + 2\omega_{1\,\max}\left\|\omega^{-1}C(s)\right\|_{\mathcal{L}_1})\frac{1}{2}l.\end{aligned} \tag{3.51}$$

We have the following theorem.

Theorem 4 *Let the adaptation gain be lower bounded as in* (3.41) *and the projection be confined to the bounds in* (3.42)*. Given the closed-loop system with uniform quantization* (2.1) *and the $\mathcal{L}_1$ adaptive controller defined by* (3.30)-(3.32)*, subject to the $\mathcal{L}_1$-norm condition in* (3.26)*, and the closed-loop reference system in* (3.34)*, if $\|x_0\|_\infty \leq \rho_{x_r}$, then we have the performance bounds*

$$\begin{aligned}&\|x_{\rm ref}\|_{\mathcal{L}_\infty} \leq \rho_{x_r}\,,\ \|u_{\rm ref}\|_{\mathcal{L}_\infty} \leq \rho_{u_r}\,,\ \|x\|_{\mathcal{L}_\infty} \leq \rho_{x_{\rm unif}}\,, \\ &\|u_{\rm q}\|_{\mathcal{L}_\infty} \leq \rho_{u_{\rm unif}}\,,\ \|\tilde{x}\|_{\mathcal{L}_\infty} < \gamma_0\,,\ \|x - x_{\rm ref}\|_{\mathcal{L}_\infty} < \gamma_{x_{\rm unif}}\,, \\ &\|u_{\rm q} - u_{\rm ref}\|_{\mathcal{L}_\infty} < \gamma_{u_{\rm unif}}\,,\ \|y - y_{\rm ref}\|_{\mathcal{L}_\infty} < \|C\|_\infty \gamma_{x_{\rm unif}}\,,\end{aligned} \tag{3.52}$$

where $\gamma_{x_{\rm unif}}$ and $\gamma_{u_{\rm unif}}$ were defined in (3.49) *and* (3.51)*, respectively.*

Proof. See Appendix B.4.

Remark 17 *The performance bounds in* (3.52) *are decoupled into two terms, one of which depends linearly upon l, representing the quantization interval length for the uniform quantizer, and the other is independent of the quantizer's parameters. When l decreases to zero and there is no quantization, the corresponding term vanishes, and the performance bounds reduce to the ones in Theorem 1 in [30], as to be expected.*

Remark 18 *As discussed in Section 3.8, ρ_{x_r} characterizes the positive invariant sets for the state of the closed-loop reference system, while $\rho_{x_{\log}}$ and $\rho_{x_{\text{unif}}}$ characterize the positive invariant sets for the state of the closed-loop adaptive system with logarithmic and uniform quantization, respectively. We notice that, since $\bar{\gamma}_x$ can be set to be arbitrarily small, $\rho_{x_{\log}}$ and $\rho_{x_{\text{unif}}}$ can approximate ρ_{x_r} arbitrarily closely in both cases.*

3.8.6 Performance bounds in the case of nonzero trajectory initialization error

In previous subsections we analyzed the performance bounds, assuming the predictor can be initialized perfectly using the initial condition. While in state feedback this is ideally true, the initialization process can be affected by hardware noise and latencies. This section analyzes the effect of non-zero trajectory initialization errors on the performance bounds.

To streamline the subsequent analysis, we consider a simplified version of (3.22), limiting it to SISO systems with matched uncertainty, constant unknown parameter and uniform quantization, i.e.

$$\begin{aligned} &\dot{x}(t) = A_m x(t) + b(\omega u_{\text{q}}(t) + \theta^\top x(t) + \sigma(t))\,,\ x(0) = x_0\,,\\ &y(t) = c^\top x(t)\,, \quad u_{\text{q}}(t) = Q_{\text{unif}}(u(t))\,, \end{aligned} \tag{3.53}$$

where $\omega \in \mathbb{R}$ is an unknown constant, $b, c \in \mathbb{R}^n$ are known constant vectors, $\theta \in \mathbb{R}^n$ is an unknown constant vector, and $\sigma(t) \in \mathbb{R}$ is the unknown disturbance.

Let $\omega \in [\omega_l, \omega_u]$, $\theta \in \Theta$, $|\sigma(t)| \leq \sigma_b$, $|\dot{\sigma}(t)| \leq d_\sigma$, $\forall t \geq 0$.

We consider the following state predictor:

$$\dot{\hat{x}}(t) = A_m \hat{x}(t) + b(\hat{\omega}(t) u_{\text{q}}(t) + \hat{\theta}^\top(t) x(t) + \hat{\sigma}(t)), \hat{x}(0) = \hat{x}_0, \tag{3.54}$$

where $\hat{x}_0 \neq x_0$ in general.

The adaptive laws in this case are

$$\begin{aligned}\dot{\hat{\omega}}(t) =& \Gamma \mathrm{Proj}(\hat{\omega}(t), -\tilde{x}^\top(t) P b u_{\mathrm{q}}(t)),\\ \dot{\hat{\theta}}(t) =& \Gamma \mathrm{Proj}(\hat{\theta}(t), -x(t)\tilde{x}^\top(t) P b),\\ \dot{\hat{\sigma}}(t) =& \Gamma \mathrm{Proj}(\hat{\sigma}(t), -\tilde{x}^\top(t) P b).\end{aligned}$$

The controller takes the form

$$u(s) = -kD(s)(\hat{\eta}(s) - k_g r(s)), \tag{3.55}$$

where $\hat{\eta}(s)$ is the Laplace transform of $\hat{\eta}(t)$, $\hat{\eta}(t) = \hat{\omega}(t)u(t) + \hat{\theta}^\top(t)x(t) + \hat{\sigma}(t)$, $k_g = -1/(c\top A_m^{-1} b)$, and $D(s)$ and k are introduced in (3.25) and (3.32).

Lemma 7 ([39]) *For the system in* (3.53) *and the $\mathcal{L}_1$ adaptive controller with the predictor in* (3.54)*, the prediction error is upper bounded by $\|\tilde{x}(t)\| \leq \rho(t)$, $\forall$ $t \geq 0$, where*

$$\begin{aligned}\rho(t) \triangleq& \sqrt{\frac{\left(V(0) - \frac{\theta_n}{\Gamma}\right) \mathrm{e}^{-\alpha t}}{\lambda_{\min}(P)}} + \sqrt{\frac{\theta_n}{\lambda_{\min}(P)\Gamma}},\ \alpha \triangleq \frac{\lambda_{\min}(Q)}{\lambda_{\max}(P)},\\ \theta_n \triangleq& 4 \max_{\theta \in \Theta} \|\theta\|_2^2 + 4\sigma_b^2 + (\omega_u - \omega_l)^2 + \frac{4\sigma_b d_\sigma}{\alpha},\end{aligned}$$

with $V(t)$ being the Lyapunov function

$$V(\tilde{x}(t), \tilde{\theta}(t), \tilde{\omega}(t), \tilde{\sigma}(t)) = \tilde{x}^\top(t) P \tilde{x}(t) + \Gamma^{-1}\tilde{\theta}^\top(t)\tilde{\theta}(t) + \Gamma^{-1}\tilde{\omega}^2(t) + \Gamma^{-1}\tilde{\sigma}^2(t),$$

$P = P^\top > 0$, $Q = Q^\top > 0$, $\tilde{x}(t)$ being defined in Section 3.7.2, and $\tilde{\theta}(t) = \hat{\theta}(t) - \theta$, $\tilde{\omega}(t) = \hat{\omega}(t) - \omega$, $\tilde{\sigma}(t) = \hat{\sigma}(t) - \sigma(t)$.

The proof is similar to the one in [39] and is thus omitted.

For an m input n output stable proper transfer function $F(s)$ with impulse response $f(t)$, let

$$\Psi_F(t) = \max_{i=1,\cdots,n} \sqrt{\sum_{j=1}^{m} f_{ij}^2(t)}, \tag{3.56}$$

where $f_{ij}(t)$ is the i^{th} row j^{th} column of the impulse response matrix of $F(s)$.

Lemma 8 ([39]) *Consider an m input n output stable proper transfer function $F(s)$, and let $p(s) = F(s)q(s)$. If $\|q(t)\| \leq \mu(t)$, then $\|p(t)\|_\infty \leq \Psi_F(t) * \mu(t)$, where $*$ is the convolution operation.*

Theorem 5 *Given the system in* (3.53) *and the $\mathcal{L}_1$ adaptive controller with the predictor in* (3.54)*, the following bounds hold for all $t \geq 0$*

$$\|x(t) - x_{\rm ref}(t)\|_\infty \leq \gamma(t)\,, \tag{3.57}$$

$$\|u_{\rm q}(t) - u_{\rm ref}(t)\|_\infty \leq \Psi_{H_4}(t) * \gamma(t) + \Psi_{H_5}(t) * (\rho(t) + \|\tilde{x}_{in}(t)\|) + \Psi_{H_6}(t) * (\omega_u - \omega_l)\frac{1}{2}l + \frac{1}{2}l, \tag{3.58}$$

where $\tilde{x}_{in}(t)$ is the inverse Laplace transform of $\tilde{x}_{in}(s)$, Ψ_{H_i} is defined in (3.56)*, and*

$$\begin{aligned}
&\tilde{x}_{in}(s) = (s\mathbb{I} - A_m)^{-1}(\hat{x}_0 - x_0)\,,\\
&\gamma(t) = \Psi_{H_1}(t) * (\rho(t) + \|\tilde{x}_{in}(t)\|) + \Psi_{H_2}(t) * (\omega_u - \omega_l)\frac{1}{2}l + \Psi_{H_3}(t) * |\omega|\frac{1}{2}l\,,\\
&H_1(s) = (\mathbb{I} - G(s)\theta^\top)^{-1}C(s)\,, \quad H_2(s) = H_1(s)H(s)\,,\\
&G(s) = H(s)(1 - C(s))\,, \quad H(s) = (s\mathbb{I} - A_m)^{-1}b\,,\\
&H_3(s) = (\mathbb{I} - G(s)\theta^\top)^{-1}H(s)\,, \quad H_4(s) = -\frac{C(s)\theta^\top}{\omega}\,,\\
&H_5(s) = \frac{C(s)}{\omega}\frac{1}{c_o^\top H(s)}c_o^\top\,, \quad H_6(s) = H_5(s)H(s)\,.
\end{aligned}$$

Proof. See Appendix B.5.

3.9 Simulation

Consider the system

$$\begin{aligned}
\dot{x}(t) =& A_m x(t) + B_m\omega u_{\rm q}(t) + f_\Delta(x(t), z(t), t)\,,\\
y(t) =& Cx(t)\,,\ u_{\rm q}(t) = Q(u(t))\,,\ x(0) = [0\ 0\ 0]^\top,
\end{aligned}$$

where

$$A_m = \begin{bmatrix} -1 & 0 & 0 \\ 0 & 0 & 1 \\ 0 & -1 & -1.8 \end{bmatrix}, B_m = \begin{bmatrix} 1 & 0 \\ 0 & 0 \\ 1 & 1 \end{bmatrix}, \tag{3.59}$$

$$C = \begin{bmatrix} 1 & 0 & 0 \\ 0 & 1 & 0 \end{bmatrix}, \ \omega = \begin{bmatrix} 1 & -0.2 \\ -0.2 & 1.1 \end{bmatrix}, \tag{3.60}$$

while $\omega \in \mathbb{R}^{2\times 2}$ is assumed to be within the convex set

$$\Omega = \{\omega | \omega = \omega^\top, \omega_{11} \in [1, 1.3], \omega_{12} \in [-0.2, 0.1], \omega_{22} \in [1, 1.3]\}.$$

The (unknown) nonlinear function f_Δ is given by

$$f_\Delta(x, z, t) = \begin{bmatrix} 0.033x^\top x + 0.1 \tanh(\frac{1}{2}x_1)x_1 + 0.1z^2 \\ -0.015x_3^2 - 0.01(1 - \mathrm{e}^{-0.3t}) + 0.05z \\ -0.1x_3 \cos(t) + 0.1z^2 \end{bmatrix}.$$

The internal unmodeled dynamics are given by

$$\begin{aligned} \dot{x}_{z1}(t) =& x_{z2}(t) \\ \dot{x}_{z2}(t) =& -0.3 \sin x_{z1}(t) - 0.7x_{z2}(t), \\ z(t) =& 0.25 \left(x_{z1}(t) - x_{z2}(t)\right) + z_u(t) \\ z_u(s) =& \frac{-s+1}{\frac{s^2}{0.1^2} + \frac{0.8s}{0.1} + 1} \begin{bmatrix} \frac{1}{5} & -\frac{1}{10} & \frac{1}{5} \end{bmatrix} x(s), \end{aligned}$$

where $[x_{z1}(0)\ x_{z2}(0)] = [-0.1\ 0.1]$, $L_z = 0.8465$, $B_z = 0.05$.

In the implementation of the $\mathcal{L}_1$ controller, we set $Q = \mathbb{I}_3$,

$$\Gamma = 10^4, \quad D(s) = \frac{1}{s(\frac{s}{25}+1)(\frac{s}{70}+1)(\frac{s^2}{40^2}+\frac{1.8s}{40}+1)}\mathbb{I}_2,$$
$$K = \begin{bmatrix} 8 & 0 \\ 0 & 8 \end{bmatrix}, \quad K_g(s) \equiv K_g = -(CA_m^{-1}B_m)^{-1} = \begin{bmatrix} 1 & 0 \\ -1 & 1 \end{bmatrix}.$$

From this selection of $D(s)$ and K we can compute the norms in (3.26):

$$\max_{\omega\in\Omega} \{\|G_m(s)\|_{\mathcal{L}_1} + \|G_{um}(s)\|_{\mathcal{L}_1}\ell_0\} = 0.7125,$$

$$\max_{\omega\in\Omega}\{\|H_{xm}(s)C(s)K_g(s)\|_{\mathcal{L}_1}\|r\|_{\mathcal{L}_\infty}\} = 0.3188,$$

and $\|s(s\mathbb{I}-A_m)^{-1}\|_{\mathcal{L}_1} = 2.1004$. There exists $\rho_{x_r} = 1$, such that $\forall\omega\in\Omega$

$$\begin{aligned}\|G_m(s)\|_{\mathcal{L}_1} + \|G_{um}(s)\|_{\mathcal{L}_1}\ell_0 &\leq 0.7125\\ &< \frac{\rho_{x_r} - 0.3188 - \|s(s\mathbb{I}-A_m)^{-1}\|_{\mathcal{L}_1}\rho_0}{L_{1\rho_{x_r}}\rho_{x_r}+B_0}(=0.7534)\\ &< \frac{\rho_{x_r} - \|H_{xm}(s)C(s)K_g(s)\|_{\mathcal{L}_1}\|r\|_{\mathcal{L}_\infty} - \|s(s\mathbb{I}-A_m)^{-1}\|_{\mathcal{L}_1}\rho_0}{L_{1\rho_{x_r}}\rho_{x_r}+B_0},\end{aligned}$$

where $\bar{\rho}_{x_r} = 1.3$, $\rho_0 = 0.01$, $L_{1\rho_x} = 0.8661$, $L_{2\rho_x} = 0.0533$, $B_{10} = 0.01$, $B_{20} = 0$. This verifies that the selected $D(s)$ and K ensure that the $\mathcal{L}_1$ norm condition in (3.26) holds.

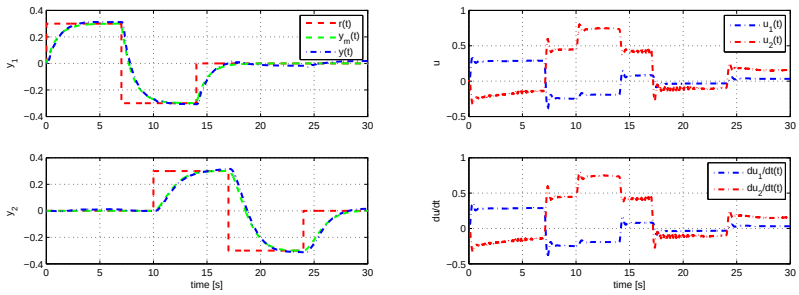

Figure 3.9: $y(t)$, $y_m(t)$ and $r(t)$ for step references $r(t) = [0.3u(t) - 0.6u(t-7) + 0.3u(t-14)\ 0.3u(t-10) - 0.6u(t-17) + 0.6(t-24)]^\top$ with uniform quantizer, $l = 0.05$.

The projection bounds can be chosen conservatively as

$$\begin{aligned}&\hat{\theta}_1(t) \in [-0.8661, 0.8661]\mathbf{1}_m\,,\ \hat{\sigma}_1(t) \in [-5,5]\mathbf{1}_m\,,\\ &\hat{\theta}_2(t) \in [-0.0533, 0.0533]\mathbf{1}_{(n-m)},\ \hat{\sigma}_2(t) \in [-5,5]\mathbf{1}_{(n-m)},\\ &\hat{\omega}_{11}(t), \hat{\omega}_{22}(t) \in [0.25, 3]\,,\ \hat{\omega}_{12}(t), \hat{\omega}_{21}(t) \in [-0.2, 0.2]\,,\end{aligned}$$

where $\mathbf{1}_r \in \mathbb{R}^r$ represents the vector with all elements being 1. With this design, the closed-loop performance is shown in Figure 3.9. The $\mathcal{L}_1$ controller drives the closed-loop system response close to the desired system response $y_m(t)$, as stated in the control objective.

Now consider another plant, where f_Δ is the following (unknown) nonlinear

function:

$$f_\Delta(x,z,t)=A_\Delta x(t)+\begin{bmatrix} \frac{1}{3}x^\top x+\tanh(\frac{1}{2}x_1)x_1+z \\ \frac{1}{2}\text{sech}(x_2)x_2-\frac{1}{5}x_3^2-\frac{1}{2}(1-\mathrm{e}^{-0.3t})+\frac{1}{2}z \\ -x_3\cos(t)+z^2 \end{bmatrix},$$

$$A_\Delta = \begin{bmatrix} 0.2 & -0.2 & -0.3 \\ 0.1 & -0.4 & 0.3 \\ -0.1 & 0 & -0.9 \end{bmatrix}.$$

The internal unmodeled dynamics are given by

$$\begin{aligned} \dot{x}_{z1}(t) =& x_{z2}(t) \\ \dot{x}_{z2}(t) =& -x_{z1}(t)+0.8\left(1-x_{z1}^2(t)\right)x_{z2}(t), \\ z(t) =& 0.1\left(x_{z1}(t)-x_{z2}(t)\right) + z_u(t) \\ z_u(s) =& \frac{-s+1}{\frac{s^2}{0.1^2}+\frac{0.8s}{0.1}+1}\begin{bmatrix} 1 & -2 & 1 \end{bmatrix}x(s), \end{aligned}$$

with $[x_{z1}(0)\ x_{z2}(0)] = [x_{z1_0}\ x_{z2_0}]$.

We choose conservatively $L_{1\rho_x} = L_{2\rho_x} = 40$ and $B_{10} = B_{20} = 5$, and let the other parameters be defined as in the previous case. The projection bounds can be chosen as

$$\begin{aligned} &\hat{\theta}_1(t) \in [-40,\ 40]\mathbf{1}_m, \quad \hat{\sigma}_1(t) \in [-5,\ 5]\mathbf{1}_m, \\ &\hat{\theta}_2(t) \in [-40,\ 40]\mathbf{1}_{(n-m)}, \quad \hat{\sigma}_2(t) \in [-5,\ 5]\mathbf{1}_{(n-m)}, \\ &\hat{\omega}_{11}(t), \hat{\omega}_{22}(t) \in [0.25,\ 3], \ \ \hat{\omega}_{12}(t), \hat{\omega}_{21}(t) \in [-0.2,\ 0.2], \end{aligned}$$

where $\mathbf{1}_r \in \mathbb{R}^r$ is the vector with all elements being 1.

The next two figures show the system performance with logarithmic quantization.

Plots in Figure 3.10 show the cases where the reference signal is the sum of step functions. In both cases, the reference signal has different amplitudes in different channels, and the system output tracks the desired signal. When the quantization is coarse, the tracking error is larger. When the quantization is sufficiently dense, the tracking error is reduced and is close to the case without quantization.

Figure 3.11 shows the performance of $\mathcal{L}_1$ adaptive controller in the presence of unmodeled dynamics and unmatched uncertainties. We compare the case using

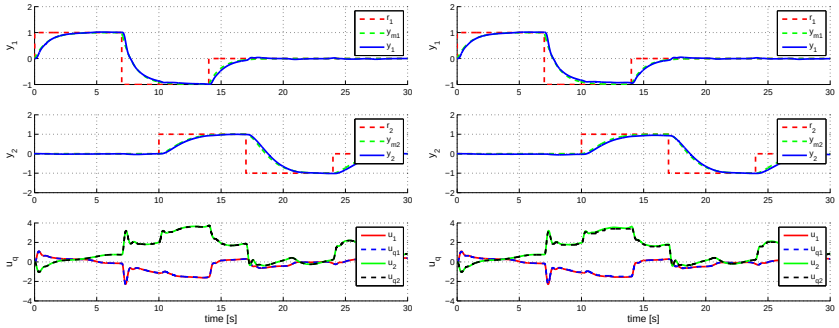

Figure 3.10: $y(t)$, $y_m(t)$ and $r(t)$ for step references $r(t) = [u(t) - 2u(t-7) + u(t-14)\ u(t-10) - 2u(t-17) + u(t-24)]^\top$ with logarithmic quantizer, $\rho = 0.99$ and $\rho = 0.95$, respectively.

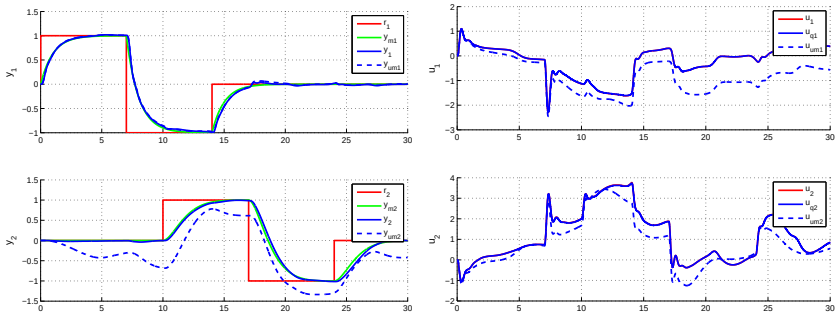

Figure 3.11: Performance of $\mathcal{L}_1$ controller with logarithmic quantization ($\rho = 0.99$) and step reference.

the $\mathcal{L}_1$ adaptive controller (solid line) with the case without the compensation term ($\hat{\eta}_{2m}(t)$ in (3.33)) for the unmatched uncertainty in the control law (dashed line). Without this term, the system output significantly deviates from the ideal response to the step reference. This demonstrates the significance of the compensation term.

These figures also show the tracking of different steps. For different amplitudes of steps, the controller provides scaled control signals and scaled system outputs, per (3.47), consistently with the properties of $\mathcal{L}_1$ adaptive control theory.

Figure 3.12 shows the system response to sinusoidal reference signals. For uniform quantization, the results are similar, as shown in Figure 3.13.

Further, we vary the unmodeled dynamics and the nonlinear function f_Δ. For instance, in Figure 3.14, we show the simulation results with the following param-

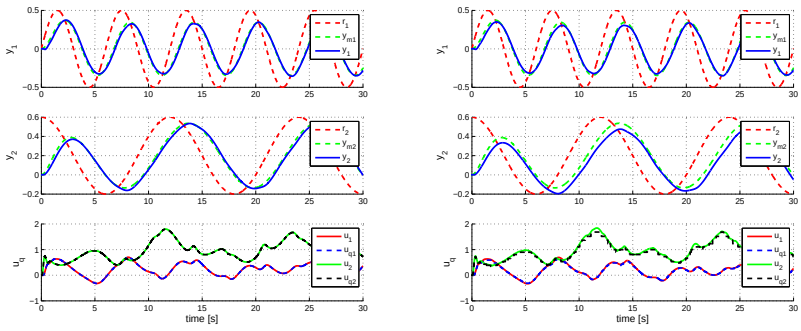

(a) $\rho = 0.99$ (b) $\rho = 0.9$

Figure 3.12: $y(t)$, $y_m(t)$ and $r(t)$ for sinusoidal references $r(t) = [0.5\sin(\frac{\pi}{3}t)\ 0.2 + 0.8\cos(\frac{\pi}{6}t)]^\top$ and logarithmic quantizer.

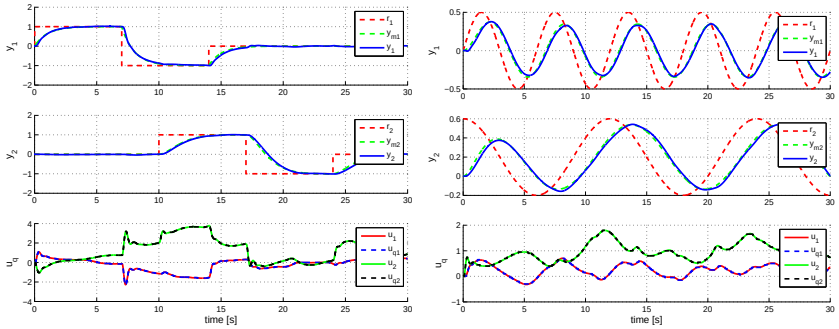

Figure 3.13: $y(t)$, $y_m(t)$ and $r(t)$ for uniform quantizer ($l = 0.05$), with step references and sinusoidal references, respectively.

eters:

$$A_\Delta = \begin{bmatrix} 0.1 & -0.4 & 0.5 \\ -0.5 & 0.5 & 0 \\ -0.2 & 0.3 & 0.5 \end{bmatrix}, \quad \omega = \begin{bmatrix} 0.8 & -0.1 \\ 0.1 & 0.8 \end{bmatrix},$$

where the internal unmodeled dynamics are given by

$$\begin{aligned} \dot{x}_{z1}(t) &= 10\,(x_{z2}(t) - x_{z1}(t)) \\ \dot{x}_{z2}(t) &= x_{z1}(t)\,(28 - x_{z3}(t)) - x_{z2}(t) \\ \dot{x}_{z3}(t) &= x_{z1}(t)x_{z2}(t) - \tfrac{8}{3}x_{z3}(t) \\ z(t) &= \tfrac{1}{300}\,(x_{z1}(t) + x_{z2}(t) + x_{z3}(t))\ . \end{aligned} \tag{3.61}$$

Similar to Figure 3.11, where we consider the case without the compensation

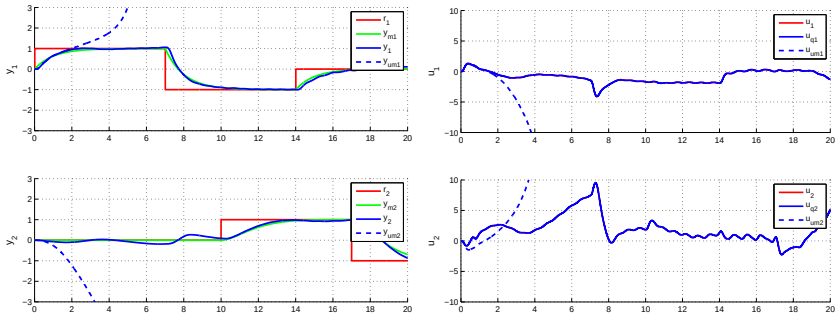

Figure 3.14: Performance of $\mathcal{L}_1$ controller with uniform quantizer ($l = 0.05$) and step reference.

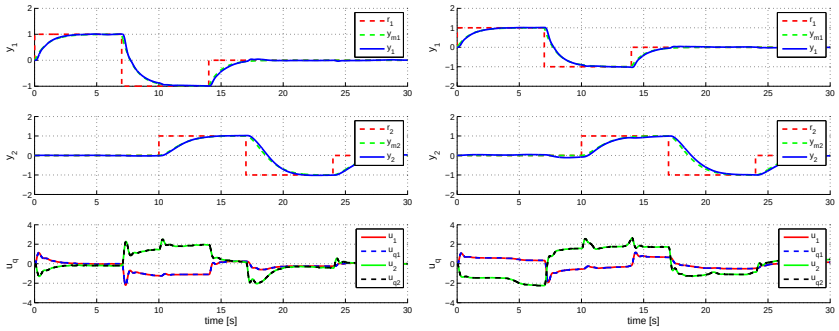

Figure 3.15: $y(t)$, $y_m(t)$ and $r(t)$ for uniform quantizer where $l = 0.05$, with the nonlinear function $f_{\Delta 1}$ and $f_{\Delta 2}$, respectively.

for the unmatched uncertainty (dashed line). In this case of uncertainties, the system becomes unstable.

In the two plots in Figure 3.15, the nonlinear function $f_\Delta(x, z, t)$ in the model is replaced respectively by

$$f_{\Delta 1}(x, z, t) = A_\Delta x(t) + \begin{bmatrix} \tanh(x_1)x_1 \\ \text{sech}(x_2)x_2 \\ -x_3 \cos(\frac{1}{2}t) + z^2 \end{bmatrix},$$

$$f_{\Delta 2}(x, z, t) = A_\Delta x(t) + \begin{bmatrix} x_3^3 \\ z^2 + z \\ \sin x_1 \cos(x_2^2) \end{bmatrix},$$

while all other parameters are the same as in Figure 3.10.

Figures 3.14 and 3.15 show the cases with different internal unmodeled dynamics and nonlinear functions. The $\mathcal{L}_1$ adaptive controller ensures that the system output tracks the desired signal closely and smoothly. We note that in all these

cases we have not redesigned or retuned the $\mathcal{L}_1$ adaptive controller.

3.10 Control and communication synthesis

In this chapter, we have seen input-quantized uncertain systems, the $\mathcal{L}_1$ adaptive controller for quantized systems, and the closed-loop system performance. As shown in Sections 3.4 and 3.8, two critical parameters govern the performance bounds: one is the adaptation rate Γ, while the other is the quantization density. With the explicit performance bounds in mind, given the dynamics of a plant and required error envelope, the performance analysis will in turn guide the design of adaptation rate and quantization density. Thus, the controller parameter and coding schemes are determined.

For example, consider the system in (3.4) with parameters in (3.21) and uniform quantization with interval length l. The closed-loop performance bounds are given by

$$\|e_x\|_{\mathcal{L}_\infty} \leq \gamma_{xu}, \quad \|e_u\|_{\mathcal{L}_\infty} \leq \gamma_{uu},$$

where

$$\begin{aligned}
\gamma_{xu} =& \frac{1}{2} l \left\| \left(\mathbb{I} - G(s)\theta^\top\right)^{-1} H(s) \right\|_{\mathcal{L}_1} \\
&+ \|(\mathbb{I} - G(s)\theta^\top)^{-1}[G(s)\theta^\top + (C(s)-1)\mathbb{I}]\|_{\mathcal{L}_1} \sqrt{\frac{\theta_{2\max}}{\lambda_{\min}(P)\Gamma}}, \\
\gamma_{uu} =& \left\| C(s) \frac{1}{c_o^\top H(s)} c_o^\top \right\|_{\mathcal{L}_1} \sqrt{\frac{\theta_{2\max}}{\lambda_{\min}(P)\Gamma}} + \|C(s)\theta^\top\|_{\mathcal{L}_1} \gamma_{xu} + \frac{1}{2} l \,.
\end{aligned}$$

Compute the $\mathcal{L}_1$ norms of the transfer functions:

$$\begin{aligned}
&\left\| \left(\mathbb{I} - G(s)\theta^\top\right)^{-1} H(s) \right\|_{\mathcal{L}_1} = 1.0777, \\
&\|(\mathbb{I} - G(s)\theta^\top)^{-1}[G(s)\theta^\top + (C(s)-1)\mathbb{I}]\|_{\mathcal{L}_1} = 1.1299, \\
&\left\| C(s) \frac{1}{c_o^\top H(s)} c_o^\top \right\|_{\mathcal{L}_1} = 320.9, \\
&\|C(s)\theta^\top\|_{\mathcal{L}_1} = 8.5.
\end{aligned}$$

Thus, if the closed-loop system state and control are required to stay within $\pm\gamma_1$,

$\pm\gamma_2$ around the reference system state and control, respectively, the adaptation rate Γ and the quantization interval length l need to satisfy

$$0.5389l + \frac{47.4338}{\sqrt{\Gamma}} \leq \gamma_1, \quad 5.0803l + \frac{1.38 \times 10^{-4}}{\sqrt{\Gamma}} \leq \gamma_2.$$

We can visualize the performance with respect to the parameters in Figure 3.16a. For example, if the requirement for the state tracking error is $\gamma_1 = 1$, we see that the parameters selection should be within the upper left corner inside the contour of value 1. One conservative selection could be $l = 0.5$, $\Gamma = 5 \times 10^3$, and by Theorem 1 the corresponding quantization and control are guaranteed to lead the closed-loop system to satisfy the performance requirement.

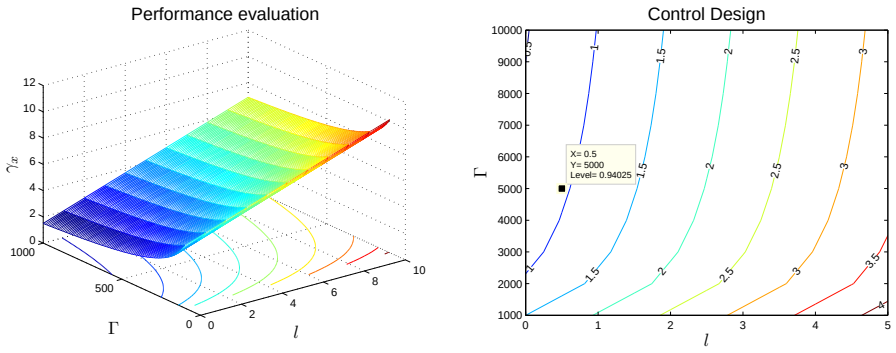

(a) $\gamma_x(l, \Gamma)$ (b) Contour

Figure 3.16: Performance dependence on adaptation rate and input quantization.

CHAPTER 4

STATE FEEDBACK CONTROL FOR STATE-QUANTIZED SYSTEMS

"Knowledge of the self is the mother of all knowledge." –Khalil Gibran

This chapter studies uncertain systems with both state and input quantization. One scenario is a networked control system, where the plant and the controller are connected through a communication network, as shown in Figure 4.1. Specifically, we analyze the quantization effect of the system. To communicate over the network, the state is quantized and sent over the network to the controller. At the other end, the generated control is preprocessed, quantized, and sent to control the plant.

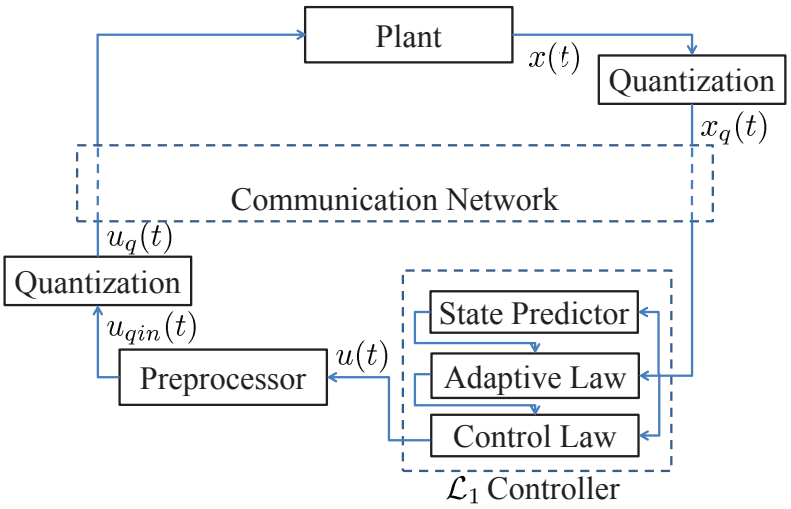

Figure 4.1: Quantized system with $\mathcal{L}_1$ adaptive controller.

For the plant dynamics, we consider two cases, the first part in this chapter is devoted to linear systems with matched uncertainties, while the second half is on more general nonlinear systems with unmatched uncertainties.

4.1 State-quantized systems with matched uncertainties

The first part of this chapter comprised of this and next three sections considers the plant dynamics given by

$$\begin{aligned}\dot{x}(t) =& A_m x(t) + b\left(-\theta^\top x(t) + u_{\rm q}(t)\right), \quad x(0) = x_0,\\ y(t) =& c^\top x(t),\\ x_{\rm q}(t) =& Q_x(x(t)), \quad u_{\rm q}(t) = Q_u(u_{\rm qin}(t)),\end{aligned} \tag{4.1}$$

where A_m is a known $n \times n$ Hurwitz matrix, $b, c \in \mathbb{R}^n$ are known constant vectors, $\theta \in \mathbb{R}^n$ is an unknown constant vector, $x(t) \in \mathbb{R}^n$ is the system state vector (measured), $y(t) \in \mathbb{R}$ is the regulated output, $u_{\rm qin}(t)$ is the designed control signal, and $Q_x(\cdot)$ and $Q_u(\cdot)$ are the quantization functions for state and input respectively.

Assumption 7 *The unknown parameter θ belongs to a given compact convex set Θ_B, $\theta \in \Theta_B$. Let $\theta_{1\max} \triangleq \max_{\theta\in\Theta_B} \|\theta\|_1$.*

The objective is to design an adaptive controller that would compensate for the uncertainties in the system and ensure analytically quantifiable uniform transient and steady-state performance bounds in the presence of both input and state quantization.

4.2 Control design

In this section we present the $\mathcal{L}_1$ adaptive controller for the system in (4.1). In this case, the state predictor, the adaptive law and the control law make use of only quantized-states instead of the real values. The state predictor is adjusted to incorporate the quantization and maintain a structure similar to that of the plant.

We consider the following state predictor:

$$\begin{aligned}\dot{\hat{x}}(t) =& A_m \hat{x}(t) + b(-\hat{\theta}^\top(t) x_{\rm q}(t) + u_{\rm q}(t))\\ \hat{y}(t) =& c^\top \hat{x}(t), \quad \hat{x}(0) = x_0,\end{aligned} \tag{4.2}$$

where $\hat{x}(t) \in \mathbb{R}^n$, $\hat{y}(t) \in \mathbb{R}$ are the state and the output of the state predictor and $\hat{\theta}(t) \in \mathbb{R}^n$ is an estimate of the parameter θ. The projection-type adaptive law for

$\hat{\theta}(t)$ is given by

$$\dot{\hat{\theta}}(t) = \Gamma \mathrm{Proj}(\hat{\theta}(t), x_{\mathrm{q}}(t)\tilde{x}_{\mathrm{q}}^{\top}(t)Pb),\ \hat{\theta}(0) = \hat{\theta}_0, \tag{4.3}$$

where $\tilde{x}_{\mathrm{q}}(t) \triangleq \hat{x}(t) - x_{\mathrm{q}}(t)$ is the error between prediction and quantized state, $\Gamma > 0$ is the adaptation rate, $\mathrm{Proj}(\cdot,\cdot)$ denotes the projection operator (Definition 3), which ensures that $\hat{\theta}(t) \in \Theta_B$ for all $t \geq 0$, and $P = P^{\top} > 0$ solves the algebraic Lyapunov equation $A_m^{\top}P + PA_m = -Q$ for some symmetric $Q > 0$. The control signal is defined by

$$u(s) = C(s)\left(\hat{\eta}_{\mathrm{q}}(s) + k_g r(s)\right)\ ,\ u_{\mathrm{qin}}(t) = f(u(t)), \tag{4.4}$$

where $k_g \triangleq 1/(c^{\top}H(0))$, $H(s) \triangleq (s\mathbb{I} - A_m)^{-1}b$, $\hat{\eta}_{\mathrm{q}}(t) \triangleq \hat{\theta}^{\top}(t)x_{\mathrm{q}}(t)$, $u_{\mathrm{qin}}(t)$ is a modified control signal, and the function f is selected according to an appropriate quantization method, while $C(s)$ is a BIBO stable and strictly proper transfer function with DC gain $C(0) = 1$, and its state-space realization assumes zero initialization. Let

$$G(s) \triangleq H(s)(C(s) - 1)\,. \tag{4.5}$$

The $\mathcal{L}_1$ adaptive controller consists of (4.2) - (4.4), with $C(s)$ verifying the following upper bound for the $\mathcal{L}_1$ norm of $G(s)$

$$\lambda \triangleq \|G(s)\|_{\mathcal{L}_1}\theta_{1\,\max} < 1. \tag{4.6}$$

4.3 Performance analysis

4.3.1 Stability of reference system

In order to compare the closed-loop system performance, we use the reference system introduced in (3.10) and (3.11), whose stability is established in Lemma 12.

By Lemma 12, the two transfer functions $(\mathbb{I}-G(s)\theta^{\top})^{-1}$ and $(\mathbb{I}-G(s)\theta^{\top})^{-1}G(s)$

are BIBO stable. Let

$$\begin{aligned}\rho_{x_r} &\triangleq k_g\|(\mathbb{I}-G(s)\theta^\top)^{-1}H(s)C(s)\|_{\mathcal{L}_1}\|r\|_{\mathcal{L}_\infty}\\ &\quad+\|(\mathbb{I}-G(s)\theta^\top)^{-1}\|_{\mathcal{L}_1}\|(s\mathbb{I}-A_m)^{-1}x_0\|_{\mathcal{L}_\infty},\\ \rho_{u_r} &\triangleq \|C(s)\theta^\top\|_{\mathcal{L}_1}\rho_{x_r}+k_g\|r\|_{\mathcal{L}_\infty},\end{aligned}$$

and the bounds in (3.13) and (3.14) can be written as

$$\|x_{\rm ref}\|_{\mathcal{L}_\infty}\le\rho_{x_r},\quad \|u_{\rm ref}\|_{\mathcal{L}_\infty}\le\rho_{u_r}, \tag{4.7}$$

4.3.2 Prediction error

Let $\tilde{x}(t)\triangleq\hat{x}(t)-x(t)$, and $\tilde{\theta}(t)\triangleq\hat{\theta}(t)-\theta$. From (4.1) and (4.2), we have the prediction error dynamics

$$\dot{\tilde{x}}(t)=A_m\tilde{x}(t)+b\big(\theta^\top x(t)-\hat{\theta}^\top(t)x_{\rm q}(t)\big),\tilde{x}(0)=0\,. \tag{4.8}$$

Consider the Lyapunov function

$$V(t)=\tilde{x}^\top(t)P\tilde{x}(t)+\tilde{\theta}(t)^\top\Gamma^{-1}\tilde{\theta}(t),$$

where P and Γ are defined in (4.3). Take the derivative of $V(t)$ and substitute (4.8) into $\dot{V}(t)$ to get

$$\begin{aligned}\dot{V}(t)=&\tilde{x}(t)^\top A_m^\top P\tilde{x}(t)+\tilde{x}(t)^\top PA_m\tilde{x}(t)\\ &-2\tilde{x}(t)^\top Pb\tilde{\theta}(t)^\top x_{\rm q}(t)-2\tilde{x}(t)^\top Pb\theta^\top x_{\rm qe}(t)+2\tilde{\theta}^\top\Gamma^{-1}\dot{\tilde{\theta}}\,,\end{aligned}$$

Note that

$$\tilde{x}(t)=\hat{x}(t)-x(t)=\hat{x}(t)-x_{\rm q}(t)+x_{\rm q}(t)-x(t)=\tilde{x}_{\rm q}(t)+x_{\rm qe}(t),$$

where $x_{\rm qe}(t)=x_{\rm q}(t)-x(t)$ is the quantization error of the system state and $\tilde{x}_{\rm q}(t)$ is defined in (4.3). Then the derivative of $V(t)$ can be written as

$$\begin{aligned}\dot{V}(t)=&\tilde{x}(t)^\top A_m^\top P\tilde{x}(t)+\tilde{x}(t)^\top PA_m\tilde{x}(t)-2\tilde{x}_{\rm q}(t)^\top Pb\tilde{\theta}(t)^\top x_{\rm q}(t)\\ &+2\tilde{\theta}^\top\Gamma^{-1}\dot{\tilde{\theta}}-2x_{\rm qe}(t)^\top Pb\tilde{\theta}(t)^\top x_{\rm q}(t)-2\tilde{x}(t)^\top Pb\theta^\top x_{\rm qe}(t)\,.\end{aligned}$$

The design of adaptive law in (4.3) ensures that

$$\dot{V}(t) \leq -\tilde{x}(t)^\top Q\tilde{x}(t) - 2x_{\rm qe}(t)^\top Pb\tilde{\theta}(t)^\top x_{\rm q}(t) - 2\tilde{x}(t)^\top Pb\theta^\top x_{\rm qe}(t)\,, \quad (4.9)$$

where $\theta_{1\max}$ is defined in Assumption 9, $\tilde{\theta}_{1\max} \triangleq \max_{\theta_a\in\Theta_B}$.

Following the Lyapunov analysis and the bounds on the quantization errors we have the following lemma.

Lemma 9 *For the system in (4.1) and the controller defined by (4.4), if $\|x_t\|_{\mathcal{L}_\infty} \leq \rho_x$ and the state quantization is the hysteresis quantization with quantization interval length d_x, we have the following bound*

$$\|\tilde{x}_t\|_{\mathcal{L}_\infty} \leq \max\left\{\sqrt{\frac{\theta_{2\max}}{\lambda_{\min}(P)\Gamma}}, c_{\tilde{x}hu}(d_x,\rho_x)\right\}\,, \quad (4.10)$$

$$c_{\tilde{x}hu}(d_x,\rho_x) \triangleq \frac{\|Pb\|_2\theta_{1\max}d_x + \sqrt{c_{\Delta hu}(d_x,\rho_x)}}{2\lambda_{\min}(Q)}\,, \quad (4.11)$$

$$c_{\Delta hu}(d_x,\rho_x) \triangleq (\|Pb\|_2\theta_{1\max}d_x)^2 + 4\lambda_{\min}(Q)d_x\|Pb\|_1\tilde{\theta}_{1\max}\left(\rho_x + \frac{1}{2}d_x\right), \quad (4.12)$$

where $\theta_{1\max}$ is given in Assumption 9, $\theta_{2\max} \triangleq 4\max_{\theta_a\in\Theta_B}\|\theta\|_2^2$.

4.3.3 Performance bounds

Let the error signals be defined by

$$e_x(t) = x(t) - x_{\rm ref}(t)\,,\ e_u(t) = u_{\rm q}(t) - u_{\rm ref}(t)\,. \quad (4.13)$$

Let $\bar{\gamma}_{xhu} > 0$ be an arbitrary positive number, and let

$$\rho_{xhu} = \rho_{x_r} + \bar{\gamma}_{xhu}\,, \quad (4.14)$$

$$\begin{aligned}
\gamma_{xhu} &= \gamma_{xohu} + \gamma_{xqhu} + \epsilon\,, \quad (4.15)\\
\gamma_{xohu} &= \|(\mathbb{I} - G(s)\theta^\top)^{-1}[G(s)\theta^\top + (C(s)-1)\mathbb{I} + \mathbb{I}]\|_{\mathcal{L}_1}\\
&\qquad \max\left\{\sqrt{\tfrac{\theta_{2\max}}{\lambda_{\min}(P)\Gamma}}, c_{\tilde{x}hu}(d_x,\rho_{xhu})\right\}\,,\\
\gamma_{xqhu} &= \frac{1}{2}\|(\mathbb{I} - G(s)\theta^\top)^{-1}H(s)\|_{\mathcal{L}_1}d_u\,,
\end{aligned}$$

where $\epsilon > 0$ is a small positive number, $c_{\tilde{x}hu}(d_x, \rho_{xhu})$ is defined in (4.11), and d_x and d_u are the quantization interval lengths of the hysteresis quantization on x and u, respectively. If Γ is sufficiently large, and d_x and d_u are sufficiently small, such that $\gamma_{xhu} = \gamma_{xohu} + \gamma_{xqhu} + \epsilon < \bar{\gamma}_{xhu}$, the error $e_x(t)$ is strictly upper bounded by

$$\|e_{x'_t}\|_{\mathcal{L}_\infty} < \gamma_{xhu} < \bar{\gamma}_{xhu} \,.$$

Similarly, let

$$\rho_{uhu} = \rho_{u_r} + \gamma_{uhu} \,, \tag{4.16}$$

where

$$\gamma_{uhu} = \|C(s)\theta^\top\|_{\mathcal{L}_1}\gamma_{xhu} + \Big\|C(s)\frac{1}{c_o^\top H(s)}c_o^\top\Big\|_{\mathcal{L}_1}\max\Big\{\sqrt{\tfrac{\theta_{2\max}}{\lambda_{\min}(P)\Gamma}}, c_{\tilde{x}hu}(d_x, \rho_{xhu})\Big\}. \tag{4.17}$$

Theorem 6 *Consider the system in (4.1) and the controller in (4.4). In the case of hysteresis quantization, if the quantization interval lengths are d_x and d_u for the state and the input, respectively, then the tracking errors are upper bounded by*

$$\begin{aligned} &\|x - x_{\rm ref}\|_{\mathcal{L}_\infty} \le \gamma_{xhu} \,, \quad \|u - u_{\rm ref}\|_{\mathcal{L}_\infty} \le \gamma_{uhu} \,, \\ &\|x\|_{\mathcal{L}_\infty} \le \rho_{xhu}, \quad \|u\|_{\mathcal{L}_\infty} \le \rho_{uhu} \,, \end{aligned} \tag{4.18}$$

where ρ_{xhu}, γ_{xhu}, ρ_{uhu}, γ_{uhu} are given by (4.14)*,* (4.15)*,* (4.16) *and* (4.17)*.*

Proof. See Appendix B.6.

4.4 Simulation

Consider the system in (4.1) with

$$A_m = \begin{bmatrix} 0 & 1 \\ -1 & -1.4 \end{bmatrix}, \; b = \begin{bmatrix} 0 \\ 1 \end{bmatrix}, \; c = \begin{bmatrix} 1 \\ 0 \end{bmatrix}, x_0 = \begin{bmatrix} 1 \\ 1 \end{bmatrix}, \; \theta = \begin{bmatrix} 4 \\ -4.5 \end{bmatrix},$$

and let $\Theta_B = \{\theta_1 \in [-10, 10], \theta_2 \in [-10, 10]\}$, which gives $\theta_{1\max} = 20$. Let $C(s) = \frac{\omega}{s+\omega}$, where $\omega = 50$, and let the adaptation rate be $\Gamma = 10^6$.

We now show the performance of $\mathcal{L}_1$ adaptive controller with hysteresis quantization under different reference signals without any retuning of the controller.

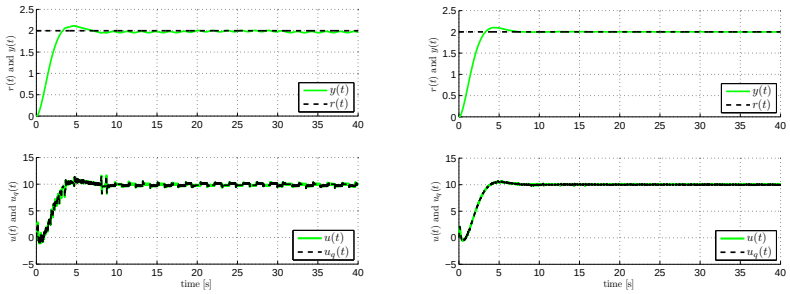

(a) $d_x = 0.1$, $d_u = 0.2$ (b) $d_x = 0.01$, $d_u = 0.02$

Figure 4.2: $y(t)$ and $u(t)$ with step references $r(t) = 2$.

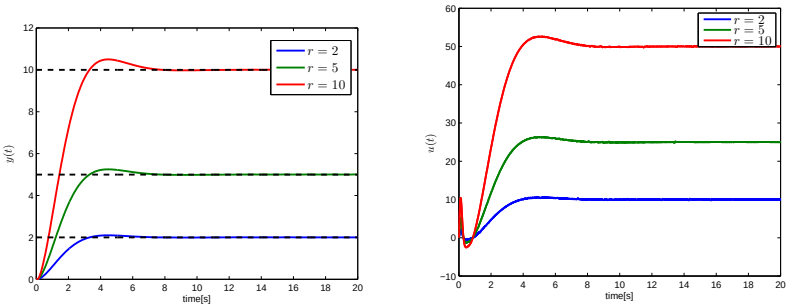

(a) $y(t)$ (b) $u(t)$

Figure 4.3: $y(t)$ and $u(t)$ with $d_x = 0.01$, $d_u = 0.02$ and step references $r(t) = 2\,, 5\,, 10$.

First, we see that with hysteresis quantization for both state and input signals the system output $y(t)$ tracks the reference signal $r(t)$. Figure 4.2a shows the output of the system with uniform quantization, tracking a step reference signal. In both cases, the designed $\mathcal{L}_1$ controller leads to desired performance in the whole time span, as guaranteed by the uniform transient performance bounds derived in Section 4.3.

Second, the comparison of Figures 4.2a and 4.2b shows the effect of quantization density on the system performance. In Figure 4.2a, a small tracking error is visible between $y(t)$ and $r(t)$. In the latter case in Figure 4.2b, where the quantization interval lengths are reduced to $\frac{1}{10}$ of the former values, the quantization becomes finer. The output $y(t)$ almost coincides with $r(t)$. This shows that the performance bound decreases as the quantization density increases.

Next, we show the scaled response of the closed-loop system to different reference signals. Figures 4.3a and 4.3b show the performance of the system output $y(t)$ and the input $u(t)$ in the case of uniform quantization with quantization intervals $d_x = 0.01$, $d_u = 0.02$ and step references $r = 2\,, 5\,, 10$. We note that it leads to scaled control inputs and system outputs for scaled reference inputs.

We finally notice that we do not redesign or retune the $\mathcal{L}_1$ controller in these simulations, from one reference input to another, or from one quantizer to the other.

4.5 State-quantized systems with unmatched uncertainties

In this and the next three sections, we consider the system dynamics described by:

$$\dot{x}(t) = A_m x(t) + B_m \omega u_{\mathrm{q}}(t) + f(x(t), z(t), t)\,,\ x(0) = x_0\,, \tag{4.19a}$$

$$\dot{x}_z(t) = g\left(x_z(t), x(t), t\right)\,, \quad x_z(0) = x_{z0}\,, \tag{4.19b}$$

$$z(t) = g_o\left(x_z(t), t\right)\,, \tag{4.19c}$$

$$y(t) = Cx(t)\,, \tag{4.19d}$$

$$u_{\mathrm{q}}(t) = Q_u(u(t))\,, \tag{4.19e}$$

$$x_{\mathrm{q}}(t) = Q_x(x(t)) \tag{4.19f}$$

where $x(t) \in \mathbb{R}^n$ is the system state vector; $u_{\mathrm{q}}(t) \in \mathbb{R}^m$ ($n \geq m$) is the quantized control signal; $y(t) \in \mathbb{R}^m$ is the regulated output; A_m is a known Hurwitz $n \times n$ matrix; $B_m \in \mathbb{R}^{n\times m}$ and $C \in \mathbb{R}^{m\times n}$ are known constant matrices, with $\mathrm{rank}(B_m) = m$; $\omega \in \mathbb{R}^{m\times m}$ is the unknown high-frequency gain matrix; $z(t)$ and $x_z(t)$ are the output and the state vector of internal unmodeled dynamics, defined in (4.19b) and (4.19c), respectively; $f(\cdot)$ $g_o(\cdot)$, and $g(\cdot)$ are unknown nonlinear functions, Lipschitz continuous in x, z, x_z, respectively, and continuous in t; $u(t)$ is the designed control signal; x_{q} is the quantized state used by the controller as feedback signal; and $Q_u(\cdot)$ and $Q_x(\cdot)$ are the input and state quantization functions, respectively (Quantization schemes introduced in Section 2.3 and Section 2.4.). The initial condition x_0 is assumed to be inside a known set, specifically $\|x_0\|_\infty \leq \rho_0$ with known $\rho_0 > 0$.

State equation (4.19a) can be rewritten as

$$\begin{aligned}\dot{x}(t) =& A_m x(t) + B_m\left(\omega u_{\mathrm{q}}(t) + f_1(x(t), z(t), t)\right) + B_{um} f_2(x(t), z(t), t)\,,\\ x(0) =& x_0\,,\end{aligned} \tag{4.20}$$

where $B_{um} \in \mathbb{R}^{n\times(n-m)}$ is a constant matrix such that

$$B_m^\top B_{um} = 0, \quad \operatorname{rank}([B_m\ B_{um}]) = n,$$

and $f_1(\cdot)$, $f_2(\cdot)$ are unknown nonlinear functions such that

$$\begin{bmatrix} f_1(x(t), z(t), t) \\ f_2(x(t), z(t), t) \end{bmatrix} = \begin{bmatrix} B_m & B_{um} \end{bmatrix}^{-1} f(x(t), z(t), t)\,.$$

Here $f_1(\cdot)$ represents the matched part of the uncertain function $f(\cdot)$, whereas $B_{um} f_2(\cdot)$ represents the unmatched part (cross-coupling dynamics).

Assume that Assumptions 2-6 hold. Given a piecewise continuous, bounded reference signal $r(t)$, the control objective is to design an adaptive state feedback controller for the quantized system to ensure that $y(t)$ tracks the output response $y_m(t)$ of the following system:

$$M(s) \triangleq C\left(s\mathbb{I} - A_m\right)^{-1} B_m K_g(s),$$

both in transient and steady-state, where $K_g(s)$ is a feedforward prefilter.

4.6 Control design

State predictor: We consider the following state predictor

$$\begin{aligned}\dot{\hat{x}}(t) =& A_m\hat{x}(t) + B_m(\hat{\omega}(t)u_{\mathrm{q}}(t) + \hat{\theta}_1(t)\|x_{\mathrm{q}_t}\|_{\mathcal{L}_\infty} + \hat{\sigma}_1(t))\\ &+ B_{um}(\hat{\theta}_2(t)\|x_{\mathrm{q}_t}\|_{\mathcal{L}_\infty} + \hat{\sigma}_2(t)),\ \hat{x}(0) = x_0,\end{aligned} \tag{4.21}$$

where $\hat{\omega}(t) \in \mathbb{R}^{m\times m}$, $\hat{\theta}_1(t) \in \mathbb{R}^m$, $\hat{\sigma}_1(t) \in \mathbb{R}^m$, $\hat{\theta}_2(t) \in \mathbb{R}^{n-m}$, and $\hat{\sigma}_2(t) \in \mathbb{R}^{n-m}$ are the adaptive estimates.

Adaptive laws: The adaptation laws for $\hat{\omega}(t)$, $\hat{\theta}_1(t)$, $\hat{\sigma}_1(t)$, $\hat{\theta}_2(t)$, and $\hat{\sigma}_2(t)$ are defined as

$$
\begin{aligned}
\dot{\hat{\omega}}(t) &= \Gamma \mathrm{Proj}(\hat{\omega}(t), -(\tilde{x}_{\mathrm{q}}^{\top}(t) P B_m)^{\top} u_{\mathrm{q}}^{\top}(t)), \\
\dot{\hat{\theta}}_1(t) &= \Gamma \mathrm{Proj}(\hat{\theta}_1(t), -(\tilde{x}_{\mathrm{q}}^{\top}(t) P B_m)^{\top} \|x_{\mathrm{q}_t}\|_{\mathcal{L}_\infty}), \\
\dot{\hat{\theta}}_2(t) &= \Gamma \mathrm{Proj}(\hat{\theta}_2(t), -(\tilde{x}_{\mathrm{q}}^{\top}(t) P B_{um})^{\top} \|x_{\mathrm{q}_t}\|_{\mathcal{L}_\infty}), \\
\dot{\hat{\sigma}}_1(t) &= \Gamma \mathrm{Proj}(\hat{\sigma}_1(t), -(\tilde{x}_{\mathrm{q}}^{\top}(t) P B_m)^{\top}), \\
\dot{\hat{\sigma}}_2(t) &= \Gamma \mathrm{Proj}(\hat{\sigma}_2(t), -(\tilde{x}^{\top}(t) P B_{um})^{\top}),
\end{aligned} \tag{4.22}
$$

where $\hat{\omega}(0) = \hat{\omega}_0$, $\hat{\theta}_i(0) = \hat{\theta}_{i_0}$, $\hat{\sigma}_i(0) = \hat{\sigma}_{i_0}$, $i = 1, 2$; $\tilde{x}_{\mathrm{q}}(t) = \hat{x}(t) - x_{\mathrm{q}}(t)$; $\Gamma \in \mathbb{R}^+$ is the adaptation gain; $P = P^{\top} > 0$ is the solution to the algebraic Lyapunov equation $A_m^{\top} P + P A_m = -Q$, $Q = Q^{\top} > 0$; and the projection operator $\mathrm{Proj}(\cdot, \cdot)$ is given in Definition 3 in the Appendix. The projection operator ensures that $\hat{\omega}(t) \in \Omega$, $\|\hat{\theta}_i(t)\|_\infty \leq \theta_{b_i}$, $\|\hat{\sigma}_i(t)\|_\infty \leq \sigma_{b_i}$, $i = 1, 2$, for all $t > 0$, where θ_{b_i} and σ_{b_i} depend on the bounds of x in different cases (defined in (3.36)).

Control law: We first design the control signal $u(t)$, and the input for the quantization $u_{\mathrm{qin}}(t)$ is designed according to different types of quantizers. The control law is generated by

$$
u(t) = -K D(s) \hat{\eta}_{\mathrm{q}}(s)\,, \tag{4.23}
$$

where $\hat{\eta}_{\mathrm{q}}(s)$ is the Laplace transform of the signal

$$
\hat{\eta}_{\mathrm{q}}(t) = \hat{\omega}(t) u(t) + \hat{\eta}_{1\mathrm{q}}(t) + \hat{\eta}_{2m\mathrm{q}}(t) - r_g(t)\,, \tag{4.24}
$$

with $r_g(s) = K_g(s) r(s)$, $\hat{\eta}_{2m\mathrm{q}}(s) = H_m^{-1}(s) H_{um}(s) \hat{\eta}_{2\mathrm{q}}(s)$, the transfer functions are defined by $H_{xm}(s) \triangleq (s\mathbb{I}_n - A_m)^{-1} B_m$, $H_{xum}(s) \triangleq (s\mathbb{I}_n - A_m)^{-1} B_{um}$, $H_m(s) \triangleq C H_{xm}(s) = C(s\mathbb{I}_n - A_m)^{-1} B_m$, $H_{um}(s) \triangleq C H_{xum}(s) = C(s\mathbb{I}_n - A_m)^{-1} B_{um}$, and $\hat{\eta}_{1\mathrm{q}}(t)$ and $\hat{\eta}_{2\mathrm{q}}(t)$ are defined by

$$
\hat{\eta}_{i\mathrm{q}}(t) = \hat{\theta}_i(t) \|x_{\mathrm{q}_t}\|_{\mathcal{L}_\infty} + \hat{\sigma}_i(t),\ i = 1, 2.
$$

The design of the control law (4.23) involves a strictly proper $m \times m$ transfer matrix $D(s)$ and a matrix gain $K \in \mathbb{R}^{m \times m}$, which lead to a strictly proper stable transfer matrix

$$
C(s) \triangleq \omega K \left(\mathbb{I}_m + D(s) \omega K\right)^{-1} D(s) \tag{4.25}
$$

with DC gain $C(0) = \mathbb{I}_m$. The choice of $D(s)$ needs to ensure also that $C(s) H_m^{-1}(s)$

is a proper stable transfer matrix. For a particular class of systems, a possible choice for $D(s)$ might be $D(s) = \frac{1}{s}\mathbb{I}_m$, which yields a strictly proper $C(s)$ of the form $C(s) = \omega K \left(s\mathbb{I}_m + \omega K\right)^{-1}$, with the condition that the choice of K must ensure that $-\omega K$ is Hurwitz.

For proofs of stability and performance bounds, the choices of $D(s)$ and K also need to ensure that there exists $\rho_{x_r} > \rho_0$, such that

$$\begin{aligned}&\|G_m(s)\|_{\mathcal{L}_1} + \|G_{um}(s)\|_{\mathcal{L}_1}\ell_0 \\ &\qquad \leq \frac{\rho_{x_r} - \|H_{xm}(s)C(s)K_g(s)\|_{\mathcal{L}_1}\|r\|_{\mathcal{L}_\infty} - \|s(s\mathbb{I} - A_m)^{-1}\|_{\mathcal{L}_1}\rho_0}{L_{1\rho_{x_r}}\rho_{x_r} + B_0}, \quad (4.26)\end{aligned}$$

where

$$G_m(s) \triangleq H_{xm}(s)(\mathbb{I}_m - C(s)),\ G_{um}(s) \triangleq (\mathbb{I}_n - H_{xm}(s)C(s)H_m^{-1}(s)C)H_{xum}(s),$$

$\ell_0 \triangleq L_{2\rho_{x_r}}/L_{1\rho_{x_r}}$, $B_0 \triangleq \max\{B_{10}, \frac{B_{20}}{\ell_0}\}$, $K_g(s)$ is the proper stable feedforward prefilter, $L_{1\rho_{x_r}}$ and $L_{2\rho_{x_r}}$ are defined by

$$L_{i\nu} \triangleq \frac{\bar{\nu}}{\nu} d_{f_{xi}}(\bar{\nu}), \quad \forall \nu > 0, \quad \bar{\nu} \triangleq \max\{\nu + \bar{\gamma}_x,\ L_z(\nu + \bar{\gamma}_x) + B_z\}, \quad (4.27)$$

and $\bar{\gamma}_x > 0$ is an arbitrary, small constant.

For the analysis results in the following section to hold, the inequality in (4.26) is only a sufficient condition and is required only for the real ω. However, since ω is unknown, (4.26) cannot be used to guide the filter design. More conservatively, we can make the choices of $D(s)$ and K to ensure that for all $\omega \in \Omega$ there exists a constant $\rho_{x_r} > \rho_0$, such that (4.26) holds.

4.7 Performance analysis

4.7.1 Prediction error

We see that if the bounds in (3.35) hold, then Lemma 5 implies that the system in (4.20) can be rewritten over $\tau \in [0, t]$ as

$$\begin{aligned}\dot{x}(\tau) =& A_m x(\tau) + B_m \left(\omega u_{\mathrm{q}}(\tau) + \theta_1(\tau)\|x_\tau\|_{\mathcal{L}_\infty} + \sigma_1(\tau)\right) \\ &+ B_{um} \left(\theta_2(\tau)\|x_\tau\|_{\mathcal{L}_\infty} + \sigma_2(\tau)\right) , \\ y(\tau) =& Cx(\tau) , \quad x(0) = x_0 ,\end{aligned} \tag{4.28}$$

where $\theta_1(\tau)$, $\sigma_1(\tau)$, $\theta_2(\tau)$, and $\sigma_2(\tau)$ are unknown bounded time-varying signals with bounded derivatives. Let the prediction error be $\tilde{x}(t) \triangleq \hat{x}(t) - x(t)$. The prediction error dynamics can be obtained by comparing (4.28) and (4.21)

$$\begin{aligned}\dot{\tilde{x}}(t) =& A_m \tilde{x}(t) + B_m \left(\tilde{\omega}(t) u_{\mathrm{q}}(t) + \hat{\theta}_1(t)\|x_{\mathrm{q}_t}\|_{\mathcal{L}_\infty} - \theta_1(t)\|x_t\|_{\mathcal{L}_\infty} + \tilde{\sigma}_1(t)\right) \\ &+ B_{um} \left(\hat{\theta}_2(t)\|x_{\mathrm{q}_t}\|_{\mathcal{L}_\infty} - \theta_2(t)\|x_t\|_{\mathcal{L}_\infty} + \tilde{\sigma}_2(t)\right) , \quad \tilde{x}(0) = 0.\end{aligned} \tag{4.29}$$

Lemma 10 *Given the system in* (4.20) *and the $\mathcal{L}_1$ adaptive controller defined by* (4.21)*,* (4.22)*, and* (4.23) *subject to the $\mathcal{L}_1$-norm condition in* (4.26)*, if the state quantization is of uniform type with interval length d_x, and the state and input are bounded by*

$$\|x_t\|_{\mathcal{L}_\infty} \leq \rho_x, \quad \|u_t\|_{\mathcal{L}_\infty} \leq \rho_u, \tag{4.30}$$

then we have

$$\|\tilde{x}_t\|_{\mathcal{L}_\infty} \leq \sqrt{\frac{\theta_{hu}(d_x, \Gamma)}{\lambda_{\min(P)}}},$$

where $\theta_{hu}(d_x, \Gamma)$ is defined by

$$\begin{aligned}\theta_{hu}(d_x, \Gamma) \triangleq& \frac{4}{\Gamma} \left(\omega_{F\max} + m\theta_{b_1}^2 + m\sigma_{b_1}^2 + (n-m)\theta_{b_2}^2 + (n-m)\sigma_{b_2}^2\right) \\ &+ \lambda_{\max}(P)\tilde{x}_{hu}^2(d_x, \Gamma),\end{aligned} \tag{4.31}$$

$$\tilde{x}_{hu}(d_x,\Gamma) = \frac{c_1(d_x)+\sqrt{c_1^2(d_x)+4\lambda_{\min}(Q)\left(c_2(d_x)+\frac{c_3}{\Gamma}\right)}}{2\lambda_{\min}(Q)}.$$

$$\begin{aligned}
c_1(d_x) =& \big(m\|PB_m\|_2\theta_{b_1}+(n-m)\|PB_{um}\|_2\theta_{b_2}\big)d_x,\\
c_2(d_x) =& m\tilde{\omega}_{1\max}\|PB_m\|_1 d_x(\frac{1}{2}d_u+\rho_u)\\
&+2\left(m\|PB_m\|_1\theta_{b_1}+(n-m)\|PB_{um}\|_1\theta_{b_2}\right)(\rho_x+\frac{1}{2}d_x)d_x\\
&+2\left(m\|PB_m\|_1\sigma_{b_1}+(n-m)\|PB_{um}\|_1\sigma_{b_2}\right)d_x,\\
c_3 =& 4\left(m\theta_{b_1}d_{\theta_1}+m\sigma_{b_1}d_{\sigma_1}+(n-m)\theta_{b_2}d_{\theta_2}+(n-m)\sigma_{b_2}d_{\sigma_2}\right).
\end{aligned}$$

Proof. See Section B.7 in Appendix B.

Remark 19 *Note that in the definition of $\theta_{hu}(d_x,\Gamma)$ in* (4.31)*, $c_1(d_x)$ is a linear function of d_x, $c_2(d_x)$ is a monotonically increasing function of d_x, and c_3 is a constant dependent on system parameters. Hence, $\theta_{hu}(d_x,\Gamma)$ is monotonically increasing in d_x, and monotonically decreasing in Γ, $\lim_{d_x\to 0,\Gamma\to\infty}\theta_{hu}(d_x,\Gamma)=0$. We see that one can improve the state quantization or increase the adaptation rate to systematically decrease the prediction error.*

Lemma 11 *Given the system in* (4.20) *and the $\mathcal{L}_1$ adaptive controller defined by* (4.21)*,* (4.22)*, and* (4.23)*, subject to the $\mathcal{L}_1$-norm condition in* (4.26)*, if the state and input quantization is of logarithmic type with density and hysteresis factor ρ_{qx}, p_{hx}, ρ_{qu}, p_{hu}, respectively, and the state and input are bounded by*

$$\|x_t\|_{\mathcal{L}_\infty}\le\rho_x,\quad \|u_t\|_{\mathcal{L}_\infty}\le\rho_u, \tag{4.32}$$

then we have

$$\|\tilde{x}_t\|_{\mathcal{L}_\infty}\le\sqrt{\frac{\theta_{hl}(\delta_{ex},\delta_{eu},\Gamma)}{\lambda_{\min(P)}}},$$

where $\theta_{hl}(\delta_{ex}, \delta_{eu}, \Gamma)$ *is defined by*

$$\theta_{hl}(\delta_{ex}, \delta_{eu}, \Gamma) \triangleq \frac{4}{\Gamma}\left(\omega_{F\max} + m\theta_{b_1}^2 + m\sigma_{b_1}^2 + (n-m)\theta_{b_2}^2 + (n-m)\sigma_{b_2}^2\right) + \lambda_{\max}(P)\tilde{x}_{hl}^2(\delta_{ex}, \delta_{eu}, \Gamma)$$

$$\delta_{ex} = \frac{\rho_{\mathrm{q}x} + p_{hx}(1+\rho_{\mathrm{q}x})}{\rho_{\mathrm{q}x} - p_{hx}(1-\rho_{\mathrm{q}x})}, \quad \delta_{eu} = \frac{\rho_{\mathrm{q}u} + p_{hu}(1+\rho_{\mathrm{q}u})}{\rho_{\mathrm{q}u} - p_{hu}(1-\rho_{\mathrm{q}u})},$$

$$\tilde{x}_{hl}(\delta_{ex}, \delta_{eu}, \Gamma) = \frac{c_4(\delta_{ex}) + \sqrt{c_4^2(\delta_{ex}) + 4\lambda_{\min}(Q)\left(c_5(\delta_{ex}, \delta_{eu}, \rho_x) + \frac{c_3}{\Gamma}\right)}}{2\lambda_{\min}(Q)},$$

$$c_4(\delta_{ex}) = 2\left(m\theta_{b_1}\|PB_m\|_2 + (n-m)\theta_{b_2}\|PB_{um}\|_2\right)\delta_{ex}\rho_x,$$

$$\begin{aligned} c_5(\delta_{ex}, \delta_{eu}, \rho_x) = {} & 2m\|PB_m\|_1\tilde{\omega}_{1\max}\delta_{ex}\rho_x(1+\delta_{eu})\rho_u + 4m\|PB_m\|_1\theta_{b_1}\delta_{ex}(1+\delta_{ex})\rho_x^2 \\ & + 4m\|PB_m\|_1\sigma_{b_1}\delta_{ex}\rho_x + 4(n-m)\|PB_m\|_1\theta_{b_2}\delta_{ex}(1+\delta_{ex})\rho_x^2 \\ & + 4(n-m)\|PB_m\|_1\sigma_{b_2}\delta_{ex}\rho_x. \end{aligned}$$

Proof. The proof is similar to Lemma 10 and is thus omitted. □

Remark 20 *The prediction error bound in Lemma 11 involves the quantity* $\theta_{hl}(\delta_{ex}, \delta_{eu}, \Gamma)$*, where* $c_4(\delta_{ex})$ *and* $c_5(\delta_{ex}, \delta_{eu}, \rho_x)$ *are monotonically increasing functions of* δ_{ex}*, and* c_6 *is a constant determined by system parameters. Hence,* $\theta_{hl}(\delta_{ex}, \delta_{eu}, \Gamma)$ *is monotonically increasing in* δ_{ex}*, and monotonically decreasing in* Γ*,*

$$\lim_{\delta_{ex}\to 0, \Gamma\to\infty} \theta_{hl}(\delta_{ex}, \delta_{eu}, \Gamma) = 0.$$

Thus the prediction error can be systematically reduced by improving the state quantization or increasing the adaptation rate.

4.7.2 Transient and steady-state performance

For analyzing the closed-loop performance, we consider the theoretical reference system with full knowledge of the uncertainties introduced in (3.34) in Section 3.8.1. The stability of the reference system is established in Lemma 4.

Hysteresis uniform quantization

We have seen that the reference system is BIBO stable. Now we show that using the $\mathcal{L}_1$ adaptive control, the response of the closed-loop system is close to that of the reference system, and the state and input signals can be bounded by some constants defined as

$$\rho_{x_{hu}} \triangleq \rho_{x_r} + \bar{\gamma}_{x_{hu}}, \tag{4.33}$$

$$\gamma_{x_{hu}} \triangleq \gamma_{x\mathrm{o}_{hu}} + \gamma_{x\mathrm{q}_{hu}} + \epsilon, \tag{4.34}$$

$$\gamma_{x\mathrm{o}_{hu}} \triangleq \frac{\|H_{xm}(s)C(s)H_m^{-1}(s)C\|_{\mathcal{L}_1}}{1 - \|G_m(s)\|_{\mathcal{L}_1}L_{1\rho_{x_r}} - \|G_{um}(s)\|_{\mathcal{L}_1}L_{2\rho_{x_r}}}\gamma_{0_{hu}},$$

$$\gamma_{x\mathrm{q}_{hu}} \triangleq \frac{\|H_{xm}(s)\omega\|_{\mathcal{L}_1} + \|H_{xm}(s)C(s)\|_{\mathcal{L}_1}\tilde{\omega}_{1\max}}{1 - \|G_m(s)\|_{\mathcal{L}_1}L_{1\rho_{x_r}} - \|G_{um}(s)\|_{\mathcal{L}_1}L_{2\rho_{x_r}}}\frac{1}{2}d_u,$$

where $\bar{\gamma}_{x_{hu}}$ is an arbitrary, small positive constant, and $\gamma_{0_{hu}}$, d_u and ϵ are small positive constants such that $\gamma_{x_{hu}} < \bar{\gamma}_{x_{hu}}$. Let

$$\rho_{u_{hu}} \triangleq \rho_{u_r} + \gamma_{u_{hu}}\,, \tag{4.35}$$

$$\begin{aligned}\gamma_{u_{hu}} \triangleq\ & \left(\|\omega^{-1}C(s)\|_{\mathcal{L}_1}L_{1\rho_{x_r}} + \|\omega^{-1}C(s)H_m^{-1}(s)H_{um}(s)\|_{\mathcal{L}_1}L_{2\rho_{x_r}}\right)\gamma_{x_{hu}} \\ & + \|\omega^{-1}C(s)H_m^{-1}(s)C\|_{\mathcal{L}_1}\gamma_{0_{hu}} + \|\omega^{-1}C(s)\|_{\mathcal{L}_1}\tilde{\omega}_{1\max}\frac{1}{2}d_u.\end{aligned} \tag{4.36}$$

The performance results are summarized in the following theorem.

Theorem 7 *Consider the closed-loop system with uniform quantization* (2.6) *and the $\mathcal{L}_1$ adaptive controller defined by* (4.21)-(4.23)*, subject to the $\mathcal{L}_1$-norm condition in* (4.26)*. If the adaptation rate Γ and the quantization interval length d_x are selected such that $\sqrt{\frac{\theta_{hu}(d_x,\Gamma)}{\lambda_{\min}(P)}} < \gamma_{0_{hu}}$, and the initial condition $\|x_0\|_\infty \leq \rho_{x_r}$, then we have the performance bounds*

$$\begin{aligned}&\|x_{\mathrm{ref}}\|_{\mathcal{L}_\infty} \leq \rho_{x_r}\,,\ \|u_{\mathrm{ref}}\|_{\mathcal{L}_\infty} \leq \rho_{u_r}\,,\ \|x\|_{\mathcal{L}_\infty} \leq \rho_{x_{hu}}\,, \\ &\|u\|_{\mathcal{L}_\infty} \leq \rho_{u_{hu}}\,,\ \|\tilde{x}\|_{\mathcal{L}_\infty} < \gamma_{0_{hu}}\,,\ \|x - x_{\mathrm{ref}}\|_{\mathcal{L}_\infty} < \gamma_{x_{hu}}\,, \\ &\|u - u_{\mathrm{ref}}\|_{\mathcal{L}_\infty} < \gamma_{u_{hu}}\,,\ \|y - y_{\mathrm{ref}}\|_{\mathcal{L}_\infty} < \|C\|_\infty\gamma_{x_{hu}}\,,\end{aligned} \tag{4.37}$$

where $\gamma_{x_{hu}}$ and $\gamma_{u_{hu}}$ were defined in (4.33) *and* (4.35) *respectively.*

Proof. See Section B.8 in Appendix B.

Remark 21 *Recall that the prediction error bound $\sqrt{\frac{\theta_{hu}(d_x,\Gamma)}{\lambda_{\min}(P)}}$ can be systematically reduced by improving the state quantization (reducing the quantization in-*

terval length d_x) or increasing the adaptation rate, as stated by Remark 19, and $\lim_{d_x\to 0,\Gamma\to\infty}\theta_{hu}(d_x,\Gamma)=0$. *Thus for any* $\gamma_{0_{hu}}>0$, *there always exists* $d_x>0$, $\Gamma>0$, *such that* $\sqrt{\frac{\theta_{hu}(d_x,\Gamma)}{\lambda_{\min}(P)}}<\gamma_{0_{hu}}$.

Remark 22 *The performance bounds in* (4.37) *consist of two terms, one of which depends linearly upon d_u, representing the quantization interval length for the uniform input quantization, while the other is determined by the state quantization parameter d_x and the adaptation rate Γ. In the limiting case, when d_x goes to zero, the closed-loop system reduces to the input quantization case, and the performance bounds reduce to the ones in [40]. When d_x and d_u decrease to zero and there is no quantization, the corresponding term vanishes, and the performance bounds reduce to the classical ones in Theorem 1 in [20], as to be expected.*

Hysteresis logarithmic quantization

In the case of hysteresis logarithmic quantization, similarly, we show that the response of the closed-loop system with the $\mathcal{L}_1$ adaptive control is close to that of the reference system, and the state and input signals can be bounded by the following constants

$$\rho_{x_{hl}} \triangleq \rho_{x_r}+\bar{\gamma}_{x_{hl}}, \tag{4.38}$$

$$\gamma_{x_{hl}} \triangleq \gamma_{x\mathrm{o}_{hl}}+\gamma_{x\mathrm{q}_{hl}}+\epsilon, \tag{4.39}$$

$$\gamma_{x\mathrm{o}_{hl}} \triangleq \frac{c_{ep}(\delta_{eu})\gamma_{0_{hl}}}{1-\|G_m(s)\|_{\mathcal{L}_1}L_{1\rho_{x_r}}-\|G_{um}(s)\|_{\mathcal{L}_1}L_{2\rho_{x_r}}-c_{ex}(\delta_{eu})\delta_{eu}}$$

$$\gamma_{x\mathrm{q}_{hl}} \triangleq \frac{c_{eu}(\delta_{eu})\rho_{u_r}\delta_{eu}}{1-\|G_m(s)\|_{\mathcal{L}_1}L_{1\rho_{x_r}}-\|G_{um}(s)\|_{\mathcal{L}_1}L_{2\rho_{x_r}}-c_{ex}(\delta_{eu})\delta_{eu}},$$

where $\bar{\gamma}_{x_{hl}}$ is an arbitrary, small positive constant, and $\gamma_{0_{hl}}$, δ_{eu} and ϵ are small positive constants such that $\gamma_{x_{hl}}<\bar{\gamma}_{x_{hl}}$. Let

$$\rho_{u_{hl}} \triangleq \rho_{u_r}+\gamma_{u_{hl}}, \tag{4.40}$$

$$\gamma_{u_{hl}} \triangleq c_{dx}(\delta_{eu})\gamma_{x_{hl}}+\frac{\|\omega^{-1}C(s)H_m^{-1}(s)C\|_{\mathcal{L}_1}}{1-\|\omega^{-1}C(s)\|_{\mathcal{L}_1}\tilde{\omega}_{1\max}\delta_{eu}}\gamma_{0_{hl}}$$
$$+\frac{\|\omega^{-1}C(s)\|_{\mathcal{L}_1}\tilde{\omega}_{1\max}}{1-\|\omega^{-1}C(s)\|_{\mathcal{L}_1}\tilde{\omega}_{1\max}\delta_{eu}}\rho_{u_r}\delta_{eu}, \tag{4.41}$$

and the coefficients are given by

$$
\begin{aligned}
&c_{ex}(\delta_{eu}) \triangleq c_{ed}c_{dx}(\delta_{eu}),\\
&c_{ed} \triangleq \left(\|H_{xm}(s)\omega\|_{\mathcal{L}_1} + \|H_{xm}(s)C(s)\|_{\mathcal{L}_1}\tilde{\omega}_{1\max}\right),\\
&c_{dx}(\delta_{eu}) \triangleq \frac{\|\omega^{-1}C(s)\|_{\mathcal{L}_1}L_{1\rho_{x_r}} + \|\omega^{-1}C(s)H_m^{-1}(s)H_{um}(s)\|_{\mathcal{L}_1}L_{2\rho_{x_r}}}{1-\|\omega^{-1}C(s)\|_{\mathcal{L}_1}\tilde{\omega}_{1\max}\delta_{eu}}\\
&c_{ep}(\delta_{eu}) \triangleq \|H_{xm}(s)C(s)H_m^{-1}(s)C\|_{\mathcal{L}_1} + c_{ep2}\delta_{eu},\\
&c_{ep2}(\delta_{eu}) \triangleq c_{ed}\frac{\|\omega^{-1}C(s)H_m^{-1}(s)C\|_{\mathcal{L}_1}}{1-\|\omega^{-1}C(s)\|_{\mathcal{L}_1}\tilde{\omega}_{1\max}\delta_{eu}},\\
&c_{eu}(\delta_{eu}) \triangleq \frac{c_{ed}}{1-\|\omega^{-1}C(s)\|_{\mathcal{L}_1}\tilde{\omega}_{1\max}\delta_{eu}}.
\end{aligned}
$$

The performance results are summarized in the following theorem.

Theorem 8 *Consider the closed-loop system with hysteresis logarithmic quantization, and the $\mathcal{L}_1$ adaptive controller defined by* (4.21)-(4.23)*, subject to the $\mathcal{L}_1$-norm condition in* (4.26)*. If the adaptation rate Γ and the quantization density δ_{ex} are selected such that $\sqrt{\frac{\theta_{hl}(\delta_{ex},\delta_{eu},\Gamma)}{\lambda_{\min}(P)}} < \gamma_{0_{hl}}$, and the initial condition $\|x_0\|_\infty \leq \rho_{x_r}$, then we have the performance bounds*

$$
\begin{aligned}
&\|x_{\rm ref}\|_{\mathcal{L}_\infty} \leq \rho_{x_r}\,,\ \|u_{\rm ref}\|_{\mathcal{L}_\infty} \leq \rho_{u_r}\,,\ \|x\|_{\mathcal{L}_\infty} \leq \rho_{x_{hl}}\,,\\
&\|u_{\rm q}\|_{\mathcal{L}_\infty} \leq \rho_{u_{hl}}\,,\ \|\tilde{x}\|_{\mathcal{L}_\infty} < \gamma_{0_{hl}}\,,\ \|x-x_{\rm ref}\|_{\mathcal{L}_\infty} < \gamma_{x_{hl}}\,,\\
&\|u_{\rm q}-u_{\rm ref}\|_{\mathcal{L}_\infty} < \gamma_{u_{hl}}\,,\ \|y-y_{\rm ref}\|_{\mathcal{L}_\infty} < \|C\|_\infty\gamma_{x_{hl}}\,,
\end{aligned}
\tag{4.42}
$$

where $\gamma_{x_{hl}}$ and $\gamma_{u_{hl}}$ were defined in (4.39) *and* (4.41) *respectively.*

Proof. See Section B.9 in Appendix B.

Remark 23 *As introduced in Sections 4.6 and 3.8.1, ρ_{x_r} characterizes the positive invariant sets for the state of the closed-loop reference system, while $\rho_{x_{hu}}$ and $\rho_{x_{hl}}$ characterize the positive invariant sets for the state of the closed-loop adaptive system with uniform and logarithmic quantization, respectively. We notice that, since $\bar{\gamma}_{x_{hu}}$ and $\bar{\gamma}_{x_{hl}}$ can be set to be arbitrarily small, $\rho_{x_{hu}}$ and $\rho_{x_{hl}}$ can approximate ρ_{x_r} arbitrarily closely in both cases.*

4.8 Simulations

Consider the system

$$\begin{aligned}\dot{x}(t) =& A_m x(t) + B_m \omega u_{\mathrm{q}}(t) + f_\Delta(x(t), z(t), t)\,,\\ y(t) =& Cx(t)\,,\ u_{\mathrm{q}}(t) = Q_{h\mathrm{unif}}(u(t))\,,\ x(0) = [0\ 0\ 0]^\top,\end{aligned}$$

where

$$A_m = \begin{bmatrix} -1 & 0 & 0 \\ 0 & 0 & 1 \\ 0 & -1 & -1.8 \end{bmatrix}, B_m = \begin{bmatrix} 1 & 0 \\ 0 & 0 \\ 1 & 1 \end{bmatrix}, \tag{4.43}$$

$$C = \begin{bmatrix} 1 & 0 & 0 \\ 0 & 1 & 0 \end{bmatrix},\ \omega = \begin{bmatrix} 1 & -0.2 \\ -0.2 & 1.1 \end{bmatrix}, \tag{4.44}$$

while $\omega \in \mathbb{R}^{2\times 2}$ is assumed to be within the convex set $\Omega = \{\omega | \omega = \omega^\top, \omega_{11} \in [1, 1.3], \omega_{12} \in [-0.2, 0.1], \omega_{22} \in [1, 1.3]\}$. The (unknown) nonlinear function f_Δ is given by

$$f_\Delta(x, z, t) = \begin{bmatrix} 0.033x^\top x + 0.1\tanh(\frac{1}{2}x_1)x_1 + 0.1z^2 \\ -0.015x_3^2 - 0.01(1 - \mathrm{e}^{-0.3t}) + 0.05z \\ -0.1x_3\cos(t) + 0.1z^2 \end{bmatrix}.$$

The internal unmodeled dynamics are given by

$$\begin{aligned}\dot{x}_{z1}(t) =& x_{z2}(t)\\ \dot{x}_{z2}(t) =& -0.3\sin x_{z1}(t) - 0.7x_{z2}(t)\,,\\ z(t) =& 0.25\,(x_{z1}(t) - x_{z2}(t)) + z_u(t)\\ z_u(s) =& \frac{-s+1}{\frac{s^2}{0.1^2} + \frac{0.8s}{0.1} + 1}\begin{bmatrix} \frac{1}{5} & -\frac{1}{10} & \frac{1}{5} \end{bmatrix} x(s)\,,\end{aligned}$$

where $[x_{z1}(0)\ x_{z2}(0)] = [-0.1\ 0.1]$, $L_z = 0.8465$, $B_z = 0.05$.

In the implementation of the $\mathcal{L}_1$ controller, we set $Q = \mathbb{I}_3$,

$$\begin{aligned}&\Gamma = 10^4, \quad D(s) = \frac{1}{s(\frac{s}{25}+1)(\frac{s}{70}+1)(\frac{s^2}{40^2} + \frac{1.8s}{40} + 1)}\mathbb{I}_2,\\ &K = \begin{bmatrix} 8 & 0 \\ 0 & 8 \end{bmatrix}, \quad K_g(s) \equiv K_g = -(CA_m^{-1}B_m)^{-1} = \begin{bmatrix} 1 & 0 \\ -1 & 1 \end{bmatrix}.\end{aligned}$$

The projection bounds can be chosen conservatively as

$$\hat{\theta}_1(t) \in [-0.8661, 0.8661]\mathbf{1}_m\,,\ \hat{\sigma}_1(t) \in [-5, 5]\mathbf{1}_m\,,$$
$$\hat{\theta}_2(t) \in [-0.0533, 0.0533]\mathbf{1}_{(n-m)},\ \hat{\sigma}_2(t) \in [-5, 5]\mathbf{1}_{(n-m)},$$
$$\hat{\omega}_{11}(t), \hat{\omega}_{22}(t) \in [0.25, 3]\,,\ \hat{\omega}_{12}(t), \hat{\omega}_{21}(t) \in [-0.2, 0.2]\,,$$

where $\mathbf{1}_r \in \mathbb{R}^r$ represents the vector with all elements being 1.

First we show that in the presence of nonlinearity and quantization, the $\mathcal{L}_1$ adaptive controller drives the closed-loop system response to follow the reference system response $y_{\text{ref}}(t)$, as shown in Figure 4.4 and 4.5. These figures also show the scaled response of the closed-loop system to scaled reference steps. For different amplitudes of steps, the controller provides scaled control signals and scaled system outputs, which is consistent with the properties of $\mathcal{L}_1$ adaptive control theory ([20]).

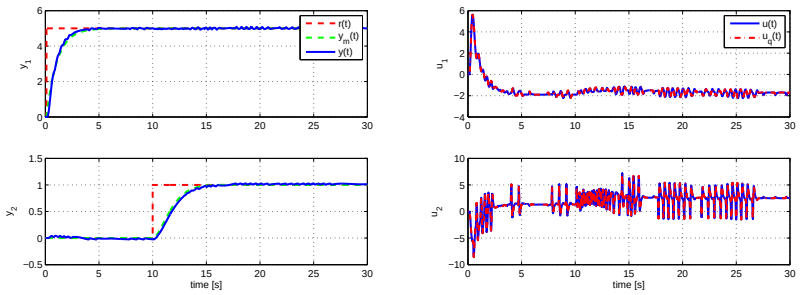

Figure 4.4: Output and control signals for step references with uniform quantization, $d_u = 0.1$, $d_x = 0.05$.

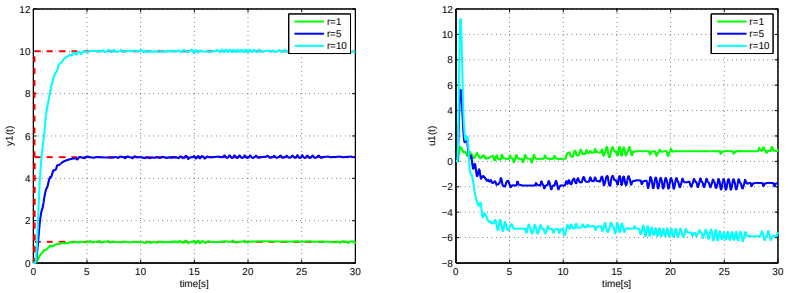

Figure 4.5: Output and control signals for step references with uniform quantization, $d_u = 0.1$, $d_x = 0.05$.

Second we show the quantization effect in the closed-loop system. As shown in Figures 4.4 and 4.6, the system output tracks the reference signal in both cases. When the quantization is coarser, the tracking error is larger. In Figure 4.6, the quantization effect is obvious while the system maintains acceptable performance. When the quantization is sufficiently dense, the quantization effect in the performance (Remark 22) tracking error is smaller. In Figure 4.6, the deviation is almost invisible and the system response is close to the case without quantization.

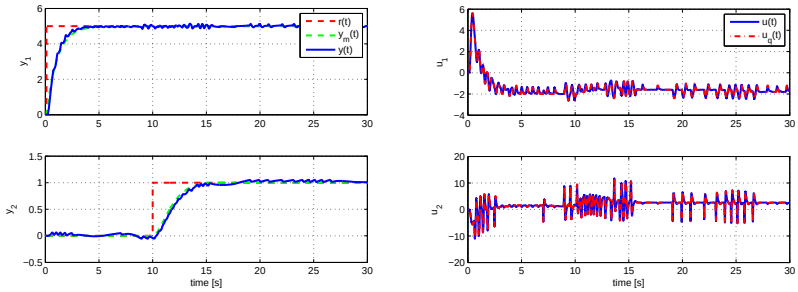

Figure 4.6: Output and control signals for step references with uniform quantization, $d_u = 0.2$, $d_x = 0.05$.

Further we see that the effects of state and control quantization schemes on the system performance have 'waterbed-like' effect. To maintain required performance for a system with both state and control quantization, if one quantization gets coarser, the other one has to be finer, and *vice versa*. From Figure 4.4 to Figure 4.6, the deviation gets more obvious as the input quantization interval enlarges. When the state quantization is improved, the performance is retained as in Figure 4.7. Recall that the performance bounds in Theorem 7 are determined by d_x, d_u and Γ, and better performance can be achieved by either improving the state or the input quantization.

Figure 4.8 shows the system performance with logarithmic quantization.

In conclusion, we see that in different cases the $\mathcal{L}_1$ adaptive controller ensures that the system output tracks the reference signal closely and smoothly. We note that in all these cases we have not redesigned or retuned the $\mathcal{L}_1$ adaptive controller.

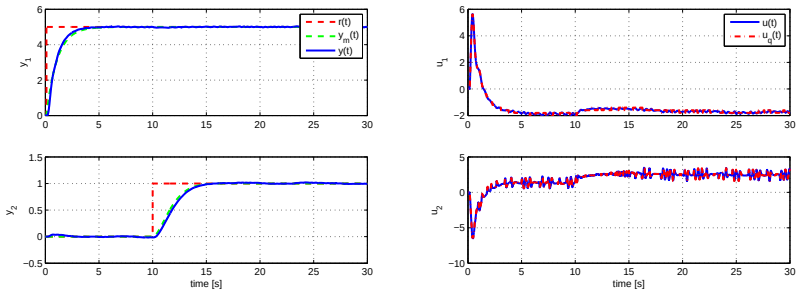

Figure 4.7: Output and control signals for step references with uniform quantization, $d_u = 0.2$, $d_x = 0.01$.

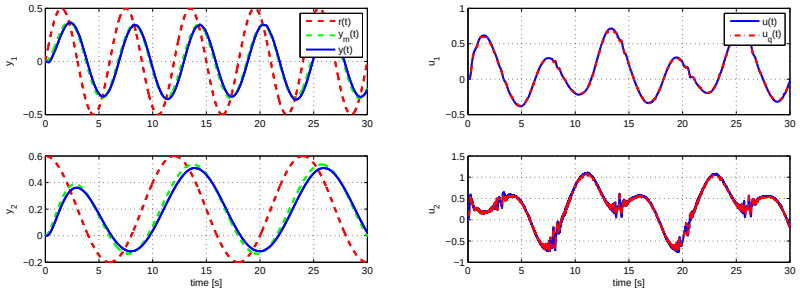

Figure 4.8: Output and control signals for sinusoidal references with logarithmic quantization, $\rho_u = 0.95$, $\rho_x = 0.99$.

CHAPTER 5

OUTPUT FEEDBACK CONTROL FOR INPUT-QUANTIZED SYSTEMS

"There is an objective reality out there, but we view it through the spectacles of our beliefs, attitudes, and values." –David G. Myers

In this chapter, we consider input-quantized uncertain systems, their control design and performance evaluation problems. Different from the previous two chapters, the system states are not available. It is shown that the controller uses the measured output information to estimate and compensate the uncertainties. The closed-loop performance is guaranteed in the presence of input quantization. At the end of the chapter, we present an application to a buck converter.

An input-quantized system is shown in Figure 5.1. The controller uses the output feedback of the plant and generates the control signal $u(t)$ for the quantization block, and the quantization block generates $u_{\mathrm{q}}(t)$ and provides it to the plant.

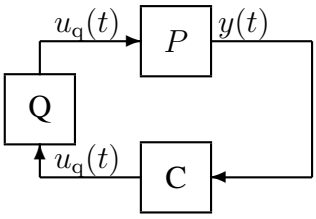

Figure 5.1: System with quantized input.

5.1 Output feedback uncertain systems

Consider the following output feedback system:

$$\begin{aligned} y(s) =& A(s)(u_{\mathrm{q}}(s) + d(s)), \quad y(0) = 0, \\ u_{\mathrm{q}}(t) =& Q(u_{ad}(t)), \end{aligned} \tag{5.1}$$

where $u_{\mathrm{q}}(t) \in \mathbb{R}$ is the quantized control, $y(t) \in \mathbb{R}$ is the system output, $A(s)$ is a strictly proper unknown transfer function, $u_{ad}(t)$ is the designed control based on output $y(t)$, $d(s)$ is the Laplace transform of the time-varying uncertainties and disturbances $d(t) = f(t, y(t))$, while f is an unknown map, subject to the following assumption.

Assumption 8 *There exist constants $L > 0$ and $L_0 > 0$, such that the inequalities*

$$|f(t, y_1) - f(t, y_2)| \leq L|y_1 - y_2|, \quad |f(t, y)| \leq L|y| + L_0$$

hold uniformly in $t \geq 0$.

We can rewrite the system as

$$\begin{aligned} y(s) =& M(s)(u_{\mathrm{q}}(s) + \sigma(s)),\ y(0) = 0, \\ \sigma(s) \triangleq& \frac{(A(s) - M(s))u_{\mathrm{q}}(s) + A(s)d(s)}{M(s)}. \end{aligned} \tag{5.2}$$

In the case of hysteresis uniform quantization, the error can be bounded by a constant

$$\Delta_u(t) \triangleq u_{\mathrm{q}}(t) - u_{ad}(t), \quad \|\Delta_u\|_{\mathcal{L}_\infty} \leq \frac{1}{2} d_u, \tag{5.3}$$

where d_u is the length of the quantization interval.

5.2 Control design

In this design for the output feedback case, the selection of $C(s)$ and $M(s)$ need to ensure that $H(s)$ is stable, and the following $\mathcal{L}_1$-norm condition

$$\|G(s)\|_{\mathcal{L}_1} L < 1 \tag{5.4}$$

holds, where

$$\begin{aligned} G(s) \triangleq& H(s)(1 - C(s)), \\ H(s) \triangleq& \frac{A(s)M(s)}{C(s)A(s) + (1 - C(s))M(s)}. \end{aligned}$$

We consider the following output predictor

$$\begin{aligned}\dot{\hat{x}}(t) =& A_m\hat{x}(t) + b_m u_{\rm q}(t) + \hat{\sigma}(t)\,,\\ \hat{y}(t) =& c_m^\top \hat{x}(t)\,, \quad \hat{x}(0) = x_0\,,\end{aligned} \tag{5.5}$$

where $\hat{\sigma}(t) \in \mathbb{R}^n$ is the vector of adaptive parameters.

Letting $\tilde{y}(t) = \hat{y}(t) - y(t)$, the estimate $\hat{\sigma}(t)$ is updated by the following adaptation law

$$\begin{aligned}\hat{\sigma}(t) =& \hat{\sigma}(iT), \quad t \in [iT, (i+1)T)\\ \hat{\sigma}(iT) =& -\Phi^{-1}(T)\mu(iT)\,, \quad i = 0, 1, 2, \cdots\,,\end{aligned} \tag{5.6}$$

with $\Phi(T)$ and $\mu(iT)$ defined by

$$\begin{aligned}\Phi(T) =& \int_0^T {\rm e}^{\Lambda A_m \Lambda^{-1}(T-\tau)}\Lambda d\tau\,,\\ \mu(iT) =& {\rm e}^{\Lambda A_m \Lambda^{-1} T}\mathbf{1}_1 \tilde{y}(iT)\,,\ i = 0, 1, 2, \cdots\,.\\ \Lambda =& \begin{bmatrix} c_m^\top \\ D\sqrt{P} \end{bmatrix}\,,\end{aligned}$$

where P is the solution to the Lyapunov equation $A_m^\top P + P A_m = -Q$, for some $Q > 0$, D is an $(n-1) \times n$ matrix such that

$$D(c_m^\top(\sqrt{P})^{-1})^\top = 0\,,$$

and Λ^{-1} exists.

The control signal is defined as follows:

$$u_{ad}(s) = C(s)r(s) - \frac{C(s)}{c_m^\top(s\mathbb{I} - A_m)^{-1}b_m} c_m^\top (s\mathbb{I} - A_m)^{-1}\hat{\sigma}(s)\,, \tag{5.7}$$

where $C(s)$ is a strictly proper low-pass filter with DC gain $C(0) = 1$.

5.3 Performance analysis

5.3.1 Closed-loop reference system

Consider the following closed-loop reference system:

$$\begin{aligned} y_{\text{ref}}(s) =& M(s)(u_{\text{ref}}(s) + \sigma_{\text{ref}}(s)) \\ u_{\text{ref}}(s) =& C(s)(r(s) - \sigma_{\text{ref}}(s)), \end{aligned} \tag{5.8}$$

where

$$\begin{aligned} \sigma_{\text{ref}}(s) =& \frac{(A(s) - M(s))u_{\text{ref}}(s) + A(s)d_{\text{ref}}(s)}{M(s)}, \\ d_{\text{ref}}(t) =& f(t, y_{\text{ref}}(t)). \end{aligned} \tag{5.9}$$

Lemma 12 *If $C(s)$ and $M(s)$ verify the $\mathcal{L}_1$ condition in* (5.4)*, the closed-loop reference system in* (5.8) *is bounded input bounded output (BIBO) stable:*

$$\|y_{\text{ref}}\|_{\mathcal{L}_\infty} \leq \rho_r \triangleq \frac{\|H(s)C(s)\|_{\mathcal{L}_1}\|r\|_{\mathcal{L}_\infty} + \|G(s)\|_{\mathcal{L}_1}L_0}{1 - \|G(s)\|_{\mathcal{L}_1}L}.$$

5.3.2 Transient and steady-state performance

Let

$$\begin{aligned} \Delta =& \|H_1(s)\|_{\mathcal{L}_1}\|r\|_{\mathcal{L}_\infty} + \|H_0(s)\|_{\mathcal{L}_1}(L\rho_r + L_0) \\ &+ \Big(\Big\|\frac{H_1(s)}{C(s)}\Big\|_{\mathcal{L}_1} + \|H_0(s)\|_{\mathcal{L}_1}\frac{\|H(s)\|_{\mathcal{L}_1}}{1 - \|G(s)\|_{\mathcal{L}_1}L}L\Big)\frac{1}{2}d_u \\ &+ \Big(\Big\|\frac{H_1(s)}{M(s)}\Big\|_{\mathcal{L}_1} + \|H_0(s)\|_{\mathcal{L}_1}\frac{\|\frac{C(s)H(s)}{M(s)}\|_{\mathcal{L}_1}}{1 - \|G(s)\|_{\mathcal{L}_1}L}L\Big)\bar{\gamma}_0, \end{aligned}$$

where $\bar{\gamma}_0 > 0$ is an arbitrary constant. Since $H_1(s)$ is BIBO stable and strictly proper, $\|H_1(s)/M(s)\|_{\mathcal{L}_1}$ is finite and, hence, Δ is a bounded.

Let $\eta_1(t) \in \mathbb{R}$ and $\eta_2(t) \in \mathbb{R}^{n-1}$ be the first and the 2-to-n elements of the row vector $\mathbf{1}_1 \mathrm{e}^{\Lambda A_m \Lambda^{-1} t}$, i.e.

$$[\eta_1(t)\ \eta_2^\top(t)] = \mathbf{1}_1 \mathrm{e}^{\Lambda A_m \Lambda^{-1} t},$$

and introduce the functions

$$\eta_3(t) = \int_0^t |\mathbf{1}_1^\top \mathrm{e}^{\Lambda A_m \Lambda^{-1}(t-\tau)} \Lambda \Phi^{-1}(T_s) \mathrm{e}^{\Lambda A_m \Lambda^{-1} T_s} \mathbf{1}_1| d\tau,$$
$$\eta_4(t) = \int_0^t |\mathbf{1}_1^\top \mathrm{e}^{\Lambda A_m \Lambda^{-1}(t-\tau)} \Lambda b_m| d\tau,$$
$$\beta_1(T_s) \triangleq \max_{t\in[0,T_s]} |\eta_1(t)|,\ \beta_2(T_s) \triangleq \max_{t\in[0,T_s]} \|\eta_2(t)\|,$$
$$\beta_3(T_s) \triangleq \max_{t\in[0,T_s]} \eta_3(t),\ \beta_4(T_s) \triangleq \max_{t\in[0,T_s]} \eta_4(t),$$
$$\alpha \triangleq \lambda_{\max}(\Lambda^{-\top} P \Lambda^{-1}) \left(\frac{2\Delta \|\Lambda^{-\top} P b_m\|}{\lambda_{\min}(\Lambda^{-\top} Q \Lambda^{-1})} \right)^2,$$
$$\varsigma(T_s) \triangleq \|\eta_2(T_s)\| \sqrt{\frac{\alpha}{\lambda_{\max}(P_2)}} + \kappa(T_s)\Delta,$$
$$\kappa(T_s) \triangleq \int_0^T |\mathbf{1}_1^\top \mathrm{e}^{\Lambda A_m \Lambda^{-1}(T_s-\tau)} \Lambda b_m| d\tau,$$

$$\Phi(T_s) \triangleq \int_0^T \mathrm{e}^{\Lambda A_m \Lambda^{-1}(T_s-\tau)} \Lambda d\tau.$$

$$\gamma_0(T_s) \triangleq \beta_1(T_s)\varsigma(T_s) + \beta_2(T_s)\sqrt{\frac{\alpha}{\lambda_{\max}(P_2)}} + \beta_3(T_s)\varsigma(T_s) + \beta_4(T_s)\Delta, \quad (5.10)$$

$$H_0(s) = \frac{A(s)}{C(s)A(s) + (1-C(s))M(s)}, H_1(s) = \frac{(A(s)-M(s))C(s)}{C(s)A(s) + (1-C(s))M(s)}$$
$$H_2(s) = \frac{C(s)A(s)}{C(s)A(s) + (1-C(s))M(s)}, H_3(s) = -\frac{M(s)C(s)}{C(s)A(s) + (1-C(s))M(s)},$$
$$H(s) = \frac{A(s)M(s)}{C(s)A(s) + (1-C(s))M(s)}. \quad (5.11)$$

Lemma 13 *Let $\gamma_0(T_s)$ be defined as in* (5.10)*. Then,*

$$\lim_{T_s\to 0} \gamma_0(T_s) = 0.$$

Lemma 14 *Consider the system in* (5.1) *and the output predictor in* (5.5)*. If T_s is chosen such that $\gamma_0(T_s) < \bar{\gamma}_0$, then we have $\|\tilde{y}\|_{\mathcal{L}_\infty} \leq \bar{\gamma}_0$.*

Theorem 9 *Consider the system in* (5.1) *and the $\mathcal{L}_1$ adaptive controller in* (5.5)*,*

(5.6), *and* (5.7). *Given* $\bar{\gamma}_0$*, if* T_s *is chosen such that* $\gamma_0(T_s) < \bar{\gamma}_0$*, then we have:*

$$\|y - y_{\text{ref}}\|_{\mathcal{L}_\infty} \leq \gamma_y, \quad \|u_{\text{q}} - u_{\text{ref}}\|_{\mathcal{L}_\infty} \leq \gamma_u, \tag{5.12}$$

where $\gamma_0(T_s)$ *is the bound on the prediction error, dependent on the sample time* T_s*, and*

$$\begin{aligned}\gamma_y =& \frac{\|H_2(s)\|_{\mathcal{L}_1}}{1 - \|G(s)\|_{\mathcal{L}_1} L} \bar{\gamma}_0 + \frac{\|H(s)\|_{\mathcal{L}_1}}{1 - \|G(s)\|_{\mathcal{L}_1} L} \frac{1}{2} d_u \\ \gamma_u =& L\|H_2(s)\|_{\mathcal{L}_1} \gamma_x + \|\frac{H_3(s)}{M(s)}\|_{\mathcal{L}_1} \bar{\gamma}_0 + \|\frac{H_3(s)}{C(s)}\|_{\mathcal{L}_1} \frac{1}{2} d_u.\end{aligned}$$

Proof. See Appendix B.10.

5.4 Application to a bulk converter

5.4.1 Circuit Diagram

The buck converter converts an unregulated DC voltage source to a regulated DC voltage source, and then supply energy to a variable load. The system consists of an inductor L, a capacitor C, and a switching cell, as shown in Figure 5.2.

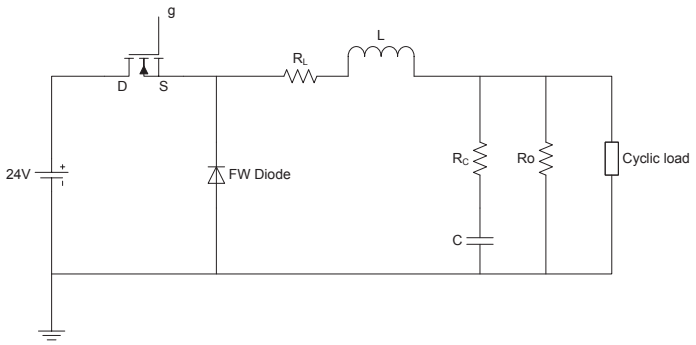

Figure 5.2: Buck converter system.

5.4.2 Polytopic model

The state-space averaged model of the buck converter is described by the following pair of equations:

$$\dot{x}(t) = \begin{cases} A_{\text{on}}x(t) + B_{\text{on}}v_s(t), & s = \text{ON}, \\ A_{\text{off}}x(t) + B_{\text{off}}v_s(t), & s = \text{OFF}. \end{cases} \tag{5.13}$$

The average linear system model is given by ([41]):

$$\dot{x}(t) = (dA_{\text{on}} + d'A_{\text{off}})x(t) + B_{\text{on}}v_u(t), \tag{5.14}$$

where d is the active fraction of the total time in a period, $x(t)$ is the state vector, $v_u(t)$ is the input, the matrices A_{on} and B_{on} are the state-space description matrices when the switch is on, and the matrix A_{off} and B_{off} are the state-space description matrices when the switch is off. The state vector and the state-space matrices are given by

$$x(t) = \begin{bmatrix} i_L(t) \\ v_C(t) \end{bmatrix}, A_{\text{on}} = A_{\text{off}} = \begin{bmatrix} 0 & \frac{1}{L} \\ \frac{1}{C} & -\frac{1}{RC} \end{bmatrix}, B_{\text{on}} = \begin{bmatrix} \frac{V_s}{L} \\ 0 \end{bmatrix}, B_{\text{off}} = \begin{bmatrix} 0 \\ 0 \end{bmatrix}.$$

5.4.3 Modulation (PWM)

The buck converter is controlled by a fixed-frequency PWM. A control signal is first generated by an adaptive controller, and then converted to a binary signal $v_u(t)$. Limited by the frequency of the PWM, the control signal is assumed to have finite resolution, which are modeled by quantization.

5.4.4 Simulation

Using the model in 5.4.2, we rewrite the buck converter by a nominal system $(A_p, B_p, c_p^\top, 0)$ with some uncertainty:

$$\begin{aligned} \dot{x}(t) =& A_p x(t) + B_p(v_u(t) + d(t)), \quad x(0) = 0, \\ y(t) =& c_p^\top x(t), \end{aligned}$$

where $A_p = A_{\text{on}=A_{\text{off}}}$, $B_p = B_{\text{off}}$, and $c_p = [01]^\top$. Then it can be written in the form of (5.1) as

$$y(s) = (s\mathbb{I} - A_p)^{-1}B_p(v_u(s) + d(s)), \quad y(0) = 0.$$

We use the output feedback adaptive controller introduced in Section 5.2 to control the supply voltage of the buck converter. Consider the case where the converter load $R = 25\Omega$, the inductance $L = 200\text{H}$, whose equivalent series resistance $R_L = 1\text{m}\Omega$, the capacitance $C = 200\text{F}$, whose equivalent series resistance $R_C = 1\text{m}\Omega$.

Figures 5.3 and 5.4 show the cases of equivalent constant current load and equivalent cyclic-varying load. We see that in the first case the steady-state output voltage stays at the assigned 12V level with no visible variations. In the second case, where the load varies by 100% periodically, the buck converter supplies a steady output voltage within 3% envelope. Thus in both cases of constant and varying loads the converter provides steady output voltage supply for the loads.

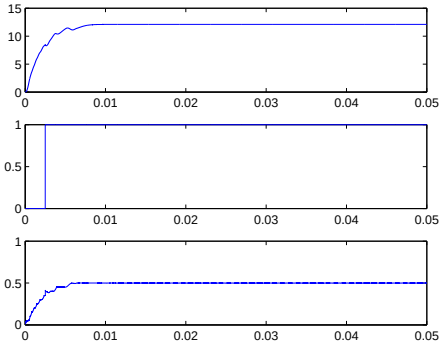

Figure 5.3: Output voltage, load, and inductor current in the case of constant load.

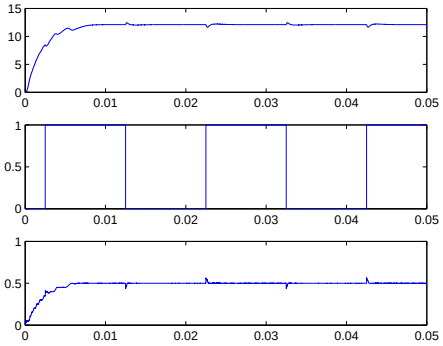

Figure 5.4: Output voltage, load, and inductor current in the case of cyclic varying load.

CHAPTER 6

STATE FEEDBACK CONTROL FOR SYSTEMS WITH INTERNAL DELAYS

"The only reason for time is so that everything doesn't happen at once." –Albert Einstein

This chapter considers control of uncertain linear systems with internal delays and disturbances, and explores the application of $\mathcal{L}_1$ adaptive controller for the trajectory control problem in directional drilling systems. In the application, the Explicit Force, Finitely Sharp, Zero Mass (EFFSZM) model is used for the steering system, in which spatial delays, modeling inaccuracies, parametric uncertainties, and noise are considered. The $\mathcal{L}_1$ adaptive controller ensures that the centerline of the borehole follows a path planned according to a priori available geologic conditions and local residential information.

6.1 Uncertain systems with internal delays

Consider a system with internal delays given by

$$\begin{aligned} \dot{x}(m) &= A_m x(m) + b_0\big(\omega u(m) + \theta_0(m)^\top x(m) + \theta_1(m)^\top x(m-\tau_1) \\ &\quad + \theta_2(m)^\top x(m-\tau_2) + \sigma(m)\big), \quad x(m) = 0\ \forall m \in [-\tau_2, 0]\,, \\ y(m) &= c_0^\top x(m)\,, \end{aligned} \tag{6.1}$$

where A_m is an $n \times n$ Hurwitz matrix by choice, $b_0, c_0 \in \mathbb{R}^n$ are known constant vectors, (A_m, b_0) is controllable, ω is an unknown constant with known sign, $\theta_0(m), \theta_1(m), \theta_2(m) \in \mathbb{R}^n$ are unknown vectors, $\tau_1, \tau_2 \in \mathbb{R}^+ (\tau_1 < \tau_2)$ are known internal delays, $\sigma(m) \in \mathbb{R}$ models the input disturbance, $x(m) \in \mathbb{R}^n$ is the system state vector (measured), $u(m) \in \mathbb{R}^m$ is the control input, and $y(m) \in \mathbb{R}$ is the regulated output.

Assumption 9 *The unknown parameters $\theta_0(m)$, $\theta_1(m)$, $\theta_2(m)$ belong to given compact convex sets Θ_0, Θ_1, Θ_2, respectively,*

$$\theta_0(m) \in \Theta_0,\ \theta_1(m) \in \Theta_1,\ \theta_2(m) \in \Theta_2,\ \forall m \geq 0.$$

Let $\theta_{\max 0} \triangleq \max_{\theta\in\Theta_0} \|\theta\|_1$, $\theta_{\max 1} \triangleq \max_{\theta\in\Theta_1} \|\theta\|_1$, $\theta_{\max 2} \triangleq \max_{\theta\in\Theta_2} \|\theta\|_1$.

The input disturbance $\sigma(m)$ is upper bounded by

$$|\sigma(m)| \leq \Delta\,,\ \forall m \geq 0\,,$$

where $\Delta \in \mathbb{R}^+$ is a known conservative bound.

Assumption 10 *Let $\theta_0(m)$, $\theta_1(m)$, $\theta_2(m)$ and $\sigma(m)$ be continuously differentiable with uniformly bounded derivatives*

$$\|\dot{\theta}_0(m)\| \leq d_{\theta 0}\,,\ \|\dot{\theta}_1(m)\| \leq d_{\theta 1}\,,$$
$$\|\dot{\theta}_2(m)\| \leq d_{\theta 2}\,,\ |\dot{\sigma}(m)| \leq d_{\sigma}\,.$$

Assumption 11 *Let $\omega \in \Omega_0 = [\omega_l, \omega_u]$, where $0 < \omega_l < \omega_u$ are given lower and upper bounds on ω.*

In the following sections, we design an adaptive controller that would compensate for the uncertainties in the system and drive the system output to track the output of a stable reference system.

6.2 Control design

In this section we present the $\mathcal{L}_1$ adaptive controller for the system in (6.1). The state predictor, adaptive law and control law are introduced as follows.

We consider the following state predictor:

$$\begin{aligned}\dot{\hat{x}}(m) =& A_m\hat{x}(m) + b_0\big(\hat{\omega}(m)u(m) + \hat{\theta}_0(m)^\top x(m) + \hat{\theta}_1(m)^\top x(m-\tau_1)\\ &+ \hat{\theta}_2(m)^\top x(m-\tau_2) + \hat{\sigma}(m)\big)\,, \quad \hat{x}(m) = 0\ \forall m \in [-\tau_2, 0]\,, \qquad (6.2)\\ \hat{y}(m) =& c_0^\top \hat{x}(m)\,,\end{aligned}$$

where $\hat{x}(m) \in \mathbb{R}^n$, $\hat{y}(m) \in \mathbb{R}$ are the state and the output of the state predictor, $\hat{\omega} \in \mathbb{R}$, $\hat{\theta}_0(m), \hat{\theta}_1(m), \hat{\theta}_2(m) \in \mathbb{R}^n$, $\hat{\sigma}(m) \in \mathbb{R}$ are estimates of the unknown

parameters ω, $\theta_0(m)$, $\theta_1(m)$, $\theta_2(m)$, and $\sigma(m)$, respectively. The projection-type adaptive laws for the estimates are given by

$$\begin{aligned}
\dot{\hat{\theta}}_0(m) =& \Gamma \mathrm{Proj}(\hat{\theta}_0(m), -\tilde{x}^\top(m) P b_0 x(m)),\ \hat{\theta}_0(0) = \hat{\theta}_{00},\\
\dot{\hat{\theta}}_1(m) =& \Gamma \mathrm{Proj}(\hat{\theta}_1(m), -\tilde{x}^\top(m) P b_0 x(m-\tau_1)),\ \hat{\theta}_1(0) = \hat{\theta}_{10},\\
\dot{\hat{\theta}}_2(m) =& \Gamma \mathrm{Proj}(\hat{\theta}_2(m), -\tilde{x}^\top(m) P b_0 x(m-\tau_2)),\ \hat{\theta}_0(0) = \hat{\theta}_{20},\\
\dot{\hat{\sigma}}(m) =& \Gamma \mathrm{Proj}(\hat{\sigma}(m), -\tilde{x}^\top(m) P b_0),\ \hat{\sigma}(0) = \hat{\sigma}_0,\\
\dot{\hat{\omega}}(m) =& \Gamma \mathrm{Proj}(\hat{\omega}(m), -\tilde{x}^\top(m) P b_0 u(m)),\ \hat{\omega}(0) = \hat{\omega}_0,
\end{aligned} \tag{6.3}$$

where $\tilde{x}(m) \triangleq \hat{x}(m) - x(m)$, $\Gamma > 0$ is the adaptation rate, $P = P^\top > 0$ solves the algebraic Lyapunov equation $A_m^\top P + P A_m = -Q$ for some symmetric $Q > 0$, and $\mathrm{Proj}(\cdot,\cdot)$ denotes the projection operator (Definition 3 in Appendix A). In the implementation of the projection operator, we use the compact sets Ω, Θ_0, Θ_1, Θ_2, and $[-\Delta, \Delta]$.

The control signal is defined by

$$u(s) = -kD(s)\left(\hat{\eta}(s) - k_g r(s)\right), \tag{6.4}$$

where $k_g \triangleq -\frac{1}{c_0^\top A_m^{-1} b_0}$, $r(s)$ and $\hat{\eta}(s)$ are the Laplace transforms of $r(m)$ and $\hat{\eta}(m) \triangleq \hat{\omega}(m)u(m) + \hat{\theta}_0^\top(m)x(m) + \hat{\theta}_1^\top(m)x(m-\tau_1) + \hat{\theta}_2^\top(m)x(m-\tau_2) + \hat{\sigma}(m)$, $k > 0$ is the feedback gain, and $D(s)$ is a strictly proper transfer function leading to a strictly proper stable

$$C(s) \triangleq \frac{\omega k D(s)}{1 + \omega k D(s)} \tag{6.5}$$

with DC gain $C(0) = 1$. One simple choice is $D(s) = \frac{1}{s}$, which yields a first order strictly proper C(s) of the following form:

$$C(s) = \frac{\omega k}{s + \omega k}.$$

The $\mathcal{L}_1$ adaptive controller consists of (6.2), (6.3) and (6.4), subject to the following $\mathcal{L}_1$ norm condition

$$\|G(s)\|_{\mathcal{L}_1}(\theta_{\max 0} + \theta_{\max 1} + \theta_{\max 2}) < 1\,, \tag{6.6}$$

where

$$H(s) \triangleq (s\mathbb{I} - A_m)^{-1} b_0\,, \quad G(s) \triangleq H(s)(C(s) - 1)\,. \tag{6.7}$$

6.3 Performance analysis

6.3.1 Stability of the reference system

Consider the reference system

$$\begin{aligned}\dot{x}_{\text{ref}}(m) =& A_m x_{\text{ref}}(m) + b_0\big(\omega u_{\text{ref}}(m) + \theta_0(m)^\top x_{\text{ref}}(m) + \theta_1(m)^\top x_{\text{ref}}(m-\tau_1) \\ &+ \theta_2(m)^\top x_{\text{ref}}(m-\tau_2) + \sigma(m)\big)\,, \quad x_{\text{ref}}(m) = 0\ \forall m \in [-\tau_2, 0]\,, \\ y_{\text{ref}}(m) =& c_0^\top x_{\text{ref}}(m)\,,\end{aligned} \tag{6.8}$$

and the reference controller

$$u_{\text{ref}}(s) = \frac{C(s)}{\omega}\big(-\eta_{\text{ref}}(s) + k_g r(s)\big)\,, \tag{6.9}$$

where $\eta_{\text{ref}}(s)$ is the Laplace transform of

$$\eta_{\text{ref}}(m) \triangleq \theta_0^\top(m) x_{\text{ref}}(m) + \theta_1^\top(m) x_{\text{ref}}(m-\tau_1) + \theta_2^\top(m) x_{\text{ref}}(m-\tau_2) + \sigma(m).$$

Lemma 15 *If the condition in* (6.6) *holds, then the reference system in* (6.8) *and* (6.9) *is BIBO stable with respect to* $r(m)$.

Proof. See Appendix B.11.

6.3.2 Prediction error

As defined in (6.3), $\tilde{x}(t) = \hat{x}(t) - x(t)$ is the error between the state of the system and the state of the predictor. From (6.1) and (6.2), we have the prediction error dynamics

$$\begin{aligned}\dot{\tilde{x}}(m) =& A_m \tilde{x}(m) + b_0\big(\tilde{\omega}(m) u(m) + \tilde{\theta}_0(m)^\top x(m) + \tilde{\theta}_1(m)^\top x(m-\tau_1) \\ &+ \tilde{\theta}_2(m)^\top x(m-\tau_2) + \tilde{\sigma}(m)\big)\,, \quad \tilde{x}(m) = 0\ \forall m \in [-\tau_2, 0]\,,\end{aligned} \tag{6.10}$$

where $\tilde{\theta}_0(m) \triangleq \hat{\theta}_0(m) - \theta_0(m)$, $\tilde{\theta}_1(m) \triangleq \hat{\theta}_1(m) - \theta_1(m)$, $\tilde{\theta}_2(m) \triangleq \hat{\theta}_2(m) - \theta_2(m)$, $\tilde{\sigma}(m) \triangleq \hat{\sigma}(m) - \sigma(m)$, and $\tilde{\omega}(m) \triangleq \hat{\omega}(m) - \omega$. Let

$$\begin{aligned}\tilde{\eta}(m) \triangleq & \tilde{\omega}(m)u(m) + \tilde{\theta}_0(m)^\top x(m) + \tilde{\theta}_1(m)^\top x(m-\tau_1) \\ & + \tilde{\theta}_2(m)^\top x(m-\tau_2) + \tilde{\sigma}(m)\,. \end{aligned} \tag{6.11}$$

Then the prediction error dynamics in (6.10) can be written as

$$\tilde{x}(s) = H(s)\tilde{\eta}(s)\,. \tag{6.12}$$

Lemma 16 *For the system in (6.1) and the controller defined by (6.4), we have the following bound*

$$\|\tilde{x}\|_{\mathcal{L}_\infty} \leq \sqrt{\frac{\theta_m}{\lambda_{\min}(P)\Gamma}}\,, \tag{6.13}$$

where

$$\theta_m \triangleq 4\sum_{i=0}^{2} \max_{\theta_i \in \Theta_i} \|\theta\|_2^2 + 4\Delta^2 + (\omega_u - \omega_l)^2 + 4\frac{\lambda_{\max}(P)}{\lambda_{\min}(Q)}(d_\theta \max_{\theta\in\Theta}\|\theta\| + d_\sigma\Delta)\,,$$

and $\lambda_{\min}(\cdot)$ is the smallest eigenvalue of a matrix.

The proof is similar to the one in [20] and is thus omitted.

6.3.3 Performance bounds

Theorem 10 *Consider the system in (6.1) and the controller in* (6.2)*,* (6.3) *and* (6.4)*. If the $\mathcal{L}_1$-norm condition in* (6.6) *holds, then the errors are upper bounded by*

$$\|x - x_{\text{ref}}\|_{\mathcal{L}_\infty} \leq \gamma_x\,,\ \|u - u_{\text{ref}}\|_{\mathcal{L}_\infty} \leq \gamma_u\,, \tag{6.14}$$

where γ_x and γ_u are given by

$$\gamma_x \triangleq \frac{\|C(s)\|_{\mathcal{L}_1}}{1-\|G(s)\|_{\mathcal{L}_1}\big(\theta_{\max 0}+\theta_{\max 1}+\theta_{\max 2}\big)}\sqrt{\frac{\theta_m}{\lambda_{\min}(P)\Gamma}},$$

$$\gamma_u \triangleq \left\|\frac{C(s)}{\omega}\right\|_{\mathcal{L}_1}\big(\theta_{\max 0}+\theta_{\max 1}+\theta_{\max 2}\big)\gamma_x + \left\|\frac{C(s)}{\omega c_o^\top H(s)}c_o^\top\right\|_{\mathcal{L}_1}\sqrt{\frac{\theta_m}{\lambda_{\min}(P)\Gamma}}\,.$$

Proof. See Appendix B.12.

6.4 Application to a rotary steerable system

6.4.1 Rotary steerable system

Directional drilling systems utilize drill pipes suspended within the borehole. The drill pipes connect with the drill rig at the surface, which rotates and applies weight on the bit. On the drill pipes stabilizers or force actuators are placed at a certain distance from the drilling bit to displace the bit and change the angle of the drilling direction while measurement-while-drilling tools are equipped to send directional data back to the surface without disturbing drilling operations. In a rotary steerable system the actual drilling trajectory depends on a variety of factors, such as assembly configuration and dimensions, lithology, dip, bit type, hole curvature, magnitude of inclination, bit weight, and rotary speed.

The directionally steered drilling system models the relationship between the centerline of the drilling hole and the actuator stimuli. By the geometry and the action of the actuators, the bit force can be computed, and approximate models can be derived. In this paper, we use the EFFSZM (Explicit Force, Finitely Sharp, Zero Mass) model given in [15], where the directional drilling system is assumed to have a force actuator on the lower collar; the bit is assumed to be finitely sharp; and the pipe work is assumed to be infinitely stiff with zero mass.

The system dynamics in the EFFSZM case is given by

$$\begin{aligned}\frac{dH(m)}{dm} =& \left(\frac{1+C_f}{b} - \frac{C_f}{d}\right) H(m) + \frac{1+C_f}{b}(V(m) - H(m-b)) \\ &+ \frac{C_f}{d} H(m-d) + \frac{b-a}{b\, WOB\, K_{anis}} F_{pad}(m)\,, \qquad (6.15) \\ \Psi(m) =& \frac{dH(m)}{dm}\,,\end{aligned}$$

where $C_f = \left(\frac{c-b}{K_{anis}} - \frac{d-b}{d-c}\frac{K_{flex}}{WOB}\right)\frac{d}{b(d-c)}$; m is the distance drilled along the direction of drilling; $H(m)$ is the lateral displacement of the borehole; a is the distance between the force actuator and the bit; b is the distance between the lower stabilizer and the bit; c is the relative position of the flex-joint to the bit; d is the position of the upper stabilizer to the bit; $V(m)$ is the actuator displacement at the lower stabilizer; WOB (Weight on Bit) is the applied drilling load; K_{anis} is the ratio of rates of penetration along and across the bit; K_{flex} is the angular spring rate of the flex joint; $F_{pad}(m)$ is the force actuator output; and $\Psi(m)$ is the measured angle of borehole-propagation with respect to the m-axis. The structure of the drilling system is shown in Figure 6.1.

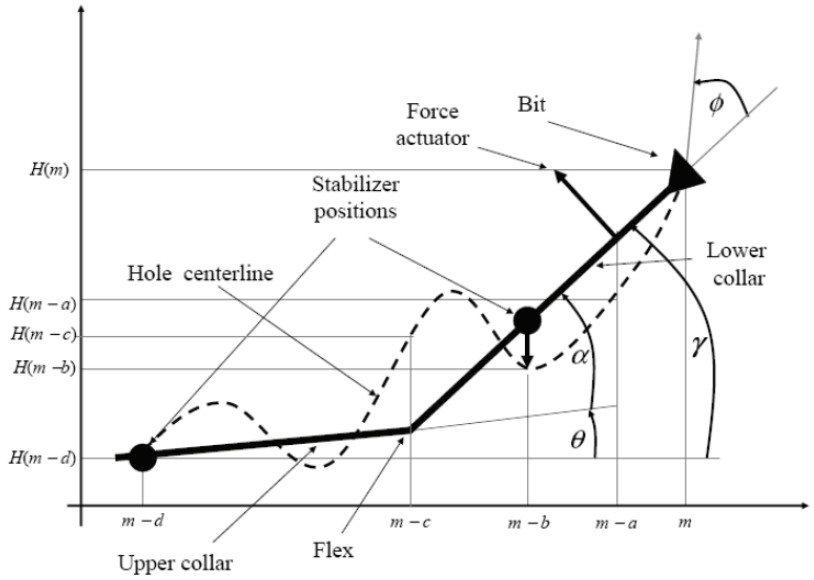

Figure 6.1: Flex-hinge directional drilling system [15].

Note that in the system described in (6.15), the independent variable is the drilled distance m instead of time t.

The model can also be written in transfer function form as

$$H(s) = \frac{\frac{1+C_f}{b}V(s) + \frac{b-a}{bW_{OB}K_{anis}}F_{pad}(s)}{s + \frac{C_f}{d}(1-e^{-sd}) - \frac{1+C_f}{b}(1-e^{-sb})},$$
$$\Psi(s) = sH(s).$$

Open-loop Performance

For different parameter settings, the response of the aforementioned system to the same input varies. In the drilling process in different rock layers, some parameters determined by the actuator and stabilizer positions and spring rates are known, such as a, b, c, d, K_{flex}, while some others such as WOB and K_{anis} are unknown, and may take different values in a compact set.

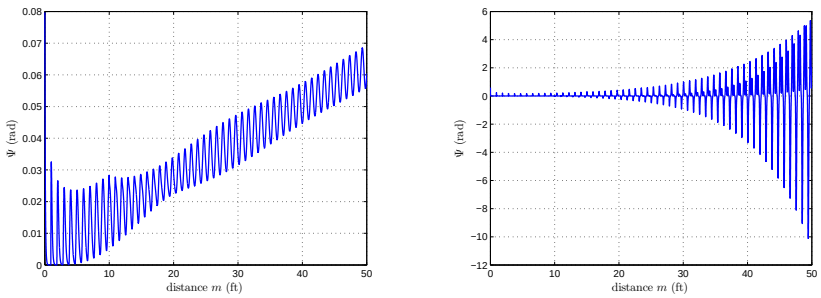

(a) $WOB = 1.5 \times 10^4$, $K_{anis} = 5$ (b) $WOB = 1 \times 10^4$, $K_{anis} = 5$

Figure 6.2: Open-loop performance for different parameter values.

Figure 6.2 shows the response of the open-loop system to a constant force $F_{pad}(m) \equiv 8.896 \times 10^3$ N. The applied drilling load and the rate ratio are $WOB = 1.5 \times 10^4$ N, $K_{anis} = 5$ and $WOB = 1 \times 10^4$ N, $K_{anis} = 1$ for Figures 6.2a and 6.2b, respectively, and detailed settings for other parameters are introduced in Subsection 6.4.2. In the first case, the system is marginally stable. The response is almost a ramp, i.e. the step response of an integrator. In the second case, the output diverges, and the system is unstable.

Model transformation

Specifically in the EFFSZM model, $x(m) \triangleq \Psi(m)$, $u(m) \triangleq \dot{F}_{pad}(m)$, $A_m < 0$ is a designed scalar, and

$$
\begin{aligned}
&b_0 = 1,\ c_0 = 1,\ \tau_1 = b,\ \tau_2 = d,\\
&\theta_0 = \left(\frac{1+C_f}{b} - \frac{C_f}{d}\right) - A_m, \theta_1 = -\frac{1+C_f}{b},\ \theta_2 = \frac{C_f}{d},\\
&\omega = \frac{b-a}{b\,WOB\,K_{anis}}, \sigma(m) = \frac{1+C_f}{b}\dot{V}(m).
\end{aligned}
$$

Remark 24 *Note that for EFFSZM model the following property holds:*

$$A_m + \theta_0 + \theta_1 + \theta_2 = 0.$$

The transfer function of the system in (6.1) *can be written as*

$$x(s) = \frac{b_0\omega}{A_m + \theta_0 + \theta_1 e^{-\tau_1 s} + \theta_2 e^{-\tau_2 s}}\big(u(s) + \sigma(s)\big)\,.$$

Thus, $s = 0$ is one of the infinitely many poles of the transfer function. The system can be at most marginally stable. This is in accordance with the open-loop cases shown in the previous subsection.

6.4.2 Test case

In this section, we discuss simulation results of a test case of a rotary steerable system. The test case is a fictitious one, but representative of controlling the angle at which a directional steering system drills with respect to the hole propagation direction. We assume that the borehole motion takes place only in the vertical plane. For simplicity of analysis we shall assume that the case is valid for ± 20 degree angles with respect to the horizontal, so that the small-angle approximation holds and the approximated EFFSZM model can be used.

For simplicity we assume that there are no delays in measuring $\Psi(m)$, or in sending down the new steering commands. The steering control commands produce the actuator force $F_{pad}(m)$ that pushes against the borehole wall.

The control objective is to servo $\Psi(m)$ to a user defined angle (assume that the system starts from 0 degrees). We assume that the driller wants to change

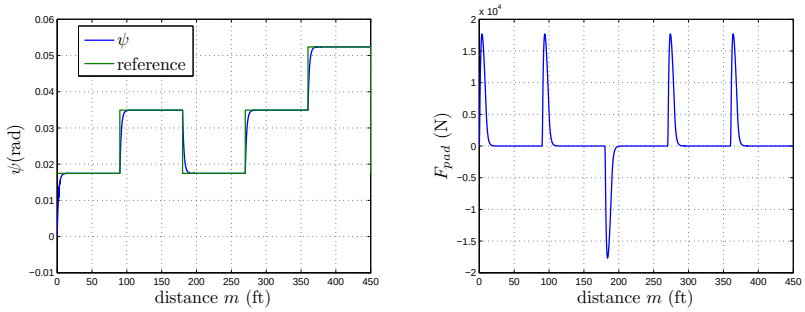

Figure 6.3: Closed-loop system with $K_{anis} = 5$ and $W_{OB} = 1.5 \times 10^4$.

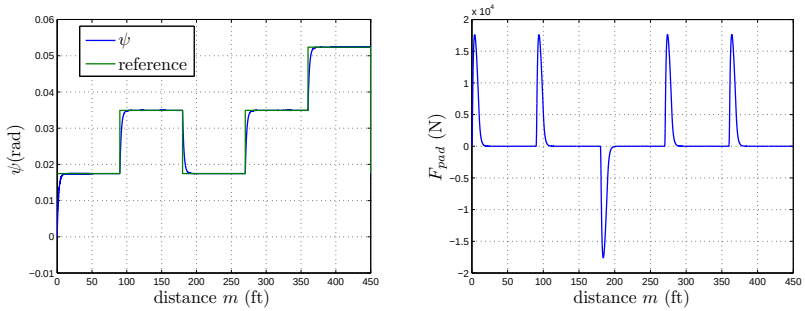

Figure 6.4: Closed-loop system (open-loop unstable) with $K_{anis} = 1$ and $W_{OB} = 1 \times 10^4$.

inclination in 1 degree random steps every 90 ft drilled.

The geometrical and structural parameters used in the EFFSZM model are fixed. The values are given by

$$a = 0.305\text{m},\ b = 0.953\text{m},\ c = 1.407\text{m},\ d = 2\text{m}, K_{flex} = 8.577 \times 10^5 \text{N} \cdot \text{m/rad}.$$

The uncertain parameters WOB and K_{anis} have the following range of variation $WOB \in [10^4, 1.6 \times 10^5]$N, $K_{anis} \in [1, 100]$.

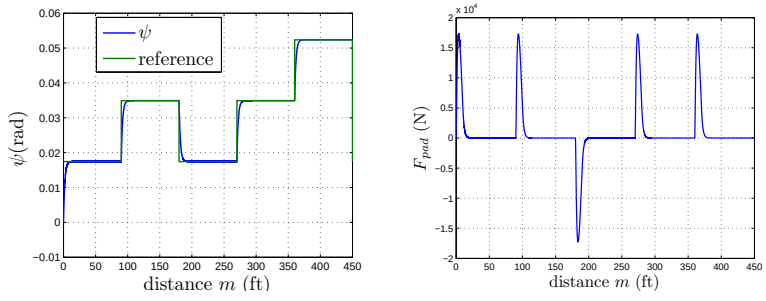

Figure 6.5: Closed-loop system with $K_{anis} = 5$ and $W_{OB} = 8.8964 \times 10^4$.

We use the $\mathcal{L}_1$ adaptive controller with the following parameters:

$$
\begin{aligned}
&A_m = -0.5\,,\ \Gamma = 10^8\,,\ k = 10^4\,,\\
&C_f \in [-252.8380, -11.1425]\,,\ \Theta_0 = [-49.7445, -1.8306]\,,\\
&\Theta_1 = [3.0249, 75.1083]\,,\ \Theta_2 = [-25.2838, -1.1142]\,,\\
&\Omega \in [5.6815 \times 10^{-8}, 9.0904 \times 10^{-5}]\,.
\end{aligned}
$$

The result of Theorem 10 ensures that $\mathcal{L}_1$ adaptive controller drives the system output close to the output of the stable reference system. It deals with internal delays and slow-varying uncertain parameters in the system. In this test case, there are further restrictions such as the actuator force limit.

We show the angle of drilling direction $\Psi(m)$ and the actuator force $F_{pad}(m)$ for three different cases.

1. $K_{anis} = 5$ and $W_{OB} = 1.5 \times 10^4$. Figure 6.3 shows the inclination angle Ψ and the control input F_{pad} after saturation. The angle tracks the command perfectly with a "growing distance" of about 10 ft, and the control signal changes smoothly.

2. $K_{anis} = 1$ and $W_{OB} = 10^4$. Under this set of parameters, the closed-loop system response is similar to the above case.

3. $K_{anis} = 5$ and $W_{OB} = 8.8964 \times 10^4$. The angle and the control signal are shown in Figure 6.5.

Recall that the open-loop performance of the first two cases is shown in Subsection 6.4.1. In the first case the open-loop system performed similar to a marginally stable system and in the second case the open-loop system is unstable. Now, as shown in Figures 6.3, 6.4, and 6.5, the closed-loop system responds to a step command uniformly in all cases.

Further, we present results for the case where the two uncertain parameters K_{anis} and W_{OB} are "distance"-varying, representing the condition changes, when the bit penetrates different rock layers, as in Figure 6.6. Note that in all cases the design of the adaptive controller is fixed (there is no retuning), and the controller adjusts to the new parameter settings and ensures that the closed-loop system maintains the desired output response.

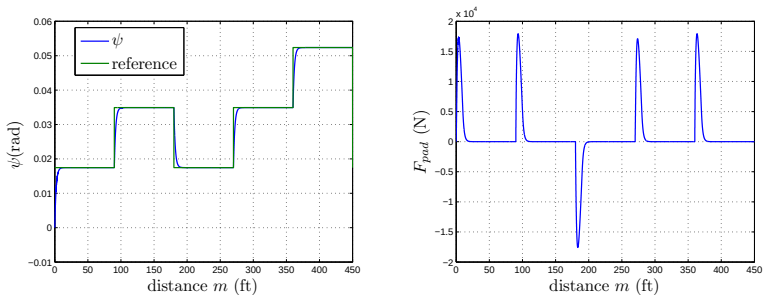

Figure 6.6: Closed-loop system with K_{anis} varies every 80 ft between 1 and 100 and W_{OB} varies every 50 ft between 10^4 and 1.6×10^5 N.

CHAPTER 7

CONCLUSION

"Learn from yesterday, live for today, hope for tomorrow. The important thing is not to stop questioning." –Albert Einstein

In this dissertation, we have considered the reference tracking control problem for quantized uncertain systems and delayed uncertain systems. Different variations of the $\mathcal{L}_1$ adaptive controller have been developed to address this control problem in the presence of quantization and system delays. The closed-loop system performance has been analyzed and the simulations/applications using the theoretical results have been shown.

The first part, comprising Chapters 2-5, is devoted to quantized uncertain systems. The quantization schemes considered are the typical uniform and logarithmic quantizations. To avoid possible chattering phenomena, hysteresis is introduced in the quantization function. The uncertainties considered include both linear and nonlinear, matched and unmatched uncertainties. In general, in all cases the designed controllers have been shown to drive the system output close to that of the reference system. The performance bounds are governed by the adaptation rate and the quantization density. Specifically, in the case of state feedback control of input-quantized systems, the performance bounds are decoupled into two terms, one determined by the adaptation rate and the other by the input quantization scheme. In the case of systems with both input and state quantizations, while the performance bounds are determined by adaptation and quantization as well, the quantization part depends on input and state quantization. The influence of the two quantization schemes on the performance has a "water-bed" like effect. In the case of output feedback systems, the performance bounds depend on the sampling time, which in a piecewise constant adaptation law reflects how fast the estimates adapt, as well as quantization. Simulations and an application to a buck converter have been used to demonstrate the theoretical results.

The second part, comprising Chapter 6, has considered systems with internal delays. The controller has been shown to compensate the uncertainties and

achieve close tracking of the reference system in the presence of internal delays. This study has been applied to control of the drilling bit in a rotary steerable system, where the spatial delays come from the difference of equipment positions. Different scenarios of significant weight on bit change, time-varying load and stabilizer vibration during drilling process, and limited control action over every period are tested. In all scenarios of this application, the drilling process has been shown to follow the pre-determined well path closely and smoothly without any retuning of the controller.

Future work will consider decentralized systems or stochastic systems with additive noise (Brownian motion). In networked control systems, quantization is closely related to coding and information theory. For transmissions of large amounts of data packages, it is natural to use stochastic models. Besides, many real systems are intrinsically random, such as the reproduction process of cells, the human decision and behavior in large groups, and various biochemical events like binding and unbinding of RNA polymerase to a gene promoter. In stochastic systems, how to model unknown but deterministic uncertainties and unpredictable stochastic uncertainties and how to control stochastic systems and evaluate performance in a statistical sense are questions to study. A similar idea of uncertainty compensation could be used in the stochastic control problem. With current estimation tools of stochastic process such as Kalman filter or particle filter, and control tools of deterministic systems such as $\mathcal{L}_1$ adaptive control, the combination could be a future direction in which to go. Other practical applications, such as power systems, are also relevant and interesting future topics.

APPENDIX A

PROJECTION OPERATOR

Definition 3 ([29]) *Given a convex compact set with a smooth boundary given by* $\Omega_c \triangleq \{\hat{\theta} \in \mathbb{R}^n | h(\hat{\theta}) \leq c\}$, $0 \leq c \leq 1$, *where* $h : \mathbb{R}^n \to \mathbb{R}$ *is the following smooth convex function* $h(\hat{\theta}) = \frac{(\epsilon_\theta+1)\hat{\theta}^\top\hat{\theta}-\theta_{\max}^2}{\epsilon_\theta\theta_{\max}^2}$, *with* $\theta_{\max}$ *being the norm bound imposed on the vector* $\hat{\theta}$, *and* $\epsilon_\theta > 0$ *being the projection tolerance bound, the projection operator* $\mathrm{Proj}(\hat{\theta}, y)$ *[29] is defined as*

$$\mathrm{Proj}(\hat{\theta}, y) \triangleq \begin{cases} y & \text{if } h(\hat{\theta}) < 0, \\ y & \text{if } h(\hat{\theta}) \geq 0 \text{ and } \nabla h^\top y \leq 0, \\ y - \frac{\nabla h}{\|\nabla h\|}\langle \frac{\nabla h}{\|\nabla h\|}, y\rangle h(\hat{\theta}) & \text{if } h(\hat{\theta}) \geq 0 \text{ and } \nabla h^\top y > 0. \end{cases}$$

Property 1 ([29]) *The projection operator* $\mathrm{Proj}(\hat{\theta}, y)$ *does not alter* y, *if* $\hat{\theta}$ *belongs to the set* $\Omega_0 \triangleq \{\hat{\theta} \in \mathbb{R}^n | h(\hat{\theta}) \leq 0\}$. *In the set* $\{\hat{\theta} \in \mathbb{R}^n | 0 \leq h(\hat{\theta}) \leq 1\}$, *if* $\nabla h^\top y > 0$, *the* $\mathrm{Proj}(\hat{\theta}, y)$ *operator subtracts a vector normal to the boundary* $\bar{\Omega}_{h(\hat{\theta})} \triangleq \{\bar{\theta} \in \mathbb{R}^n | h(\bar{\theta}) = h(\theta)\}$, *so that we get a smooth transformation from the original vector field* y *to an inward or tangent vector field for* Ω_1.

Property 2 ([29]) *Given the vectors* $y \in \mathbb{R}^n$, $\theta^* \in \Omega_0 \subset \Omega_1 \subset \mathbb{R}^n$, *and* $\theta \in \Omega_1$, *we have* $(\hat{\theta} - \theta^*)^\top(\mathrm{Proj}(\hat{\theta}, y) - y) \leq 0$.

APPENDIX B

PROOFS

B.1 Proof of Lemma 3

First, $e_x(t) = x(t) - x_{ref}(t) = \hat{x}(t) - \tilde{x}(t) - x_{ref}(t)$.

On the one hand, from (3.5) it follows that

$$\begin{aligned}\hat{x}(s) =& - H(s)\hat{\eta}(s) + H(s)u_q(s) + (s\mathbb{I} - A_m)^{-1}x_0 \\ =& -H(s)\hat{\eta}(s) + H(s)u(s) - H(s)u_{qe}(s) + (s\mathbb{I} - A_m)^{-1}x_0,\end{aligned}$$

where $\hat{\eta}(t) = \hat{\theta}^\top(t)x(t)$ is defined in Section 3.3. By (3.7), we further write

$$\hat{x}(s) = G(s)\hat{\eta}(s) + H(s)C(s)k_g r(s) - H(s)u_{qe}(s) + (s\mathbb{I} - A_m)^{-1}x_0. \quad \text{(B.1)}$$

Note that

$$\begin{aligned}\hat{\eta}(t) =& \hat{\theta}^\top(t)x(t) = \theta^\top x(t) + \tilde{\theta}^\top(t)x(t) \\ =& \theta^\top\hat{x}(t) - \theta^\top\tilde{x}(t) + \tilde{\theta}^\top(t)x(t). \quad \text{(B.2)}\end{aligned}$$

Substitute (B.2) into (B.1) to obtain

$$\begin{aligned}\hat{x}(s) =& (\mathbb{I} - G(s)\theta^\top)^{-1}H(s)C(s)k_g r(s) \\ &+ (\mathbb{I} - G(s)\theta^\top)^{-1}[-G(s)\theta^\top - (C(s) - 1)\mathbb{I}]\tilde{x}(s) \\ &+ (\mathbb{I} - G(s)\theta^\top)^{-1}H(s)u_{qe}(s) + (\mathbb{I} - G(s)\theta^\top)^{-1}(s\mathbb{I} - A_m)^{-1}x_0.\end{aligned}$$

On the other hand, in (3.12) we have

$$x_{ref}(s) = (\mathbb{I} - G(s)\theta^\top)^{-1}[H(s)C(s)k_g r(s) + (s\mathbb{I} - A_m)^{-1}x_0].$$

Subtracting $x_{ref}(s)$ from $x(s)$ gives

$$\begin{aligned} e_x(s) =&(\mathbb{I} - G(s)\theta^\top)^{-1}[-G(s)\theta^\top - (C(s)-1)\mathbb{I}]\tilde{x}(s) \\ &+ (\mathbb{I} - G(s)\theta^\top)^{-1}H(s)u_{qe}(s). \end{aligned}$$

Thus, Lemma 1 in [21] (which follows the definition of $\mathcal{L}_1$ norm) gives

$$\begin{aligned} \|e_{x_\tau}\|_{\mathcal{L}_\infty} \leq &\|(\mathbb{I} - G(s)\theta^\top)^{-1}[G(s)\theta^\top + (C(s)-1)\mathbb{I}]\|_{\mathcal{L}_1}\|\tilde{x}_\tau\|_{\mathcal{L}_\infty} \\ &+ \|((\mathbb{I} - G(s)\theta^\top)^{-1}H(s)u_{qe})_\tau\|_{\mathcal{L}_\infty}\,. \end{aligned}$$

Now we examine the error between the quantized control signal and the desired reference control signal

$$e_u(t) = u_q(t) - u_{ref}(t) = (u(t) - u_{ref}(t)) + u_{qe}(t). \tag{B.3}$$

By (3.7) and (3.11), we have

$$u(s) - u_{ref}(s) = C(s)\tilde{\eta}(s) - C(s)\theta^\top(x(s) - x_{ref}(s)),$$

where $\tilde{\eta}(t) = \tilde{\theta}^\top(t)x(t)$. Since (A_m, b) is controllable, and $H(s)$ is strictly proper and stable, there exists $c_o \in \mathbb{R}^n$ such that $c_o^\top H(s)$ is minimum phase with relative degree one (by Lemma 4 in [21]). Then

$$\begin{aligned} u(s) - u_{ref}(s) =&C(s)\frac{c_o^\top H(s)\tilde{\eta}(s)}{c_o^\top H(s)} + C(s)\theta^\top e_x(s) \\ =&C(s)\frac{1}{c_o^\top H(s)}c_o^\top\tilde{x}(s) + C(s)\theta^\top e_x(s)\,. \end{aligned}$$

Since $C(s)$ is BIBO stable and strictly proper, the complete system $C(s)\frac{1}{c_o^\top H(s)}$ is proper and BIBO stable, which implies that its $\mathcal{L}_1$ norm is bounded. Hence,

$$\|(u - u_{ref})_\tau\|_{\mathcal{L}_\infty} \leq \left\|C(s)\frac{1}{c_o^\top H(s)}c_o^\top\right\|_{\mathcal{L}_1}\|\tilde{x}_\tau\|_{\mathcal{L}_\infty} + \|C(s)\theta^\top\|_{\mathcal{L}_1}\|e_{x_\tau}\|_{\mathcal{L}_\infty}\,.$$

By (B.3), we have

$$\|e_{u_\tau}\|_{\mathcal{L}_\infty} \leq \|(u - u_{ref})_\tau\|_{\mathcal{L}_\infty} + \|u_{qe_\tau}\|_{\mathcal{L}_\infty}\,,$$

which leads to the bound in (3.17). □

B.2 Proof of Theorem 2

Following Lemma 3 and Equation (2.5), we have

$$\begin{aligned}\|e_{x_\tau}\|_{\mathcal{L}_\infty} \leq & \|(\mathbb{I}-G(s)\theta^\top)^{-1}[G(s)\theta^\top+(C(s)-1)\mathbb{I}]\|_{\mathcal{L}_1}\|\tilde{x}_\tau\|_{\mathcal{L}_\infty} \\ & + \|(\mathbb{I}-G(s)\theta^\top)^{-1}H(s)\|_{\mathcal{L}_1}\Delta\|u_\tau\|_{\mathcal{L}_\infty}. \end{aligned} \tag{B.4}$$

For the last term, note that $u(s) = C(s)(\hat{\eta}(s) + k_g r(s))$, and

$$\begin{aligned}\|u_\tau\|_{\mathcal{L}_\infty} \leq & \|C(s)\|_{\mathcal{L}_1}\|(\hat{\eta}+k_g r)_\tau\|_{\mathcal{L}_\infty} \\ \leq & \|C(s)\|_{\mathcal{L}_1}\|\hat{\eta}_\tau\|_{\mathcal{L}_\infty} + \|C(s)\|_{\mathcal{L}_1}k_g\|r_\tau\|_{\mathcal{L}_\infty}, \end{aligned} \tag{B.5}$$

where $\hat{\eta}(t) = -\hat{\theta}^\top(t)x(t) = -\hat{\theta}^\top(t)e(t) - \hat{\theta}^\top(t)x_{ref}(t)$,

$$\|\hat{\eta}_\tau\|_{\mathcal{L}_\infty} \leq \theta_{1\max}\|e_{x_\tau}\|_{\mathcal{L}_\infty} + \theta_{1\max}\|x_{ref_\tau}\|_{\mathcal{L}_\infty}. \tag{B.6}$$

Substitute (B.5) and (B.6) into (B.4) to get

$$\begin{aligned}\|e_{x_\tau}\|_{\mathcal{L}_\infty} \leq & \|(\mathbb{I}-G(s)\theta^\top)^{-1}[G(s)\theta^\top+(C(s)-1)\mathbb{I}]\|_{\mathcal{L}_1}\|\tilde{x}_\tau\|_{\mathcal{L}_\infty} \\ & + \|(\mathbb{I}-G(s)\theta^\top)^{-1}H(s)\|_{\mathcal{L}_1}\Delta\|C(s)\|_{\mathcal{L}_1}\theta_{1\max}\|e_{x_\tau}\|_{\mathcal{L}_\infty} \\ & + \|(\mathbb{I}-G(s)\theta^\top)^{-1}H(s)\|_{\mathcal{L}_1}\Delta\|C(s)\|_{\mathcal{L}_1}\theta_{1\max}\|x_{ref_\tau}\|_{\mathcal{L}_\infty} \\ & + \|(\mathbb{I}-G(s)\theta^\top)^{-1}H(s)\|_{\mathcal{L}_1}\Delta\|C(s)\|_{\mathcal{L}_1}k_g\|r_\tau\|_{\mathcal{L}_\infty}. \end{aligned}$$

Thus $\|e_{x_\tau}\|_{\mathcal{L}_\infty} \leq B_{xlog}$. Since B_{xlog} is uniform over all $\tau \in (0,\infty)$, $\|e_x\|_{\mathcal{L}_\infty} \leq B_{xlog}$.

Similarly, we substitute (2.5) into (3.17) in Lemma 3 to get

$$\|e_{u_\tau}\|_{\mathcal{L}_\infty} \leq \left\|C(s)\frac{1}{c_o^\top H(s)}c_o^\top\right\|_{\mathcal{L}_1}\|\tilde{x}_\tau\|_{\mathcal{L}_\infty} + \|C(s)\theta^\top\|_{\mathcal{L}_1}\|e_{x_\tau}\|_{\mathcal{L}_\infty} + \Delta\|u_\tau\|_{\mathcal{L}_\infty}.$$

Substituting (B.5) and (B.6) into the above inequality gives

$$\begin{aligned}\|e_{u_\tau}\|_{\mathcal{L}_\infty} \leq & \left\|C(s)\frac{1}{c_o^\top H(s)}c_o^\top\right\|_{\mathcal{L}_1}\|\tilde{x}_\tau\|_{\mathcal{L}_\infty} \\ & + \|C(s)\theta^\top\|_{\mathcal{L}_1}\|e_{x_\tau}\|_{\mathcal{L}_\infty} + \Delta\|C(s)\|_{\mathcal{L}_1}\theta_{1\max}\|e_{x_\tau}\|_{\mathcal{L}_\infty} \\ & + \Delta\|C(s)\|_{\mathcal{L}_1}\theta_{1\max}\|x_{ref_\tau}\|_{\mathcal{L}_\infty} + \Delta\|C(s)\|_{\mathcal{L}_1}k_g\|r_\tau\|_{\mathcal{L}_\infty}, \end{aligned}$$

which implies $\|e_u\|_{\mathcal{L}_\infty} \leq B_{ulog}$. Since the bound is uniform for all $\tau \in (0,\infty)$,

we have the inequality in (3.20). □

B.3 Proof of Theorem 3

(By contradiction)

Assume that the bounds in (3.47) do not hold. Then, since

$$\|x(0) - x_{\text{ref}}(0)\|_\infty = 0 < \gamma_{x_{\log}}, \quad \|u(0) - u_{\text{ref}}(0)\|_\infty = 0 < \gamma_{u_{\log}},$$

and $x(t)$, $x_{\text{ref}}(t)$, $u(t)$, and $u_{\text{ref}}(t)$ are continuous, there exists t' such that either

$$\|x(t') - x_{\text{ref}}(t')\|_\infty = \gamma_{x_{\log}}, \quad \text{or } \|u(t') - u_{\text{ref}}(t')\|_\infty = \gamma_{u_{\log}}, \tag{B.7}$$

while $\|x(\tau) - x_{\text{ref}}(\tau)\|_\infty < \gamma_{x_{\log}}$, $\|u(\tau) - u_{\text{ref}}(\tau)\|_\infty < \gamma_{u_{\log}}$, $\forall \tau \in [0, t')$, which implies that

$$\|(x - x_{\text{ref}})_{t'}\|_{\mathcal{L}_\infty} \leq \gamma_{x_{\log}}, \ \|(u - u_{\text{ref}})_{t'}\|_{\mathcal{L}_\infty} \leq \gamma_{u_{\log}}. \tag{B.8}$$

It follows from Assumption 5 that

$$\|z_{t'}\|_{\mathcal{L}_\infty} \leq L_z \left(\|x_{\text{ref}\,t'}\|_{\mathcal{L}_\infty} + \gamma_{x_{\log}} \right) + B_z \,. \tag{B.9}$$

Then, Lemma 12 implies that

$$\|x_{\text{ref}\,t'}\|_{\mathcal{L}_\infty} \leq \rho_{x_r}, \quad \|u_{\text{ref}\,t'}\|_{\mathcal{L}_\infty} \leq \rho_{u_r}. \tag{B.10}$$

Using the definitions of $\rho_{x_{\log}}$ and $\rho_{u_{\log}}$ in (3.43) and (3.45), together with the bounds in (B.8) and (B.10), we have $\|x_{t'}\|_{\mathcal{L}_\infty} \leq \rho_{x_r} + \gamma_{x_{\log}} \leq \rho_{x_{\log}}$, $\|u_{t'}\|_{\mathcal{L}_\infty} \leq \rho_{u_r} + \gamma_{u_{\log}} \leq \rho_{u_{\log}}$. Hence, if one chooses the adaptive gain according to (3.41) and the projection is confined to the bounds in (3.42), Lemma 6 implies that

$$\|\tilde{x}_{t'}\|_{\mathcal{L}_\infty} < \gamma_0 \,. \tag{B.11}$$

Next, let $\tilde{\eta}(t) = \tilde{\omega}(t)u(t) + \tilde{\eta}_1(t) + \tilde{\eta}_{2m}(t)$, where $\tilde{\eta}_{2m}(t)$ is the signal with Laplace transform $\tilde{\eta}_{2m}(s) = H_m^{-1}(s)H_{um}(s)\tilde{\eta}_2(s)$, and $\tilde{\eta}_1(t)$ and $\tilde{\eta}_2(t)$ were de-

fined in (3.39). It follows from (3.32) that

$$\chi(s) = D(s)\big(\omega u(s) + \eta_1(s) + H_m^{-1}(s)H_{um}(s)\eta_2(s) - K_g(s)r(s) + \tilde{\eta}(s)\big),$$

where $\eta_1(s)$, $\eta_2(s)$, and $\tilde{\eta}(s)$ are the Laplace transforms of the signals $\eta_1(t)$, $\eta_2(t)$ (defined in (3.39)), and $\tilde{\eta}(t)$, respectively. Consequently

$$\begin{aligned}\chi(s) = &\left(\mathbb{I}_m + D(s)\omega K\right)^{-1} D(s)\big(\eta_1(s) \\ &+ H_m^{-1}(s)H_{um}(s)\eta_2(s) - K_g(s)r(s) + \tilde{\eta}(s)\big)\,,\end{aligned}$$

which leads to

$$\begin{aligned}u(s) = &- K\left(\mathbb{I}_m + D(s)\omega K\right)^{-1} D(s)\big(\eta_1(s) \\ &+ H_m^{-1}(s)H_{um}(s)\eta_2(s) - K_g(s)r(s) + \tilde{\eta}(s)\big)\,.\end{aligned} \tag{B.12}$$

Using the definition of $C(s)$ in (3.25), one can write

$$\omega u(s) = -C(s)\big(\eta_1(s) + H_m^{-1}(s)H_{um}(s)\eta_2(s) - K_g(s)r(s) + \tilde{\eta}(s)\big).$$

The input quantization error is given by $u_{\mathrm{qe}}(t) = u_{\mathrm{q}}(t) - u(t)$. The system in (3.22) consequently takes the form

$$\begin{aligned}x(s) = &G_m(s)\eta_1(s) + G_{um}(s)\eta_2(s) - H_{xm}(s)C(s)\tilde{\eta}(s) \\ &+ H_{xm}(s)\omega u_{\mathrm{qe}}(s) + H_{xm}(s)C(s)K_g(s)r(s) + r_0(s).\end{aligned} \tag{B.13}$$

Next, let $e(t) \triangleq x(t) - x_{\mathrm{ref}}(t)$. From (3.34) and (B.13) we have

$$\begin{aligned}e(s) = &G_m(s)\left(\eta_1(s) - \eta_{1\mathrm{ref}}(s)\right) + G_{um}(s)\left(\eta_2(s) - \eta_{2\mathrm{ref}}(s)\right) \\ &+ H_{xm}(s)\omega u_{\mathrm{qe}}(s) - H_{xm}(s)C(s)\tilde{\eta}(s)\,, \qquad e(0) = 0\,.\end{aligned}$$

Moreover, it follows from the error dynamics in (3.40) that

$$\begin{aligned}H_m^{-1}(s)C\tilde{x}(s) = &\tilde{\eta}_u(s) + \tilde{\eta}_1(s) + H_m^{-1}(s)H_{um}(s)\tilde{\eta}_2(s) + \tilde{\eta}_{u\mathrm{q}}(s) \\ = &\tilde{\eta}(s) + \tilde{\eta}_{u\mathrm{q}}(s)\,,\end{aligned}$$

where $\tilde{\eta}_u(s)$ is the Laplace transform of $\tilde{\eta}_u(t) = \tilde{\omega}(t)u(t)$, and $\tilde{\eta}_{u\mathrm{q}}(s)$ is the

Laplace transform of $\tilde{\eta}_{u\mathrm{q}}(t) = \tilde{\omega}(t)u_{\mathrm{qe}}(t)$. The two equations above lead to

$$\begin{aligned} e(s) =& G_m(s)\left(\eta_1(s) - \eta_{1\mathrm{ref}}(s)\right) + G_{um}(s)\left(\eta_2(s) - \eta_{2\mathrm{ref}}(s)\right) \\ & - H_{xm}(s)C(s)H_m^{-1}(s)C\tilde{x}(s) + H_{xm}(s)\omega u_{\mathrm{qe}}(s) + H_{xm}(s)C(s)\tilde{\eta}_{u\mathrm{q}}(s). \end{aligned}$$

Therefore, we have

$$\begin{aligned} \|e_{t'}\|_{\mathcal{L}_\infty} \leq & \|G_m(s)\|_{\mathcal{L}_1} \|(\eta_1 - \eta_{1\mathrm{ref}})_{t'}\|_{\mathcal{L}_\infty} + \|G_{um}(s)\|_{\mathcal{L}_1} \|(\eta_2 - \eta_{2\mathrm{ref}})_{t'}\|_{\mathcal{L}_\infty} \\ & + \left\|H_{xm}(s)C(s)H_m^{-1}(s)C\right\|_{\mathcal{L}_1} \|\tilde{x}_{t'}\|_{\mathcal{L}_\infty} + \|H_{xm}(s)\omega\|_{\mathcal{L}_1} \left\|u_{\mathrm{qe}_{t'}}\right\|_{\mathcal{L}_\infty} \\ & + \|H_{xm}(s)C(s)\|_{\mathcal{L}_1} \left\|\tilde{\eta}_{u\mathrm{q}_{t'}}\right\|_{\mathcal{L}_\infty}. \end{aligned} \tag{B.14}$$

For the first two terms, substituting (B.10) in (B.9) one obtains

$$\|z_{t'}\|_{\mathcal{L}_\infty} \leq L_z\left(\rho_{x_r} + \gamma_{x_{\log}}\right) + B_z,$$

and hence

$$\begin{aligned} \|X_{t'}\|_{\mathcal{L}_\infty} &\leq \max\left\{\rho_{x_r} + \gamma_{x_{\log}}, L_z(\rho_{x_r} + \gamma_{x_{\log}}) + B_z\right\} \leq \bar{\rho}_{x_r}, \\ \|X_{\mathrm{ref}\,t'}\|_{\mathcal{L}_\infty} &\leq \max\left\{\rho_{x_r}, L_z(\rho_{x_r} + \gamma_{x_{\log}}) + B_z\right\} \leq \bar{\rho}_{x_r}. \end{aligned}$$

Assumption 3 implies that, for $i = 1, 2$, we have

$$\begin{aligned} \|(\eta_i - \eta_{i\mathrm{ref}})_{t'}\|_{\mathcal{L}_\infty} \leq & d_{f_{xi}}(\bar{\rho}_{x_r}) \|(X - X_{\mathrm{ref}})_{t'}\|_{\mathcal{L}_\infty} \\ = & d_{f_{xi}}(\bar{\rho}_{x_r}) \|(x - x_{\mathrm{ref}})_{t'}\|_{\mathcal{L}_\infty}. \end{aligned} \tag{B.15}$$

For the last term, we have $\left\|\tilde{\eta}_{u\mathrm{q}_{t'}}\right\|_{\mathcal{L}_\infty} \leq 2\omega_{1\max} \left\|u_{\mathrm{qe}_{t'}}\right\|_{\mathcal{L}_\infty}$, where $\omega_{1\max}$ is defined in (3.28). Then, from (B.14) we have

$$\begin{aligned} \|e_{t'}\|_{\mathcal{L}_\infty} \leq & \|G_m(s)\|_{\mathcal{L}_1} d_{f_{x1}}(\bar{\rho}_{x_r}) \|e_{t'}\|_{\mathcal{L}_\infty} + \|G_{um}(s)\|_{\mathcal{L}_1} d_{f_{x2}}(\bar{\rho}_{x_r}) \|e_{t'}\|_{\mathcal{L}_\infty} \\ & + \left\|H_{xm}(s)C(s)H_m^{-1}(s)C\right\|_{\mathcal{L}_1} \|\tilde{x}_{t'}\|_{\mathcal{L}_\infty} + \|H_{xm}(s)\omega\|_{\mathcal{L}_1} \left\|u_{\mathrm{qe}_{t'}}\right\|_{\mathcal{L}_\infty} \\ & + \|H_{xm}(s)C(s)\|_{\mathcal{L}_1} 2\omega_{1\max} \left\|u_{\mathrm{qe}_{t'}}\right\|_{\mathcal{L}_\infty}. \end{aligned} \tag{B.16}$$

The quantization error of the logarithmic quantizer is bounded by

$$\left\|u_{\mathrm{qe}_{t'}}\right\|_{\mathcal{L}_\infty} \leq \Delta \|u_{t'}\|_{\mathcal{L}_\infty}. \tag{B.17}$$

To bound $\|u_{t'}\|_{\mathcal{L}_\infty}$ in the above inequality, note that

$$\|u_{t'}\|_{\mathcal{L}_\infty} \leq \left\|u_{\mathrm{ref}_{t'}}\right\|_{\mathcal{L}_\infty} + \|(u-u_{\mathrm{ref}})_{t'}\|_{\mathcal{L}_\infty}, \tag{B.18}$$

where $\left\|u_{\mathrm{ref}_{t'}}\right\|_{\mathcal{L}_\infty} \leq \rho_{u_r}$ by Lemma 12. From (B.12) and (3.34), $u(t)-u_{\mathrm{ref}}(t)$ can be bounded as follows:

$$\begin{aligned}\|(u-u_{\mathrm{ref}})_{t'}\|_{\mathcal{L}_\infty} \leq{}& \left\|\omega^{-1}C(s)\right\|_{\mathcal{L}_1} \|(\eta_1-\eta_{1\mathrm{ref}})_{t'}\|_{\mathcal{L}_\infty} \\ &+ \left\|\omega^{-1}C(s)H_m^{-1}(s)H_{um}(s)\right\|_{\mathcal{L}_1} \|(\eta_2-\eta_{2\mathrm{ref}})_{t'}\|_{\mathcal{L}_\infty} \\ &+ \left\|\omega^{-1}C(s)H_m^{-1}(s)C\right\|_{\mathcal{L}_1} \|\tilde{x}_{t'}\|_{\mathcal{L}_\infty} + \left\|\omega^{-1}C(s)\right\|_{\mathcal{L}_1} \left\|\tilde{\eta}_{u\mathrm{q}_{t'}}\right\|_{\mathcal{L}_\infty},\end{aligned}$$

and the bound in (B.15) leads to

$$\begin{aligned}\|(u-u_{\mathrm{ref}})_{t'}\|_{\mathcal{L}_\infty} \leq{}& \left\|\omega^{-1}C(s)\right\|_{\mathcal{L}_1} d_{fx1}(\bar{\rho}_{x_r}) \|e_{t'}\|_{\mathcal{L}_\infty} \\ &+ \left\|\omega^{-1}C(s)H_m^{-1}(s)H_{um}(s)\right\|_{\mathcal{L}_1} d_{fx2}(\bar{\rho}_{x_r}) \|e_{t'}\|_{\mathcal{L}_\infty} \\ &+ \left\|\omega^{-1}C(s)H_m^{-1}(s)C\right\|_{\mathcal{L}_1} \|\tilde{x}_{t'}\|_{\mathcal{L}_\infty} + 2\omega_{1\max} \left\|\omega^{-1}C(s)\right\|_{\mathcal{L}_1} \|u_{\mathrm{qe}}\|_{\mathcal{L}_\infty}.\end{aligned} \tag{B.19}$$

Substitute (B.18) and (B.19) into (B.17) to get

$$\begin{aligned}\left\|u_{\mathrm{qe}_{t'}}\right\|_{\mathcal{L}_\infty} \leq{}& \frac{\Delta\rho_{u_r}}{1-2\omega_{1\max}\Delta\left\|\omega^{-1}C(s)\right\|_{\mathcal{L}_1}} + \frac{\Delta\left\|\omega^{-1}C(s)H_m^{-1}(s)C\right\|_{\mathcal{L}_1}}{1-2\omega_{1\max}\Delta\left\|\omega^{-1}C(s)\right\|_{\mathcal{L}_1}} \|\tilde{x}_{t'}\|_{\mathcal{L}_\infty} \\ &+ \frac{\Delta\big(\left\|\omega^{-1}C(s)\right\|_{\mathcal{L}_1} d_{fx1}(\bar{\rho}_{x_r}) + \left\|\omega^{-1}C(s)H_m^{-1}(s)H_{um}(s)\right\|_{\mathcal{L}_1} d_{fx2}(\bar{\rho}_{x_r})\big)}{1-2\omega_{1\max}\Delta\left\|\omega^{-1}C(s)\right\|_{\mathcal{L}_1}} \|e_{t'}\|_{\mathcal{L}_\infty},\end{aligned} \tag{B.20}$$

which together with (B.16) lead to the upper bound

$$\|e_{t'}\|_{\mathcal{L}_\infty} \leq \gamma_{x\mathrm{o}_{\log}} + \gamma_{x\mathrm{q}_{\log}} < \gamma_{x_{\log}}, \tag{B.21}$$

where $\gamma_{x\mathrm{o}_{\log}}$, $\gamma_{x\mathrm{q}_{\log}}$, and $\gamma_{x_{\log}}$ were defined in (3.44).

For the tracking error of the control signal, we have

$$\left\|(u_{\mathrm{q}}-u_{\mathrm{ref}})_{t'}\right\|_{\mathcal{L}_\infty} = \left\|(u_{\mathrm{q}}-u+u-u_{\mathrm{ref}})_{t'}\right\|_{\mathcal{L}_\infty} \left\|u_{\mathrm{qe}_{t'}}\right\|_{\mathcal{L}_\infty} + \|(u-u_{\mathrm{ref}})_{t'}\|_{\mathcal{L}_\infty}.$$

From (B.19) and (B.20), we have

$$\begin{aligned}\|(u_{\mathrm{q}}-u_{\mathrm{ref}})_{t'}\|_{\mathcal{L}_\infty} &\le c_{eu}(L_{1\rho_{x_r}},L_{2\rho_{u_r}})(\gamma_{x_{\log}}-\epsilon)\\ &\quad+\left\|\omega^{-1}C(s)H_m^{-1}(s)C\right\|_{\mathcal{L}_1}\|\tilde{x}_{t'}\|_{\mathcal{L}_\infty}+(1+2\omega_{1\max}\left\|\omega^{-1}C(s)\right\|_{\mathcal{L}_1})\|u_{\mathrm{qe}}\|_{\mathcal{L}_\infty}\\ &\le \frac{1+2\omega_{1\max}\|\omega^{-1}C(s)\|_{\mathcal{L}_1}}{1-2\omega_{1\max}\Delta\|\omega^{-1}C(s)\|_{\mathcal{L}_1}}\Delta\rho_{u_r}+\frac{(1+\Delta)\|\omega^{-1}C(s)H_m^{-1}(s)C\|_{\mathcal{L}_1}}{1-2\omega_{1\max}\Delta\|\omega^{-1}C(s)\|_{\mathcal{L}_1}}\gamma_0\\ &\quad+\frac{(1+\Delta)c_{eu}(L_{1\rho_{x_r}},L_{2\rho_{u_r}})}{1-2\omega_{1\max}\Delta\|\omega^{-1}C(s)\|_{\mathcal{L}_1}}(\gamma_{x_{\log}}-\epsilon)<\gamma_{u_{\log}},\end{aligned}$$

where $\gamma_{x_{\log}}$ and $\gamma_{u_{\log}}$ were defined in (3.44) and (3.46).

Thus, the inequality above and (B.21) contradict the assumption in (B.7) that the tracking error hits $\gamma_{x_{\log}}$ or $\gamma_{u_{\log}}$. So the error is upper bounded and (3.47) holds.

B.4 Proof of Theorem 4

This proof is similar to the proof of Theorem 3.

From (B.16), we have

$$\begin{aligned}\|e_{t'}\|_{\mathcal{L}_\infty} \le{}& \|G_m(s)\|_{\mathcal{L}_1} d_{f_{x1}}(\bar{\rho}_{x_r})\|e_{t'}\|_{\mathcal{L}_\infty}+\|G_{um}(s)\|_{\mathcal{L}_1} d_{f_{x2}}(\bar{\rho}_{x_r})\|e_{t'}\|_{\mathcal{L}_\infty}\\ &+\left\|H_{xm}(s)C(s)H_m^{-1}(s)C\right\|_{\mathcal{L}_1}\|\tilde{x}_{t'}\|_{\mathcal{L}_\infty}+\|H_{xm}(s)\omega\|_{\mathcal{L}_1}\left\|u_{\mathrm{qe}_{t'}}\right\|_{\mathcal{L}_\infty}\\ &+\|H_{xm}(s)C(s)\|_{\mathcal{L}_1}2\omega_{1\max}\left\|u_{\mathrm{qe}_{t'}}\right\|_{\mathcal{L}_\infty}. \qquad \text{(B.22)}\end{aligned}$$

Substitute (B.11) and (2.2) into (B.22):

$$\begin{aligned}\|e_{t'}\|_{\mathcal{L}_\infty} \le{}& \|G_m(s)\|_{\mathcal{L}_1} d_{f_{x1}}(\bar{\rho}_{x_r})\|e_{t'}\|_{\mathcal{L}_\infty}+\|G_{um}(s)\|_{\mathcal{L}_1} d_{f_{x2}}(\bar{\rho}_{x_r})\|e_{t'}\|_{\mathcal{L}_\infty}\\ &+\|H_{xm}(s)\omega\|_{\mathcal{L}_1}\frac{1}{2}l+\left\|H_{xm}(s)C(s)H_m^{-1}(s)C\right\|_{\mathcal{L}_1}\gamma_0\\ &+\|H_{xm}(s)C(s)\|_{\mathcal{L}_1}\omega_{1\max}l.\end{aligned}$$

Using the notation in (3.29), we have

$$\begin{aligned}\|e_{t'}\|_{\mathcal{L}_\infty} &\le c_{de}(d_{f_{x1}}(\bar{\rho}_{x_r}),d_{f_{x2}}(\bar{\rho}_{x_r}))\|e_{t'}\|_{\mathcal{L}_\infty}+c_{xe}\gamma_0+c_{ue}\frac{1}{2}l\\ &\le c_{de}(L_{1\rho_{x_r}},L_{2\rho_{x_r}})\|e_{t'}\|_{\mathcal{L}_\infty}+c_{xe}\gamma_0+c_{ue}\frac{1}{2}l,\end{aligned}$$

which implies

$$\|e_{t'}\|_{\mathcal{L}_\infty} \leq \frac{c_{xe}\gamma_0 + c_{ue}\frac{1}{2}l}{1 - c_{de}(L_{1\rho_{x_r}}, L_{2\rho_{x_r}})} \leq \gamma_{x\mathrm{o}_{\mathrm{unif}}} + \gamma_{x\mathrm{q}_{\mathrm{unif}}} < \gamma_{x_{\mathrm{unif}}}.$$

On the other hand, we have

$$\left\|(u_{\mathrm{q}} - u_{\mathrm{ref}})_{t'}\right\|_{\mathcal{L}_\infty} = \left\|(u_{\mathrm{q}} - u + u - u_{\mathrm{ref}})_{t'}\right\|_{\mathcal{L}_\infty} \leq \left\|u_{\mathrm{qe}_{t'}}\right\|_{\mathcal{L}_\infty} + \left\|(u - u_{\mathrm{ref}})_{t'}\right\|_{\mathcal{L}_\infty}.$$

From (B.19), we have

$$\begin{aligned}
\left\|(u_{\mathrm{q}} - u_{\mathrm{ref}})_{t'}\right\|_{\mathcal{L}_\infty} &\leq c_{eu}(L_{1\rho_{x_r}}, L_{2\rho_{u_r}})(\gamma_{x_{\mathrm{unif}}} - \epsilon) \\
&\quad + \left\|\omega^{-1}C(s)H_m^{-1}(s)C\right\|_{\mathcal{L}_1} \|\tilde{x}_{t'}\|_{\mathcal{L}_\infty} + (1 + 2\omega_{1\max}\left\|\omega^{-1}C(s)\right\|_{\mathcal{L}_1}) \|u_{\mathrm{qe}}\|_{\mathcal{L}_\infty} \\
&\leq c_{eu}(L_{1\rho_{x_r}}, L_{2\rho_{u_r}})(\gamma_{x_{\mathrm{unif}}} - \epsilon) + \left\|\omega^{-1}C(s)H_m^{-1}(s)C\right\|_{\mathcal{L}_1} \gamma_0 \\
&\quad + (1 + 2\omega_{1\max}\left\|\omega^{-1}C(s)\right\|_{\mathcal{L}_1})\frac{1}{2}l \\
&< \gamma_{u_{\mathrm{unif}}},
\end{aligned}$$

where $\gamma_{x_{\mathrm{unif}}}$ and $\gamma_{u_{\mathrm{unif}}}$ were defined in (3.49) and (3.51).

B.5 Proof of Theorem 5

Similar to previous definitions, let $\tilde{\eta}(t) \triangleq \tilde{\omega}(t)u(t) + \tilde{\theta}^\top(t)x(t) + \tilde{\sigma}(t)$. It follows from (3.55) and (3.25) that

$$u(s) = \frac{C(s)}{\omega}(-\theta^\top x(s) - \sigma(s) + k_g r(s) - \tilde{\eta}(s)). \tag{B.23}$$

From (3.53), the closed-loop system is

$$\begin{aligned}
x(s) = H(s)\big(&C(s)k_g r(s) - (C(s) - 1)(\theta^\top x(s) + \sigma(s)) \\
&- C(s)\tilde{\eta}(s) + \omega u_{\mathrm{qe}}(s)\big) + x_{in}(s),
\end{aligned}$$

where $u_{\mathrm{qe}}(t)$ is the input quantization error.

In the case with constant θ, the reference system is given by

$$\begin{aligned} x_{\rm ref}(s)=&H(s)\big(C(s)k_g r(s)-(C(s)-1)(\theta^\top x_{\rm ref}(s)+\sigma(s))\big)+x_{in}(s),\\ u_{\rm ref}(s) =& \frac{C(s)}{\omega}\left(-\theta^\top x_{\rm ref}(s) - \sigma(s) + k_g r(s)\right) . \end{aligned} \tag{B.24}$$

Recall that $e(t) = x(t) - x_{\rm ref}(t)$. We get

$$\begin{aligned} e(s) =&H(s)\big((1 - C(s))\theta^\top e(s) - C(s)\tilde{\eta}(s) + \omega u_{\rm qe}(s)\big)\\ =& - H_1(s)H(s)\tilde{\eta}(s) - H_2(s)\omega u_{\rm qe}(s) . \end{aligned}$$

It follows from (3.53) and (3.54) that

$$\tilde{x}(s) = H(s)\tilde{\eta}(s) + H(s)\tilde{\eta}_{u\rm q}(s) + \tilde{x}_{in}(s) , \tilde{\eta}_{u\rm q}(t) = \tilde{\omega}(t)u_{\rm qe}(t) ,$$

and consequently

$$e(s) = -H_1(s)(\tilde{x}(s) - \tilde{x}_{in}(s)) + H_1(s)H(s)\tilde{\eta}_{u\rm q}(s) - H_3(s)\omega u_{\rm qe}(s).$$

Using the upper bound from Lemma 7, we have

$$\|\tilde{x}(t) - \tilde{x}_{in}(t)\| \leq \|\tilde{x}(t)\| + \|\tilde{x}_{in}(t)\| \leq \rho(t) + \|\tilde{x}_{in}(t)\| ,$$

which together with (2.2) and Lemma 8 lead to the upper bound in (3.57).

Notice that from (B.23) and (B.24) it follows that

$$\begin{aligned} u_{\rm q}(s) - u_{\rm ref}(s) &= u(s) - u_{\rm ref}(s) + u_{\rm qe}(s)\\ &= -\frac{C(s)\theta^\top}{\omega}e(s) - \frac{C(s)}{\omega}\tilde{\eta}(s) + u_{\rm qe}(s)\\ &= -\frac{C(s)\theta^\top}{\omega}e(s) - \frac{C(s)}{\omega}\frac{1}{c_o^\top H(s)}c_o^\top H(s)\tilde{\eta}(s) + u_{\rm qe}(s)\\ &=H_4(s)e(s)-H_5(s)(\tilde{x}(s)-\tilde{x}_{in}(s))+H_5(s)H(s)\tilde{\eta}_{u\rm q}(s)+u_{\rm qe}(s). \end{aligned}$$

From this equality, Lemma 8 leads to the bound in (3.58).

Last but not least, the above bounds in both (3.57) and (3.58) are derived using a conservative estimate $\|\tilde{x}(t) - \tilde{x}_{in}(t)\| \leq \|\tilde{x}(t)\| + \|\tilde{x}_{in}(t)\|$, which leads to conservative upper bound of $\|\tilde{x}(t) - \tilde{x}_{in}(t)\|$. In fact, $\tilde{x}(t)$ and $\tilde{x}_{in}(t)$ tend to cancel each other in certain cases, leading to very small transient deviation.

B.6 Proof of Theorem 6

(By contradiction) Assume the bounds in (4.18) do not hold. Since

$$\|e_x(0)\|_\infty = 0 < \gamma_{xhu}, \quad \|e_u(0)\|_\infty = 0 < \gamma_{uhu},$$

and $x(t)$, $x_{\mathrm{ref}}(t)$, $u(t)$, and $u_{\mathrm{ref}}(t)$ are continuous, there exists t' such that $e_x(\tau)$ and $e_u(\tau)$ are within the bounds for $\tau < t'$:

$$\|e_x(\tau)\|_\infty < \gamma_{xhu}, \quad \|e_u(\tau)\|_\infty < \gamma_{uhu}, \quad \forall \tau \in [0, t'),$$

and hit the bound at t', i.e.

$$\text{either } \|e_x(t')\|_\infty = \gamma_{xhu}, \text{ or } \|e_u(t')\|_\infty = \gamma_{uhu}. \tag{B.25}$$

When $t \leq t'$, $\|e_x(t)\|_\infty \leq \gamma_{xhu}$, we have $\|e_{x_{t'}}\|_{\mathcal{L}_\infty} \leq \gamma_{xhu}$, $\|x_{t'}\|_{\mathcal{L}_\infty} < \rho_{xhu}$, and the inequality (4.10) in Lemma 9 holds. To use the upper bound on $\tilde{x}(t)$, $e_x(t)$ can be written as $e_x(t) = x(t) - x_{\mathrm{ref}}(t) = \hat{x}(t) - x_{\mathrm{ref}}(t) - \tilde{x}(t)$.

On one hand, from (4.2), $\hat{x}(s)$ is given by

$$\hat{x}(s) = -H(s)\hat{\eta}_{\mathrm{q}}(s) + H(s)u(s) + H(s)u_{\mathrm{qe}}(s) + (s\mathbb{I} - A_m)^{-1}x_0,$$

where $\hat{\eta}_{\mathrm{q}}(t) = \hat{\theta}^\top(t)x_{\mathrm{q}}(t)$ is defined in (4.4). By the control law in (4.4) and the definition of $\tilde{x}(t)$, we further write

$$\begin{aligned}\hat{x}(s) =& G(s)\theta^\top\hat{x}(s) - G(s)\theta^\top\tilde{x}(s) + H(s)(C(s)-1)\tilde{\eta}_{\mathrm{q}}(s) \\ &+ H(s)C(s)k_g r(s) + H(s)u_{\mathrm{qe}}(s) + (s\mathbb{I} - A_m)^{-1}x_0,\end{aligned} \tag{B.26}$$

where

$$\tilde{\eta}_{\mathrm{q}}(t) \triangleq \hat{\eta}_{\mathrm{q}}(t) - \theta^\top x(t) = \hat{\theta}^\top(t)x_{\mathrm{q}}(t) - \theta^\top x(t).$$

For the third term, note that the prediction error dynamics, given by (4.8), can be further written as

$$\tilde{x}(s) = H(s)(\theta^\top x(s) - \hat{\eta}_{\mathrm{q}}(s)) = -H(s)\tilde{\eta}_{\mathrm{q}}(s)\,. \tag{B.27}$$

Substitute (B.27) into (B.26) to obtain

$$\begin{aligned}\hat{x}(s) =& G(s)\theta^\top \hat{x}(s) - G(s)\theta^\top \tilde{x}(s) - (C(s)-1)\mathbb{I}_n \tilde{x}(s) \\ &+ H(s)C(s)k_g r(s) + H(s)u_{\mathrm{qe}}(s) + (s\mathbb{I} - A_m)^{-1}x_0,\end{aligned}$$

$$\begin{aligned}\hat{x}(s) =& (\mathbb{I} - G(s)\theta^\top)^{-1}[-G(s)\theta^\top - (C(s)-1)\mathbb{I}]\tilde{x}(s) \\ &+ (\mathbb{I} - G(s)\theta^\top)^{-1}H(s)u_{\mathrm{qe}}(s) + (\mathbb{I} - G(s)\theta^\top)^{-1}H(s)C(s)k_g r(s) \\ &+ (\mathbb{I} - G(s)\theta^\top)^{-1}(s\mathbb{I} - A_m)^{-1}x_0.\end{aligned}$$

On the other hand, note that $x_{\mathrm{ref}}(s)$ is given in (3.12). Subtracting $x_{\mathrm{ref}}(s)$ from $x(s)$ gives

$$\begin{aligned}e_x(s) =& (\mathbb{I} - G(s)\theta^\top)^{-1}[-G(s)\theta^\top - (C(s)-1)\mathbb{I}]\tilde{x}(s) - \tilde{x}(s) \\ &+ (\mathbb{I} - G(s)\theta^\top)^{-1}H(s)u_{\mathrm{qe}}(s)\,, \\ \|e_{x_{t'}}\|_{\mathcal{L}_\infty} \leq& \|(\mathbb{I} - G(s)\theta^\top)^{-1}H(s)\|_{\mathcal{L}_1}\|u_{\mathrm{qe}_{t'}}\|_{\mathcal{L}_\infty} \\ &+ \|(\mathbb{I} - G(s)\theta^\top)^{-1}[G(s)\theta^\top + (C(s)-1)\mathbb{I} + \mathbb{I}]\|_{\mathcal{L}_1}\|\tilde{x}_{t'}\|_{\mathcal{L}_\infty}\,.\end{aligned} \tag{B.28}$$

In the case of hysteresis quantization, the input quantization error is bounded by the constant $\frac{1}{2}d_u$. Thus, $e_x(t)$ is bounded by

$$\begin{aligned}\|e_{x_{t'}}\|_{\mathcal{L}_\infty} \leq& \|(\mathbb{I} - G(s)\theta^\top)^{-1}H(s)\|_{\mathcal{L}_1}\frac{1}{2}d_u \\ &+ \|(\mathbb{I} - G(s)\theta^\top)^{-1}[G(s)\theta^\top + (C(s)-1)\mathbb{I} + \mathbb{I}]\|_{\mathcal{L}_1}\|\tilde{x}_{t'}\|_{\mathcal{L}_\infty}.\end{aligned}$$

By Lemma 9, the bound can be written as

$$\|e_{x_{t'}}\|_{\mathcal{L}_\infty} \leq \gamma_{x\mathrm{o}hu} + \gamma_{x\mathrm{q}hu} < \gamma_{xhu}\,.$$

Now we examine the error between the control signal $u(t)$ and the desired reference control signal $u_{\mathrm{ref}}(t)$. By (4.4) and (3.11), we have

$$e_u(s) = C(s)\tilde{\eta}_q(s) + C(s)\theta^\top(x(s) - x_{\mathrm{ref}}(s)),$$

where $\tilde{\eta}_q(t)$ is defined in (B.26). Since (A_m, b) is controllable, and $H(s)$ is strictly proper and stable, there exists $c_o \in \mathbb{R}^n$ such that $c_o^\top H(s)$ is minimum phase with

relative degree one (by Lemma 4 in [21]). Then

$$\begin{aligned} e_u(s) &= C(s)\frac{c_o^\top H(s)\tilde{\eta}_q(s)}{c_o^\top H(s)} + C(s)\theta^\top e_x(s) \\ &= C(s)\tfrac{1}{c_o^\top H(s)} c_o^\top \tilde{x}(s) + C(s)\theta^\top e_x(s)\,. \end{aligned}$$

Since $C(s)$ is BIBO stable and strictly proper, the system $C(s)\frac{1}{c_o^\top H(s)}$ is proper and BIBO stable, which implies that its $\mathcal{L}_1$ norm is bounded. Hence,

$$\|e_{u_{t'}}\|_{\mathcal{L}_\infty} \leq \big\|C(s)\frac{1}{c_o^\top H(s)} c_o^\top\big\|_{\mathcal{L}_1} \|\tilde{x}_\tau\|_{\mathcal{L}_\infty} + \|C(s)\theta^\top\|_{\mathcal{L}_1} \|e_{x_{t'}}\|_{\mathcal{L}_\infty}. \tag{B.29}$$

If Γ is sufficiently large, δ_x and δ_u are sufficiently small, such that $\gamma_{xhu} = \gamma_{x\mathrm{o}hu} + \gamma_{x\mathrm{q}hu} + \epsilon < \bar{\gamma}_{xhu}$, the error $e_x(t)$ in (B.28) is strictly upper bounded by

$$\|e_{x'_t}\|_{\mathcal{L}_\infty} \leq \gamma_{x\mathrm{o}hu} + \gamma_{x\mathrm{q}hu} < \gamma_{xhu} < \bar{\gamma}_{xhu}\,, \tag{B.30}$$

where γ_{xhu} is defined in (4.14). Similarly, the error $e_u(t)$ in (B.29) is strictly upper bounded by

$$\|e_{u'_t}\|_{\mathcal{L}_\infty} < \gamma_{uhu}\,, \tag{B.31}$$

where γ_{uhu} is defined in (4.16).

The strict inequalities (B.30) and (B.31) contradict the assumption in (B.25). Thus the assumption does not hold and the proof is complete.

B.7 Proof of Lemma 10

If the system state and input signals are bounded for $\tau \in [0, t)$ as in (4.32), by Lemma 5, the nonlinear system can be rewritten as in (4.28), and further the prediction error dynamics are obtained in (4.29).

Consider the Lyapunov function candidate

$$\begin{aligned} V(\tilde{x}(\tau), \tilde{\omega}(\tau), \tilde{\theta}_i(\tau), \tilde{\sigma}_i(\tau)) =& \tilde{x}^\top(\tau) P \tilde{x}(\tau) \\ &+ \frac{1}{\Gamma}\left(\mathrm{tr}(\tilde{\omega}^\top(\tau)\tilde{\omega}(\tau)) + \sum_{i=1}^{2}\left(\tilde{\theta}_i^\top(\tau)\tilde{\theta}_i(\tau) + \tilde{\sigma}_i^\top(\tau)\tilde{\sigma}_i(\tau)\right)\right), \end{aligned}$$

where $\tilde{\omega}(t) = \hat{\omega}(t) - \omega$, $\tilde{\theta}_i(t) = \hat{\theta}_i(t) - \theta_i(t)$, $\tilde{\sigma}_i(t) = \hat{\sigma}_i(t) - \sigma_i(t)$, $i = 1, 2$. The

time derivative can be bounded by

$$
\begin{aligned}
&\dot{V}(\tau) = \tilde{x}^\top(\tau)PA_m\tilde{x}(\tau) + \tilde{x}^\top(\tau)A_m^\top P\tilde{x}(\tau) \\
&+ 2\tilde{x}^\top(\tau)PB_m\left(\tilde{\omega}(\tau)u_{\mathrm{q}}(\tau) + \hat{\theta}_1(\tau)\|x_{\mathrm{q}t}\|_{\mathcal{L}_\infty} - \theta_1(\tau)\|x_t\|_{\mathcal{L}_\infty} + \tilde{\sigma}_1(\tau)\right) \\
&+ 2\tilde{x}^\top(\tau)PB_{um}\left(\hat{\theta}_2(\tau)\|x_{\mathrm{q}t}\|_{\mathcal{L}_\infty} - \theta_2(\tau)\|x_t\|_{\mathcal{L}_\infty} + \tilde{\sigma}_2(\tau)\right) \\
&+ \frac{2}{\Gamma}\left(\mathrm{tr}(\tilde{\omega}^\top(\tau)\dot{\tilde{\omega}}(\tau)) + \sum_{i=1}^{2}\left(\tilde{\theta}_i^\top(\tau)\dot{\tilde{\theta}}_i(\tau) + \tilde{\sigma}_i^\top(\tau)\dot{\tilde{\sigma}}_i(\tau)\right)\right) \\
\leq &-\lambda_{\min}(Q)\|\tilde{x}(\tau)\|_2^2 + 2m\|\tilde{\omega}(\tau)\|_1\|PB_m\|_1\|x_{\mathrm{qe}}(\tau)\|_\infty\|u_{\mathrm{q}}(\tau)\|_\infty \qquad \text{(B.32)} \\
&+ 2m\|\tilde{x}(\tau)\|_2\|PB_m\|_2\|\theta_1(\tau)\|_\infty(\|x_{\mathrm{q}_\tau}\|_{\mathcal{L}_\infty} - \|x_\tau\|_{\mathcal{L}_\infty}) \\
&+ 2m\|x_{\mathrm{qe}}(\tau)\|_\infty\|PB_m\|_1\|\tilde{\theta}_1(\tau)\|_\infty\|x_{\mathrm{q}}(\tau)\|_\infty + 2m\|x_{\mathrm{qe}}(\tau)\|_\infty\|PB_m\|_1\|\tilde{\sigma}_1(\tau)\|_\infty \\
&+ 2(n-m)\|\tilde{x}(\tau)\|_2\|PB_{um}\|_2\|\theta_2(\tau)\|_\infty(\|x_{\mathrm{q}_\tau}\|_{\mathcal{L}_\infty} - \|x_\tau\|_{\mathcal{L}_\infty}) \\
&+ 2(n-m)\|x_{\mathrm{qe}}(\tau)\|_\infty\|PB_{um}\|_1\|\tilde{\theta}_2(\tau)\|_\infty\|x_{\mathrm{q}}(\tau)\|_\infty \\
&+ 2(n-m)\|x_{\mathrm{qe}}(\tau)\|_\infty\|PB_{um}\|_1\|\tilde{\sigma}_2(\tau)\|_\infty \\
&+ \frac{2}{\Gamma}\big(m\|\tilde{\theta}_1(\tau)\|_\infty\|\dot{\theta}_1(\tau)\|_\infty + m\|\tilde{\sigma}_1(\tau)\|_\infty\|\dot{\sigma}_1(\tau)\|_\infty \\
&\qquad + (n-m)\|\tilde{\theta}_2(\tau)\|_\infty\|\dot{\theta}_2(\tau)\|_\infty + (n-m)\|\tilde{\sigma}_2(\tau)\|_\infty\|\dot{\sigma}_2(\tau)\|_\infty\big),
\end{aligned}
$$

where $x_{\mathrm{qe}}(\tau) \triangleq x_{\mathrm{q}}(\tau) - x(\tau)$, and the inequality is from the projection-based adaptive law. Substitute the state quantization error bound (2.7) into (B.32) to get

$$
\begin{aligned}
\dot{V}(\tau) \leq &-\lambda_{\min}(Q)\|\tilde{x}(\tau)\|_2^2 + \big(m\|PB_m\|_2\theta_{b_1} + (n-m)\|PB_{um}\|_2\theta_{b_2}\big)d_x\|\tilde{x}(\tau)\|_2 \\
&+ m\tilde{\omega}_{1\max}\|PB_m\|_1 d_x(\frac{1}{2}d_u + \rho_u) \qquad \text{(B.33)} \\
&+ 2\left(m\|PB_m\|_1\theta_{b_1} + (n-m)\|PB_{um}\|_1\theta_{b_2}\right)(\rho_x + \frac{1}{2}d_x)d_x \\
&+ 2\left(m\|PB_m\|_1\sigma_{b_1} + (n-m)\|PB_{um}\|_1\sigma_{b_2}\right)d_x \\
&+ \frac{4}{\Gamma}\left(m\theta_{b_1}d_{\theta_1} + m\sigma_{b_1}d_{\sigma_1} + (n-m)\theta_{b_2}d_{\theta_2} + (n-m)\sigma_{b_2}d_{\sigma_2}\right),
\end{aligned}
$$

where $\tilde{\omega}_{1\max} = \max_{\omega_1,\omega_2\in\Omega}\|\omega_1 - \omega_2\|_1$. For this Lyapunov function candidate, note that on the one hand, at $\tau = 0$,

$$
V(0) \leq \frac{4}{\Gamma}\left(\omega_{F\max} + m\theta_{b_1}^2 + m\sigma_{b_1}^2 + (n-m)\theta_{b_2}^2 + (n-m)\sigma_{b_2}^2\right) \leq \theta_{hu}(d_x,\Gamma),
$$

where $\omega_{F\max} \triangleq \max_{\omega\in\Omega}\mathrm{tr}(\omega^\top\omega)$. On the other hand, for all $\tau \in [0,t)$, the

projection operator ensures that

$$\hat{\omega}(\tau) \in \Omega,\ \|\hat{\theta}_i(\tau)\|_\infty \leq \theta_{b_i},\ \|\hat{\sigma}_i(\tau)\|_\infty \leq \sigma_{b_i},\ i = 1, 2,$$

and therefore

$$\begin{aligned}\max_{\tau\in[0,t_1]} &\left(\mathrm{tr}(\tilde{\omega}^\top(\tau)\tilde{\omega}(\tau)) + \sum_{i=1}^{2} \left(\tilde{\theta}_i^\top(\tau)\tilde{\theta}_i(\tau) + \tilde{\sigma}_i^\top(\tau)\tilde{\sigma}_i(\tau) \right) \right) \\ &\leq 4\left(\omega_{F\max} + m\theta_{b_1}^2 + m\sigma_{b_1}^2 + (n-m)\theta_{b_2}^2 + (n-m)\sigma_{b_2}^2 \right). \end{aligned} \tag{B.34}$$

Then if for any $\tau > 0$, $V(\tau) > \theta_{hu}(d_x, \Gamma)$, it follows from the definition of the Lyapunov function and (B.34) that

$$\tilde{x}^\top(\tau)P\tilde{x}(\tau) \geq \lambda_{\max}(P)\tilde{x}_{hu}^2(d_x, \Gamma), \quad \|\tilde{x}(\tau)\|_2^2 \geq \tilde{x}_{hu}^2(d_x, \Gamma). \tag{B.35}$$

Then the inequality in (B.35) and (B.33) lead to $\dot{V}(\tau) < 0$.Thus, $V(\tau) < \theta_{hu}(d_x, \Gamma)$ for all $\tau \in [0, t)$. Hence,

$$\lambda_{\min}(P)\|\tilde{x}(\tau)\|_2^2 \leq \tilde{x}^\top(\tau)P\tilde{x}(\tau) \leq V(\tau), \quad \|\tilde{x}(\tau)\|_\infty \leq \|\tilde{x}(\tau)\|_2 \leq \sqrt{\frac{\theta_{hu}(d_x, \Gamma)}{\lambda_{\min(P)}}}.$$

Since the inequality holds uniformly for all $\tau \in [0, t)$, $\|\tilde{x}_t\|_{\mathcal{L}_\infty} < \sqrt{\frac{\theta_{hu}(d_x,\Gamma)}{\lambda_{\min(P)}}}$.

B.8 Proof of Theorem 7

(By contradiction)

Assume that the bounds in (4.37) do not hold. Then, since $\|x(0) - x_{\mathrm{ref}}(0)\|_\infty = 0 < \gamma_{x_{hu}}$, $\|u(0) - u_{\mathrm{ref}}(0)\|_\infty = 0 < \gamma_{u_{hu}}$, and $x(t)$, $x_{\mathrm{ref}}(t)$, $u(t)$, and $u_{\mathrm{ref}}(t)$ are continuous, there exists t' such that either

$$\|x(t') - x_{\mathrm{ref}}(t')\|_\infty = \gamma_{x_{hu}}, \quad \text{or } \|u(t') - u_{\mathrm{ref}}(t')\|_\infty = \gamma_{u_{hu}}, \tag{B.36}$$

while

$$\|x(\tau) - x_{\mathrm{ref}}(\tau)\|_\infty < \gamma_{x_{hu}},\ \|u(\tau) - u_{\mathrm{ref}}(\tau)\|_\infty < \gamma_{u_{hu}},\ \forall \tau \in [0, t'),$$

which implies that

$$\|(x - x_{\text{ref}})_{t'}\|_{\mathcal{L}_\infty} \leq \gamma_{x_{hu}},\ \|(u - u_{\text{ref}})_{t'}\|_{\mathcal{L}_\infty} \leq \gamma_{u_{hu}}. \tag{B.37}$$

It follows from Assumption 5 that

$$\|z_{t'}\| \leq L_z \left(\|x_{\text{ref}_{t'}}\|_{\mathcal{L}_\infty} + \gamma_{x_{hu}}\right) + B_z.$$

Then, Lemma 4 implies that

$$\|x_{\text{ref}_{t'}}\|_{\mathcal{L}_\infty} \leq \rho_{x_r}, \quad \|u_{\text{ref}_{t'}}\|_{\mathcal{L}_\infty} \leq \rho_{u_r}.$$

Using the definitions of $\rho_{x_{hu}}$ and $\rho_{u_{hu}}$ in (4.33) and (4.35), together with the bounds in (B.37), we have $\|x_{t'}\|_{\mathcal{L}_\infty} \leq \rho_{x_r} + \gamma_{x_{hu}} \leq \rho_{x_{hu}}$, $\|u_{t'}\|_{\mathcal{L}_\infty} \leq \rho_{u_r} + \gamma_{u_{hu}} \leq \rho_{u_{hu}}$. Hence, if one chooses the adaptive rate Γ and the quantization interval length d_x such that $\sqrt{\frac{\theta_{hu}(d_x,\Gamma)}{\lambda_{\min}(P)}} < \gamma_{0_{hu}}$, Lemma 10 implies that

$$\|\tilde{x}_{t'}\|_{\mathcal{L}_\infty} \leq \sqrt{\frac{\theta_{hu}(d_x, \Gamma)}{\lambda_{\min}(P)}} < \gamma_{0_{hu}}. \tag{B.38}$$

Comparing the closed-loop system in (4.28) and the reference system in (3.34), we have

$$\begin{aligned}\dot{e}_x(t) =& A_m e_x(t) + B_m[\omega(u_{\text{q}}(t) - u_{\text{ref}}(t)) + (\eta_1(t) - \eta_{1\text{ref}}(t))] \\ &+ B_{um}(\eta_2(t) - \eta_{2\text{ref}}(t)), \quad e_x(0) = 0.\end{aligned} \tag{B.39}$$

Taking Laplace transform of both sides leads to

$$\begin{aligned}e_x(s) =& H_{xm}(s)\omega(u_{\text{q}}(s) - u_{\text{ref}}(s)) + H_{xm}(s)(\eta_1(s) - \eta_{1\text{ref}}(s)) \\ &+ H_{xum}(s)(\eta_2(s) - \eta_{2\text{ref}}(s)),\end{aligned} \tag{B.40}$$

where $e_x(t) \triangleq x(t) - x_{\text{ref}}(t)$, $\eta_i(t) \triangleq f_i(x(t), z(t), t)$, $i = 1, 2$, and $\eta_{i\text{ref}}(t)$ is defined in (3.34).

Consider the first term

$$\omega(u_{\text{q}}(t) - u_{\text{ref}}(t)) = \omega u_{\text{qe}}(t) + \omega(u(t) - u_{\text{ref}}(t)), \tag{B.41}$$

where $u_{\mathrm{qe}}(t) \triangleq u_{\mathrm{q}}(t) - u(t)$. It follows from (3.32) that

$$u(s) = -KD(s)\big(\omega u(s) + \eta_1(s) + H_m^{-1}(s)H_{um}(s)\eta_2(s) - K_g(s)r(s) + \tilde{\eta}_{\mathrm{q}}(s)\big), \tag{B.42}$$

where $\eta_1(s)$, and $\eta_2(s)$ are the Laplace transforms of the signals $\eta_1(t)$ and $\eta_2(t)$ (defined in (B.40)), respectively; $\tilde{\eta}_{\mathrm{q}}(s)$ is the the Laplace transform of $\tilde{\eta}_{\mathrm{q}}(t)$; $\tilde{\eta}_{\mathrm{q}}(t) = \tilde{\omega}(t)u(t) + \tilde{\eta}_{1\mathrm{q}}(t) + \tilde{\eta}_{2m\mathrm{q}}(t)$; $\tilde{\eta}_{1\mathrm{q}}(t) = \hat{\eta}_{1\mathrm{q}}(t) - \eta_1(t)$; $\tilde{\eta}_{2m\mathrm{q}}(t)$ is the signal with Laplace transform $\tilde{\eta}_{2m\mathrm{q}}(s) = H_m^{-1}(s)H_{um}(s)(\hat{\eta}_{2\mathrm{q}}(s) - \eta_2(s))$. Consequently

$$\begin{aligned} u(s) = &-(\mathbb{I}_m + KD(s)\omega)^{-1} KD(s)\Big(\eta_1(s) + H_m^{-1}(s)H_{um}(s)\eta_2(s) \\ &- K_g(s)r(s) + \tilde{\eta}_{\mathrm{q}}(s)\Big). \end{aligned}$$

Using the definition of $C(s)$ in (4.25), one can write

$$\omega u(s) = -C(s)\big(\eta_1(s) + H_m^{-1}(s)H_{um}(s)\eta_2(s) - K_g(s)r(s) + \tilde{\eta}_{\mathrm{q}}(s)\big).$$

Compared with the reference control in (3.34)

$$\omega u_{\mathrm{ref}}(s) = -C(s)\big(\eta_{1\mathrm{ref}}(s) + H_m^{-1}(s)H_{um}(s)\eta_{2\mathrm{ref}}(s) - K_g(s)r(s)\big),$$

we obtain

$$\begin{aligned} \omega\left(u(s) - u_{\mathrm{ref}}(s)\right) = &-C(s)\big[(\eta_1(s) - \eta_{1\mathrm{ref}}(s)) \\ &+ H_m^{-1}(s)H_{um}(s)(\eta_2(s) - \eta_{2\mathrm{ref}}(s)) + \tilde{\eta}_{\mathrm{q}}(s)\big]. \end{aligned} \tag{B.43}$$

Note that by the definition of $\tilde{\eta}_{\mathrm{q}}(t)$ in (B.42), the predictor error dynamics in (4.29) can be rewritten as

$$\begin{aligned} &\tilde{x}(s) = H_{xm}(s)(\tilde{\omega}u_{\mathrm{q}} + \hat{\eta}_{1\mathrm{q}}(s) - \eta_1(s)) + H_{xum}(s)(\hat{\eta}_{2\mathrm{q}}(s) - \eta_2(s)), \\ &H_m^{-1}(s)C\tilde{x}(s) = \tilde{\omega}u_{\mathrm{q}} + (\hat{\eta}_{1\mathrm{q}}(s) - \eta_1(s)) + H_m^{-1}(s)H_{um}(s)(\hat{\eta}_{2\mathrm{q}}(s) - \eta_2(s)), \end{aligned}$$

and $\tilde{\eta}_{\mathrm{q}}(t)$ can be rewritten as

$$\tilde{\eta}_{\mathrm{q}}(s) = \tilde{\eta}_{u\mathrm{q}}(s) + H_m^{-1}(s)C\tilde{x}(s), \tag{B.44}$$

where $\tilde{\eta}_{u\mathrm{q}}(t) \triangleq \tilde{\omega}(t)(u(t) - u_{\mathrm{q}}(t))$. Substituting (B.41), (B.43) and (B.44) into

(B.40), we have

$$\begin{aligned} e_x(s) =& G_m(s)(\eta_1(s) - \eta_{1\mathrm{ref}}(s)) + G_{um}(s)(\eta_2(s) - \eta_{2\mathrm{ref}}(s)) \\ &+ H_{xm}(s)\omega u_{\mathrm{qe}}(t) - H_{xm}(s)C(s)\tilde{\eta}_{u\mathrm{q}}(s) - H_{xm}(s)C(s)H_m^{-1}(s)C\tilde{x}(s), \end{aligned}$$

where $G_m(s)$ and $G_{um}(s)$ are defined in (4.26). Hence, the error signal is upper bounded by

$$\begin{aligned} \|e_{x_t}\|_{\mathcal{L}_\infty} \leq& \|G_m(s)\|_{\mathcal{L}_1} L_{1\rho_{x_r}} \|e_{x_t}\|_{\mathcal{L}_\infty} + \|G_{um}(s)\|_{\mathcal{L}_1} L_{2\rho_{x_r}} \|e_{x_t}\|_{\mathcal{L}_\infty} \\ &+ \|H_{xm}(s)C(s)H_m^{-1}(s)C\|_{\mathcal{L}_1} \|\tilde{x}_t\|_{\mathcal{L}_\infty} \\ &+ (\|H_{xm}(s)\omega\|_{\mathcal{L}_1} + \|H_{xm}(s)C(s)\|_{\mathcal{L}_1} \tilde{\omega}_{1\,\max}) \|u_{\mathrm{qe}_t}\|_{\mathcal{L}_\infty}, \end{aligned} \tag{B.45}$$

where $\tilde{\omega}_{1\,\max}$ is defined in (B.33).

For the control signal, note that

$$\|u_t\|_{\mathcal{L}_\infty} \leq \|e_{u_t}\|_{\mathcal{L}_\infty} + \|u_{\mathrm{ref}_t}\|_{\mathcal{L}_\infty}, \tag{B.46}$$

where $e_u(t) = u(t) - u_{\mathrm{ref}}(t)$. Following (B.43) and (B.44), $e_u(s)$ can be rewritten as

$$\begin{aligned} (u(s) - u_{\mathrm{ref}}(s)) =& -\omega^{-1}C(s)(\eta_1(s) - \eta_{1\mathrm{ref}}(s)) \\ &- \omega^{-1}C(s)H_m^{-1}(s)H_{um}(s)(\eta_2(s) - \eta_{2\mathrm{ref}}(s)) \\ &- \omega^{-1}C(s)\tilde{\eta}_{u\mathrm{q}}(s) - \omega^{-1}C(s)H_m^{-1}(s)C\tilde{x}(s), \end{aligned}$$

$$\begin{aligned} \|e_{u_t}\|_{\mathcal{L}_\infty} \leq& \|\omega^{-1}C(s)\|_{\mathcal{L}_1} L_{1\rho_{x_r}} \|e_{x_t}\|_{\mathcal{L}_\infty} \\ &+ \|\omega^{-1}C(s)H_m^{-1}(s)H_{um}(s)\|_{\mathcal{L}_1} L_{2\rho_{x_r}} \|e_{x_t}\|_{\mathcal{L}_\infty} \\ &+ \|\omega^{-1}C(s)H_m^{-1}(s)C\|_{\mathcal{L}_1} \|\tilde{x}_t\|_{\mathcal{L}_\infty} + \|\omega^{-1}C(s)\|_{\mathcal{L}_1} \tilde{\omega}_{1\,\max} \|u_{\mathrm{qe}_t}\|_{\mathcal{L}_\infty}. \end{aligned} \tag{B.47}$$

Substituting the prediction error bound in (B.38) and the quantization bound in (2.7), we see that

$$\|(x - x_{\mathrm{ref}})_{t'}\|_\infty \leq \gamma_{xohu} + \gamma_{xqhu} < \gamma_{xhu},\ \|(u - u_{\mathrm{ref}})_{t'}\|_\infty < \gamma_{uhu},$$

which contradicts (B.36). Thus, the assumption does not hold and $\|(x - x_{\mathrm{ref}})_{t'}\|_\infty$ and $\|(u - u_{\mathrm{ref}})_{t'}\|_\infty$ are bounded by (4.37).

B.9 Proof of Theorem 8

(By contradiction)

Similar to the proof of Theorem 8, assume that the bounds in (4.42) do not hold. Similar analysis carries till (B.47). Substituting (B.46) into (B.47), we obtain

$$\begin{aligned}
&(1-\|\omega^{-1}C(s)\|_{\mathcal{L}_1}\tilde{\omega}_{1\max}\delta_{eu})\|u_t\|_{\mathcal{L}_\infty}\\
\leq&(\|\omega^{-1}C(s)\|_{\mathcal{L}_1}L_{1\rho_{x_r}}+\|\omega^{-1}C(s)H_m^{-1}(s)H_{um}(s)\|_{\mathcal{L}_1}L_{2\rho_{x_r}})\|e_{x_t}\|_{\mathcal{L}_\infty}\\
&+\|\omega^{-1}C(s)H_m^{-1}(s)C\|_{\mathcal{L}_1}\|\tilde{x}_t\|_{\mathcal{L}_\infty}+\|u_{\mathrm{ref}_t}\|_{\mathcal{L}_\infty},
\end{aligned}$$

$$\begin{aligned}
\|u_t\|_{\mathcal{L}_\infty}\leq&\frac{\|\omega^{-1}C(s)\|_{\mathcal{L}_1}L_{1\rho_{x_r}}+\|\omega^{-1}C(s)H_m^{-1}(s)H_{um}(s)\|_{\mathcal{L}_1}L_{2\rho_{x_r}}}{1-\|\omega^{-1}C(s)\|_{\mathcal{L}_1}\tilde{\omega}_{1\max}\delta_{eu}}\|e_{x_t}\|_{\mathcal{L}_\infty}\\
&+\frac{\|\omega^{-1}C(s)H_m^{-1}(s)C\|_{\mathcal{L}_1}}{1-\|\omega^{-1}C(s)\|_{\mathcal{L}_1}\tilde{\omega}_{1\max}\delta_{eu}}\|\tilde{x}_t\|_{\mathcal{L}_\infty}+\frac{1}{1-\|\omega^{-1}C(s)\|_{\mathcal{L}_1}\tilde{\omega}_{1\max}\delta_{eu}}\|u_{\mathrm{ref}_t}\|_{\mathcal{L}_\infty}.
\end{aligned}\tag{B.48}$$

Substituting the inequality (B.48) back to (B.45), we have

$$\|e_{x_t}\|_{\mathcal{L}_\infty}\leq\frac{c_{ep}(\delta_{eu})\|\tilde{x}_t\|_{\mathcal{L}_\infty}+c_{eu}(\delta_{eu})\|u_{\mathrm{ref}_t}\|_{\mathcal{L}_\infty}\delta_{eu}}{1-\|G_m(s)\|_{\mathcal{L}_1}L_{1\rho_{x_r}}-\|G_{um}(s)\|_{\mathcal{L}_1}L_{2\rho_{x_r}}-c_{ex}(\delta_{eu})\delta_{eu}}<\gamma_{x_{hl}}.\tag{B.49}$$

For the control signal, substituting (B.48) into (B.47), the error signal can be upper bounded by $\|e_{u_t}\|_{\mathcal{L}_\infty}<\gamma_{u_{hl}}$, which together with the inequality in (B.49) contradicts the assumption. Thus the assumption does not hold and the state and control signals can be upper bounded as in (4.42).

B.10 Proof of Theorem 9

Let

$$\tilde{\sigma}(s)\triangleq\frac{C(s)}{c_m^\top(s\mathbb{I}-A_m)^{-1}b_m}c_m^\top(s\mathbb{I}-A_m)^{-1}\hat{\sigma}(s)-C(s)\sigma(s).$$

It follows from (5.7) that

$$u_{\mathrm{q}}(s)=C(s)r(s)-C(s)\sigma(s)+\tilde{\sigma}(s)+\Delta_u(s),\tag{B.50}$$

and the system in (5.1) consequently takes the form:

$$y(s) = M(s)\Big(C(s)r(s) + (1 - C(s))\sigma(s) - \tilde{\sigma}(s)\Big). \tag{B.51}$$

Substituting (B.50) into (5.2), it follows from the definition of $H(s)$, $H_0(s)$ and $H_1(s)$ that

$$\sigma(s) = H_1(s)r(s) + \frac{H_1(s)}{C(s)}(\Delta_u(s) - \tilde{\sigma}(s)) + H_0(s)d(s).$$

Thus, (B.51) becomes

$$\begin{aligned} y(s) =& H_0(s)M(s)(1 - C(s))d(s) \\ &+ M(s)\big(C(s) + (1 - C(s))H_1(s)\big)\Big(r(s) + \frac{\Delta_u(s) - \tilde{\sigma}(s)}{C(s)}\Big). \end{aligned}$$

It can be verified from (5.11) that

$$\begin{aligned} &M(s)(C(s) + H_1(s)(1 - C(s))) = H(s)C(s), \\ &H_0(s)M(s) = H(s), \end{aligned}$$

and hence

$$y(s) = H(s)C(s)r(s) + H(s)\Delta_u(s) - H(s)\tilde{\sigma}(s) + H(s)(1 - C(s))d(s).$$

For the closed-loop reference system, it can be derived from (5.8) and (5.9) that

$$y_{\text{ref}}(s) = H(s)C(s)r(s) + H(s)(1 - C(s))d_{\text{ref}}(s).$$

The difference leads to the error signal

$$\begin{aligned} e(s) \triangleq& y(s) - y_{\text{ref}}(s) \\ =& H(s)(1 - C(s))(d(s) - d_{\text{ref}}(s)) + H(s)\Delta_u(s) - H(s)\tilde{\sigma}(s), \end{aligned} \tag{B.52}$$

where $d_{\text{ref}}(s)$ is defined in (5.9). The first term is upper bounded by Assumption 8 and the second term is upper bounded by (5.3). The third term can be written in terms of the estimation error. Note that the output predictor dynamics can be

written as

$$\hat{y}(s) = M(s)u(s) + c_m^\top(s\mathbb{I} - Am)^{-1}\hat{\sigma}(s).$$

Together with (5.2), the estimation error can be written as

$$\begin{aligned}\tilde{y}(s) =& c_m^\top(s\mathbb{I} - Am)^{-1}\hat{\sigma}(s) - M(s)\sigma(s)\\ =& \frac{M(s)}{C(s)}\frac{C(s)}{M(s)}c_m^\top(s\mathbb{I} - Am)^{-1}\hat{\sigma}(s) - \frac{M(s)}{C(s)}C(s)\sigma(s)\\ =& \frac{M(s)}{C(s)}\tilde{\sigma}(s).\end{aligned}$$

Thus,

$$H(s)\tilde{\sigma}(s) = \frac{C(s)H(s)}{M(s)}\frac{M(s)}{C(s)}\tilde{\sigma}(s).$$

Substituting it back into (B.52), the error is upper bounded by

$$\|e_t\|_{\mathcal{L}_\infty} \leq L\|H(s)(1 - C(s))\|_{\mathcal{L}_1}\|e_t\|_{\mathcal{L}_\infty} + \|H(s)\|_{\mathcal{L}_1}d_u + \|\frac{C(s)H(s)}{M(s)}\|_{\mathcal{L}_1}\|\tilde{y}_t\|_{\mathcal{L}_\infty}.$$

Applying Lemma 16 gives the uniform upper bound in the first inequality of (5.12).

Compare (B.50) and (5.8) to obtain

$$\begin{aligned}u_{\mathrm{q}}(s) - u_{\mathrm{ref}}(s) &= \frac{C(s)A(s)(d(s) - d_{\mathrm{ref}}(s)) - M(s)\tilde{\sigma}(s) + M(s)\Delta_u(s)}{C(s)A(s) + (1 - C(s))M(s)}\\ &= H_2(s)(d(s) - d_{\mathrm{ref}}(s)) - \frac{H_3(s)}{M(s)}\tilde{y}(s) + \frac{H_3(s)}{C(s)}\Delta_u(s).\end{aligned}$$

Similar to the analysis of the output signal, use Assumption 8, Lemma 16 and (5.3) to obtain

$$\|(u_q - u_{\mathrm{ref}})_t\|_{\mathcal{L}_\infty} \leq L\|H_2(s)\|_{\mathcal{L}_1}\gamma_x + \|\frac{H_3(s)}{M(s)}\|_{\mathcal{L}_1}\bar{\gamma}_0 + \|\frac{H_3(s)}{C(s)}\|_{\mathcal{L}_1}\frac{1}{2}d_u.$$

Since it holds uniformly for all $t > 0$, $u - u_{\mathrm{ref}}$ is uniformly bounded as in the second inequality of (5.12).

B.11 Proof of Lemma 15

Given (6.9) and (6.8), the closed-loop reference system is

$$x_{\text{ref}}(s) = G(s)\eta_{\text{ref}}(s) + H(s)C(s)k_g r(s)\,, \tag{B.53}$$

where $H(s)$ and $G(s)$ are defined in (6.7). Then from the properties of the $\mathcal{L}_1$ norm we have

$$\|x_{\text{ref}_\tau}\|_{\mathcal{L}_\infty} \leq \|G(s)\|_{\mathcal{L}_1}\|\eta_{\text{ref}_\tau}\|_{\mathcal{L}_\infty} + \|H(s)C(s)k_g\|_{\mathcal{L}_1}\|r_\tau\|_{\mathcal{L}_\infty}. \tag{B.54}$$

Note that

$$\begin{aligned}\|\eta_{\text{ref}_\tau}\|_{\mathcal{L}_\infty} \leq& \theta_{\max 0}\|x_{\text{ref}_\tau}\|_{\mathcal{L}_\infty} + \theta_{\max 1}\|x_{\text{ref}_{\tau-\tau_1}}\|_{\mathcal{L}_\infty} + \theta_{\max 2}\|x_{\text{ref}_{\tau-\tau_2}}\|_{\mathcal{L}_\infty} + \|\sigma_\tau\|_{\mathcal{L}_\infty} \\ \leq& \big(\theta_{\max 0} + \theta_{\max 1} + \theta_{\max 2}\big)\|x_{\text{ref}_\tau}\|_{\mathcal{L}_\infty} + \|\sigma_\tau\|_{\mathcal{L}_\infty}.\end{aligned} \tag{B.55}$$

Substituting (B.55) into (B.54) one obtains

$$\begin{aligned}\|x_{\text{ref}_\tau}\|_{\mathcal{L}_\infty} \leq& \|G(s)\|_{\mathcal{L}_1}\big(\theta_{\max 0} + \theta_{\max 1} + \theta_{\max 2}\big)\|x_{\text{ref}_\tau}\|_{\mathcal{L}_\infty} \\ &+ \|G(s)\|_{\mathcal{L}_1}\|\sigma_\tau\|_{\mathcal{L}_\infty} + \|H(s)C(s)k_g\|_{\mathcal{L}_1}\|r_\tau\|_{\mathcal{L}_\infty}.\end{aligned}$$

If the design of k and $D(s)$ satisfies the condition in (6.6), $\|x_{\text{ref}_\tau}\|_{\mathcal{L}_\infty}$ is uniformly bounded for all $\tau > 0$:

$$\|x_{\text{ref}_\tau}\|_{\mathcal{L}_\infty} \leq \frac{\|G(s)\|_{\mathcal{L}_1}\|\sigma\|_{\mathcal{L}_\infty} + \|H(s)C(s)k_g\|_{\mathcal{L}_1}\|r\|_{\mathcal{L}_\infty}}{1 - \|G(s)\|_{\mathcal{L}_1}\big(\theta_{\max 0} + \theta_{\max 1} + \theta_{\max 2}\big)}.$$

Hence, the closed-loop reference system is BIBO stable.

B.12 Proof of Theorem 10

Let $e_x(m) \triangleq x(m) - x_{\text{ref}}(m)$, and

$$\eta(m) \triangleq \theta_0(m)^\top x(m) + \theta_1(m)^\top x(m-\tau_1) + \theta_2(m)^\top x(m-\tau_2) + \sigma(m)\,. \tag{B.56}$$

By the definitions of $\eta(m)$ and $\tilde{\eta}(m)$ in (B.56) and (6.11), we can rewrite the control law in (6.4) as

$$u(s) = -kD(s)(\omega u(s) + \eta(s) - k_g r(s) + \tilde{\eta}(s))\,.$$

Consequently

$$u(s) = -\frac{kD(s)}{1 + k\omega D(s)}(\eta(s) - k_g r(s) + \tilde{\eta}(s))\,.$$

By the definition of $C(s)$ in (6.5), we obtain

$$u(s) = -\frac{C(s)}{\omega}(\eta(s) - k_g r(s) + \tilde{\eta}(s))\,. \tag{B.57}$$

Substituting (B.57) into (6.1), the closed-loop system can be rewritten as

$$x(s) = G(s)\eta(s) + H(s)C(s)k_g r(s) - H(s)C(s)\tilde{\eta}(s)\,,$$

where $H(s)$ and $G(s)$ are defined in (6.7). Recall that the closed-loop reference system is given in (B.53). Then,

$$\begin{aligned} e_x(s) =& G(s)\eta_e(s) - H(s)C(s)\tilde{\eta}(s) \\ =& G(s)\eta_e(s) - C(s)\tilde{x}(s)\,, \end{aligned}$$

where the second equality follows (6.12), and

$$\begin{aligned} \eta_e(m) \triangleq& \eta_{\text{ref}}(m) - \eta(m) \\ =& \theta_0(m)^\top e_x(m) + \theta_1(m)^\top e_x(m - \tau_1) + \theta_2(m)^\top e_x(m - \tau_2)\,. \end{aligned}$$

By the definition of the $\mathcal{L}_1$ norm, we have

$$\|e_\tau\|_{\mathcal{L}_\infty} \le \|G(s)\|_{\mathcal{L}_1}\|\eta_{e_\tau}\|_{\mathcal{L}_\infty} + \|C(s)\|_{\mathcal{L}_1}\|\tilde{x}_\tau\|_{\mathcal{L}_\infty}\,.$$

For $\|\eta_{e_\tau}\|_{\mathcal{L}_\infty}$ in the first term, Assumption 9 implies

$$\begin{aligned} \|\eta_{e_\tau}\|_{\mathcal{L}_\infty} \le& \theta_{\max 0}\|e_{x_\tau}\|_{\mathcal{L}_\infty} + \theta_{\max 1}\|e_{x_{\tau-\tau_1}}\|_{\mathcal{L}_\infty} + \theta_{\max 2}\|e_{x_{\tau-\tau_2}}\|_{\mathcal{L}_\infty} \\ \le& \big(\theta_{\max 0} + \theta_{\max 1} + \theta_{\max 2}\big)\|e_{x_\tau}\|_{\mathcal{L}_\infty}\,. \end{aligned} \tag{B.58}$$

Hence, the error $e_x(m)$ is upper bounded by

$$\|e_\tau\|_{\mathcal{L}_\infty} \leq \|G(s)\|_{\mathcal{L}_1}\big(\theta_{\max 0} + \theta_{\max 1} + \theta_{\max 2}\big)\|e_{x_\tau}\|_{\mathcal{L}_\infty} + \|C(s)\|_{\mathcal{L}_1}\|\tilde{x}_\tau\|_{\mathcal{L}_\infty}\,.$$

If the condition in (6.6) holds, we have

$$\|e_{x_\tau}\|_{\mathcal{L}_\infty} \leq \frac{\|C(s)\|_{\mathcal{L}_1}}{1-\|G(s)\|_{\mathcal{L}_1}\big(\theta_{\max 0} + \theta_{\max 1} + \theta_{\max 2}\big)}\|\tilde{x}_\tau\|_{\mathcal{L}_\infty}.$$

The above inequality together with Lemma 16 leads to

$$\|e_{x_\tau}\|_{\mathcal{L}_\infty} \leq \frac{\|C(s)\|_{\mathcal{L}_1}}{1-\|G(s)\|_{\mathcal{L}_1}\big(\theta_{\max 0} + \theta_{\max 1} + \theta_{\max 2}\big)}\sqrt{\frac{\theta_m}{\lambda_{\min}(P)\Gamma}},$$

which holds uniformly for all $\tau \geq 0$. Thus, the first inequality in (6.14) holds.

For the second bound in (6.14), subtract (6.9) from (B.57) to obtain

$$u(s) - u_{\text{ref}}(s) = -\frac{C(s)}{\omega}\eta_e(s) - \frac{C(s)}{\omega}\tilde{\eta}(s)\,.$$

For the first term, $\|\eta_{e_\tau}\|_{\mathcal{L}_\infty}$ is upper bounded as in (B.58). For the second term, since (A_m, b_0) is controllable, and $H(s)$ is strictly proper and stable, there exists $c_o \in \mathbb{R}^n$ such that $c_o^\top H(s)$ is minimum phase with relative degree one (by Lemma 4 in [21]). This allows for the following representation

$$-\frac{C(s)}{\omega}\tilde{\eta}(s) = -\frac{C(s)}{\omega}\frac{1}{c_o^\top H(s)}c_o^\top\tilde{x}(s)\,.$$

Since $C(s)$ is strictly proper and stable, the system $\frac{C(s)}{c_o^\top H(s)}c_o^\top$ is at least proper and stable. Thus, the error in the control signal can be bounded by

$$\begin{aligned}\|u - u_{\text{ref}}\|_{\mathcal{L}_\infty} \leq &\left\|\frac{C(s)}{\omega}\right\|_{\mathcal{L}_1}\big(\theta_{\max 0} + \theta_{\max 1} + \theta_{\max 2}\big)\|e_{x_\tau}\|_{\mathcal{L}_\infty} \\ &+ \left\|\frac{C(s)}{\omega c_o^\top H(s)}c_o^\top\right\|_{\mathcal{L}_1}\|\tilde{x}\|_{\mathcal{L}_\infty}\,.\end{aligned}$$

Finally, Lemma 16 and the first bound in (6.14) lead to the second bound.

REFERENCES

[1] R. W. Brockett and D. Liberzon, "Quantized feedback stabilization of linear systems," *IEEE Transactions on Automatic Control*, vol. 45, no. 7, pp. 1279–1289, 2000.

[2] N. Elia and S. Mitter, "Stabilization of linear systems with limited information," *IEEE Transactions on Automatic Control*, vol. 46, no. 9, pp. 1384–1400, Sep 2001.

[3] H. Ishii and T. Başar, "Remote control of LTI systems over networks with state quantization," *Systems & Control Letters*, vol. 54, no. 1, pp. 15–31, 2005.

[4] S. Yuksel and T. Başar, "Minimum rate coding for LTI systems over noiseless channels," *IEEE Transactions on Automatic Control*, vol. 51, no. 12, pp. 1878–1887, 2006.

[5] L. Vu and D. Liberzon, "Supervisory control of uncertain systems with quantized information," *International Journal of Adaptive Control and Signal Processing*, vol. 26, no. 8, pp. 739–756, 2012.

[6] L. Vu and D. Liberzon, "Stabilizing uncertain systems with dynamic quantization," in *IEEE Conference on Decision and Control*, 2008, pp. 4681–4686.

[7] Y. Sharon, D. Liberzon, and Y. Ma, "Adaptive control using quantized measurements with application to vision-only landing control," in *IEEE Conference on Decision and Control*, 2010, pp. 2511–2516.

[8] M. Raginsky, "Divergence-based characterization of fundamental limitations of adaptive dynamical systems," *Proceedings of the Forty-Eighth Annual Allerton Conference on Communication, Control, and Computing*, 2010.

[9] M. Fu and L. Xie, "The sector bound approach to quantized feedback control," *IEEE Transactions on Automatic Control*, vol. 50, no. 11, pp. 1698–1711, November 2005.

[10] T. Nakaguchi, Y. Tanji, and M. Tanaka, "Hysteresis hierarchical cellular neural networks," in *Proceedings of the 1999 International Symposium on Nonlinear Theory and its Applications*, Nov 1999, pp. 411–414.

[11] T. Nakaguchi, T. Harada, Y. Tanji, K. Jinno, and M. Tanaka, "Hierarchical cellular neural networks," in *Proceedings of the 1999 European Conference on Circuit Theory and Design*, Aug 1999, pp. 1355–1358.

[12] K. Yokosawa, Y. Tanji, and M. Tanaka, "CNN with multi-level hysteresis quantization output," in *Proceedings of the 2000 6th IEEE International Workshop on Cellular Neural Networks and Their Applications*, May 2000, pp. 407–412.

[13] F. Ceragioli, C. D. Persis, and P. Frasca, "Discontinuities and hysteresis in quantized average consensus," *Automatica*, vol. 47, no. 9, pp. 1916–1928, 2011.

[14] K. Millheim, S. Jordan, and C. Ritter, "Bottom-hole assembly analysis using the finite-element method," *Journal of Petroleum Technology*, pp. 265–274, 1978.

[15] G. C. Downton, "Directional drilling system response and stability," in *IEEE International Conference on Control Applications*, 2007, pp. 1543–1550.

[16] D. W. Dareing and B. J. Livesay, "Longitudinal and angular drill-string vibrations with damping," *Journal of Manufacturing Science and Engineering*, vol. 90, no. 4, pp. 671–679, November 1968.

[17] V. A. Dunsyevsky, A. Judzis, and W. H. Mills, "Dynamic stability of drillstrings under fluctuating weight on bit," *SPE Drilling & Completion*, vol. 2, no. 8, pp. 84–92, 1993.

[18] W. D. Aldred and M. C. Sheppard, "Drillstring vibrations: A new generation mechanism and control strategies," in *SPE Annual Technical Conference and Exhibition*, Washington, D.C, October 1992.

[19] C. Cao and N. Hovakimyan, "Stability margins of $\mathcal{L}_1$ adaptive control architecture," *IEEE Transactions on Automatic Control*, vol. 55, no. 2, February 2010.

[20] N. Hovakimyan and C. Cao, $\mathcal{L}_1$ *Adaptive Control Theory: Guaranteed Robustness with Fast Adaptation*. Philadelphia, PA: SIAM, 2010.

[21] C. Cao and N. Hovakimyan, "Design and analysis of a novel $\mathcal{L}_1$ adaptive control architecture with guaranteed transient performance," *IEEE Transactions on Automatic Control*, vol. 53, no. 2, pp. 586–591, March 2008.

[22] T. Hayakawa, H. Ishii, and K. Tsumura, "Adaptive quantized control for linear uncertain discrete-time systems," *Automatica*, vol. 45, no. 3, pp. 692–700, 2009.

[23] M. M. Polycarpou and P. A. Ioannou, "On the existence and uniqueness of solutions in adaptive control systems," *IEEE Transactions on Automatic Control*, vol. 38, no. 3, pp. 474–479, March 1993.

[24] E. Lindelöf and M. Picard, "Sur lapplication de la méthode des approximations successives aux équations différentielles ordinaires du premier ordre," *Comptes rendus hebdomadaires des séances de lAcadémie des sciences*, vol. 114, pp. 454–457, 1894.

[25] E. Picard, *Mémoire sur la théorie des équations aux dérivées partielles et la méthode des approximations successives*. Gauthier-Villars, 1890.

[26] A. F. Filippov, "Differential equations with discontinuous right-hand side," *Mathematicheskii Sbornik*, vol. 51, no. 93, pp. 99–128, 1960.

[27] A. Filippov, *Differential Equations with Discontinuous Righthand Sides*. Springer, 1988.

[28] E. Ryan, *Optimal relay and saturating control system synthesis*, ser. IEE control engineering series. P. Peregrinus on behalf of the Institution of Electrical Engineers, 1982.

[29] J. B. Pomet and L. Praly, "Adaptive nonlinear regulation: Estimation from the Lyapunov equation," *IEEE Transactions on Automatic Control*, vol. 37, no. 6, pp. 729–740, 1992.

[30] E. Xargay, N. Hovakimyan, and C. Cao, "$\mathcal{L}_1$ adaptive controller for Multi-Input Multi-Output systems in the presence of uncertain nonlinear cross-coupling," in *American Control Conference*, Baltimore, MD, 2010, (to be submitted to IEEE Transactions on Automatic Control). pp. 875–879.

[31] K.-K. Kim and N. Hovakimyan, "Development of verification and validation approaches for $\mathcal{L}_1$ adaptive control: Multi-criteria optimization for filter design," in *AIAA Guidance, Navigation and Control Conference*, Toronto, Canada, August 2010, AIAA-2010-7691.

[32] D. Li, N. Hovakimyan, C. Cao, and K. A. Wise, "Filter design for feedback-loop trade-off of $\mathcal{L}_1$ adaptive control: A linear matrix inequality approach," in *AIAA Guidance, Navigation and Control Conference*, Honolulu, HI, August 2008, AIAA-2008-6280.

[33] D. Li, V. V. Patel, C. Cao, and N. Hovakimyan, "Optimization of the time-delay margin of $\mathcal{L}_1$ adaptive controller via the design of the underlying filter," in *AIAA Guidance, Navigation and Control Conference*, Hilton Head, SC, August 2007, AIAA-2007-6646.

[34] M. A. Dahleh and J. B. Pearson, "$\mathcal{L}_1$ optimal feedback compensators for continuous-time systems," *IEEE Transactions on Automatic Control*, vol. 32, no. 4, pp. 889–895, October 1987.

[35] I. J. Diaz-Bobillo and M. A. Dahleh, "State feedback ℓ_1 optimal controllers can be dynamic," *Systems & Control Letters*, vol. 19, no. 2, pp. 87–93, August 1992.

[36] J. S. Shamma, "Nonlinear state feedback for ℓ_1 optimal control," *Systems & Control Letters*, vol. 21, no. 4, pp. 265–270, October 1993.

[37] C. Cao and N. Hovakimyan, "$\mathcal{L}_1$ adaptive controller for a class of systems with unknown nonlinearities: Part 1," in *American Control Conference*, Seatlle, WA, June 2008, pp. 4093–4098.

[38] H. Sun, N. Hovakimyan, and T. Başar, "$\mathcal{L}_1$ adaptive controller for systems with input quantization," in *American Control Conference*, Baltimore, MD, 2010, pp. 253–258.

[39] C. Cao and N. Hovakimyan, "$\mathcal{L}_1$ adaptive controller for systems with unknown time-varying parameters and disturbances in the presence of non-zero trajectory initialization error," *International Journal of Control*, vol. 81, no. 7, pp. 1147–1161, July 2008.

[40] H. Sun, N. Hovakimyan, and T. Başar, "$\mathcal{L}_1$ adaptive controller for uncertain nonlinear multi-input multi-output systems with input quantization," *IEEE Transactions on Automatic Control*, vol. 57, no. 3, pp. 565–578, March 2012.

[41] R. Middlebrook and S. Ćuk, "A general unified approach to modelling switching-converter power stages," *International Journal of Electronics Theoretical and Experimental*, vol. 42, no. 6, pp. 521–550, 1977.